IDENTIFICATION OF TIME-VARYING HUMAN JOINT DYNAMICS

Jon Bart MacNeil

A Thesis submitted to
the Faculty of Graduate Studies and Research
in partial fulfillment of the requirements for the degree of
Master of Engineering

Department of Mechanical Engineering
&
Biomedical Engineering Department
McGill University, Montréal

August, 1990

To my parents

ABSTRACT

In order to develop a comprehensive model of the motor control system, the time-varying nature of joint dynamics must be addressed However, it has not previously been possible to quantitatively observe changes in joint dynamics during a transition of state In this work, a recently developed method for identification of linear time-varying dynamic systems from ensemble data has been used to obtain models of neuromuscular dynamics during a rapid contraction The method, based on singular value decomposition, provides a series of nonparametric (impulse response function) models of a system's dynamics without *a priori* knowledge of its dynamic structure or time-variation, thus enabling study of the neuromuscular system during natural activity

Application of this method to simulated and experimental data have shown it to be robust and accurate Ankle dynamics have been tracked during voluntary isometric contraction of triceps surae, revealing behaviour more complex than second-order, characterized by a decrease in the joint's resistance to low frequency perturbations

RÉSUMÉ

Afin de développer un modèle détaillé du système de contrôle moteur, la nature de la variation temporelle de la dynamique articulaire doit être abordée. Il ne fut cependant pas possible auparavant d'observer quantitativement les changements de dynamique articulaire lors de la transition d'un état à un autre. Dans cette étude, une méthode d'identification de systèmes dynamiques linéaires et variant temporellement a été employée pour obtenir des modèles de la dynamique neuromusculaire lors de contractions rapides. La méthode, basée sur la décomposition des valeurs singulières, fournit une série de modèles non-paramétriques de la dynamique d'un système, sous forme de réponses impulsionnelles, et ce sans connaissance *a priori* de sa structure dynamique ni de la variation temporelle, permettant ainsi l'étude du système neuro-musculaire lors d'activités normales.

L'application de cette méthode à des donnés simulées et expérimentales a démontré sa robustesse et sa précision. L'évolution de la dynamique au niveau de la cheville a été suivie lors de contractions isométriques volontaires du triceps surae, révélant un comportement plus complexe que celui du deuxième ordre, et caractérisé par une diminution de la résistance de l'articulation à des perturbations de basse fréquence.

ACKNOWLEDGEMENTS

I thank Rob Kearney, my advisor, for all his guidance and monetary support, as well as for putting up with hearing "it's almost finished" at least a thousand times Thanks also to Ian Hunter, whose enthusiasm for scientific research is most certainly contagious, Serge Lafontaine, who expanded my knowledge of computers immensely, and Bob Kirsch, who also gave numerous valuable suggestions I wish to thank the students and staff of biomedical engineering for making my time at "the lab" enjoyable

My deepest appreciation to Eric and Grog, purveyors of pounds of pasta and brethren of the Bodum, for providing necessary, and not so necessary, diversions To Lynn, who made it all easier in many ways, heartfelt thanks

Finally, thanks to my parents, for their unfaltering love and support

This work was supported by NSERC, MRC, the coffee growers of Columbia, and Boulangerie St Laurent

TABLE OF CONTENTS

LIST OF FIGURES

LIST OF TABLES

1. INTRODUCTION

Joint dynamics describe the relationship between the angular position of a joint and the torques developed about it This relationship, expressed as either joint stiffness (position considered as input to the joint, torque as the output) or its inverse compliance, is not only dynamic, but also varies with a number of physiological factors, one of which is the mean level of torque developed at the joint due to muscular contraction

A knowledge of the way joint dynamics change with the level of muscular activation is essential to understand how the neuromuscular system controls posture and movement, and therefore has far-reaching implications in a number of fields, including basic neuromuscular research, diagnosis and treatment of neuromuscular disorders, prosthetic control, and robotics

In many functional actions, the dynamics of a joint change considerably in a short period of time due to rapid changes in muscular activity It is often the case that the changes occur on a time scale comparable to the duration of the system's dynamic response In order to obtain a true representation of a system exhibiting this behavior, it is essential that an approach recognizing the time-varying nature of the system's dynamics be employed

Unfortunately, the majority of studies of the dependence of joint dynamics on muscular contraction to date have employed quasi-time-invariant techniques, which assume that joint dynamics change slowly with time, allowing standard time-invariant system identification methods to be used These experiments have typically been designed to investigate the dynamics of a joint at distinct, maintained levels of contraction and therefore do not provide insight into the manner in which joint dynamics change during variations of the level of muscular contraction

The purpose of this work was two-fold

1 to evaluate the performance of a recently developed method for identification of time-varying systems from ensemble data and,

2 to employ this method to observe the changes in ankle joint dynamics that occur during a rapid isometric contraction of the calf muscles.

The body of this thesis has been organized in the following manner:

Chapter 2 provides the necessary background regarding joint dynamics and time-varying identification

Chapter 3 details the theory and implementation of a recently developed technique for time-varying identification, and discusses its potential advantages over other methods with particular reference to studies of joint dynamics

Chapter 4 describes a simulation study in which this technique was employed to identify the dynamics of a simulated time-varying system having behaviour similar to the human ankle The performance of the method was evaluated by applying it to data generated by the simulated system using different levels of additive output noise

Chapter 5 presents the results of an experiment in which the time-varying dynamics of the human ankle were identified during an increase in contraction of the calf muscles using the new method. The experimental paradigm, method of analysis, and results are discussed

Chapter 6 summarizes the major findings of this investigation, and suggests directions for future work

2. BACKGROUND

This thesis is concerned with identifying how human ankle joint dynamics vary during isometric contraction of the calf muscles Two issues are being addressed the dynamics of human joints, and time-varying system identification This chapter provides a brief introduction to the aspects of these two topics relevant to this report

2.1. JOINT DYNAMICS

In this section, the factors influencing joint dynamics will be discussed using a system identification philosophy The information flow diagram for an experiment designed to study joint dynamics using system identification techniques is presented in Figure 2 1 The elements of the block diagram indicate the various mechanisms that can affect the observed dynamics Each of these will be discussed separately below

2.1.1. MUSCLE MECHANICS

The mechanical properties of muscle are the result of the interaction of the muscle's contractile mechanics and activation dynamics

CONTRACTILE MECHANICS

Contractile mechanics determine the force generated due to changes of length of muscle under a constant level of activation. They are the external manifestation of the intrinsic process of contraction Therefore, in order to understand the influence of contractile mechanics, a brief review of the structure and function of skeletal muscle is in order

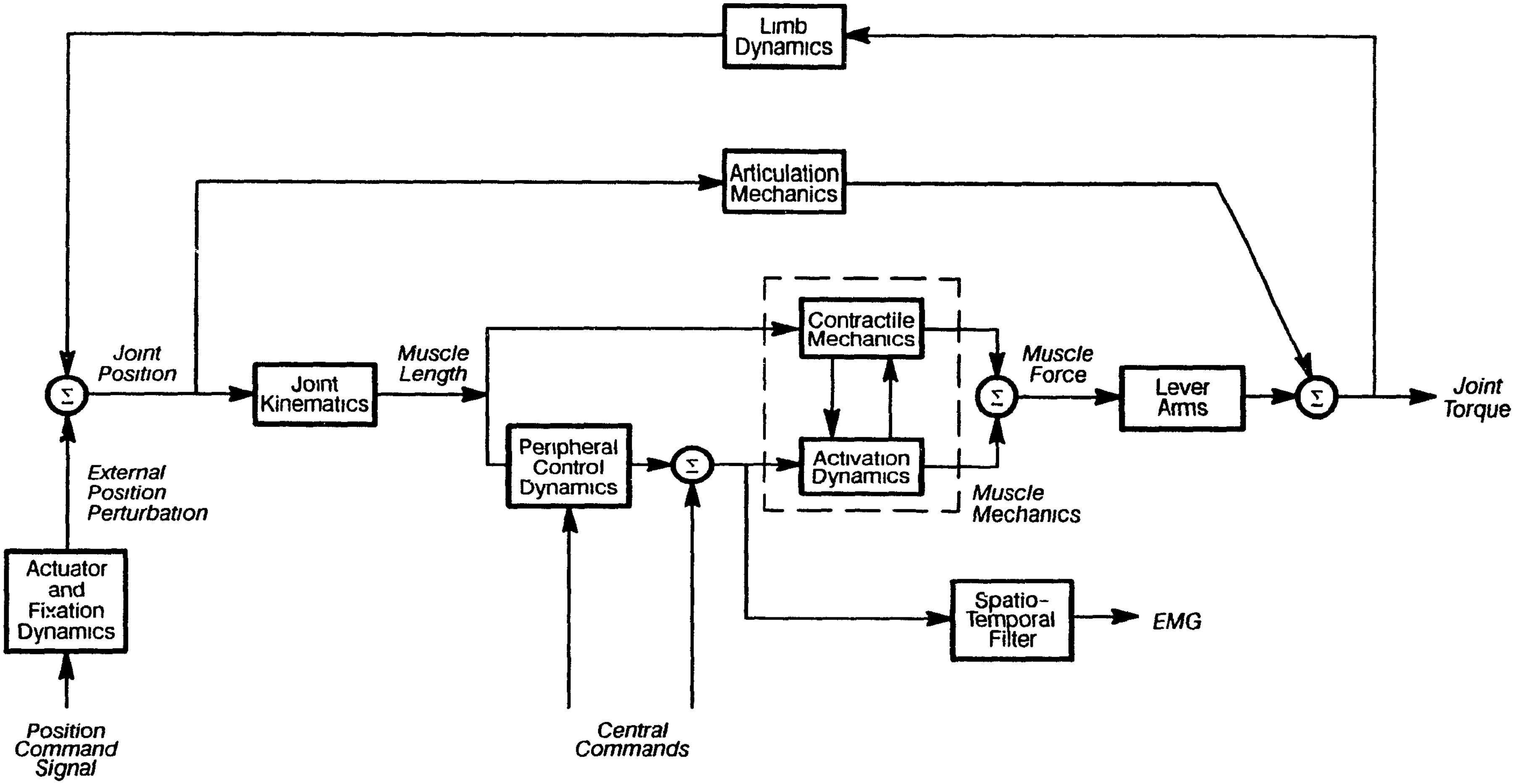

Figure 2.1. Information flow diagram for an experiment designed to investigate joint dynamics.

SKELETAL MUSCLE STRUCTURE AND FUNCTION

Whole skeletal muscle is comprised of bundles of muscle fibres held together by connective tissue (Vander, 1985) At the ends of each fibre the connective tissue joins together, forming the tendon of the whole muscle, which is attached to bone or fascia As shown in Figure 2 2, muscle fibres are formed from bundles of fibres called myofibrils These typically have diameters of approximately 2 µm and extend from one end of the fibre to the other Myofibrils are further subdivided into myofilaments, of which there are two types thick (12 to 18 nm diameter) and thin (5 to 8 nm diameter) Thin filaments are composed mainly of the proteins actin, troponin and tropomyosin, while thick filaments are primarily myosin When viewed under magnification, myofybrils have the appearance of alternating light and dark bands One unit of this periodic structure is called a sarcomere (see Figure 2 2), and is of length ranging from 1 5 to 3 6 µm, depending on muscle length The thick and thin filaments are oriented parallel to each other, thin filaments are anchored at one end of the sarcomere, with the other end overlapping the thick filaments The sliding filament theory (H E Huxley and Hanson, 1954, A F Huxley and Niedergerke, 1954) proposes that the thick and thin filaments move relative to each other, allowing the sarcomere length to vary with the degree of overlap of the thick and thin filaments

In the region of overlap, large heads of the myosin protein, known as crossbridges, are in close proximity to the actin filaments According to the crossbridge theory of muscular contraction (A F Huxley, 1957), these crossbridges attach to adjacent sites on the actin molecule, and exert force on the thin filament by rotating through an angle of approximately 45° The crossbridges cycle through a process of attachment, rotation, detachment, and reattachment at a new position on the thin filament during contraction, so that as the crossbridges exert force on the thin filaments, the sarcomere length decreases The collective effort of the immense number of crossbridges in muscle fibre results in the generation of considerable force and shortening action observed in contracting muscle fibre Crossbridge activity does not necessarily cause muscle shortening, however For isometric contractions, where muscle length is unchanged, force is still generated via crossbridge cycling

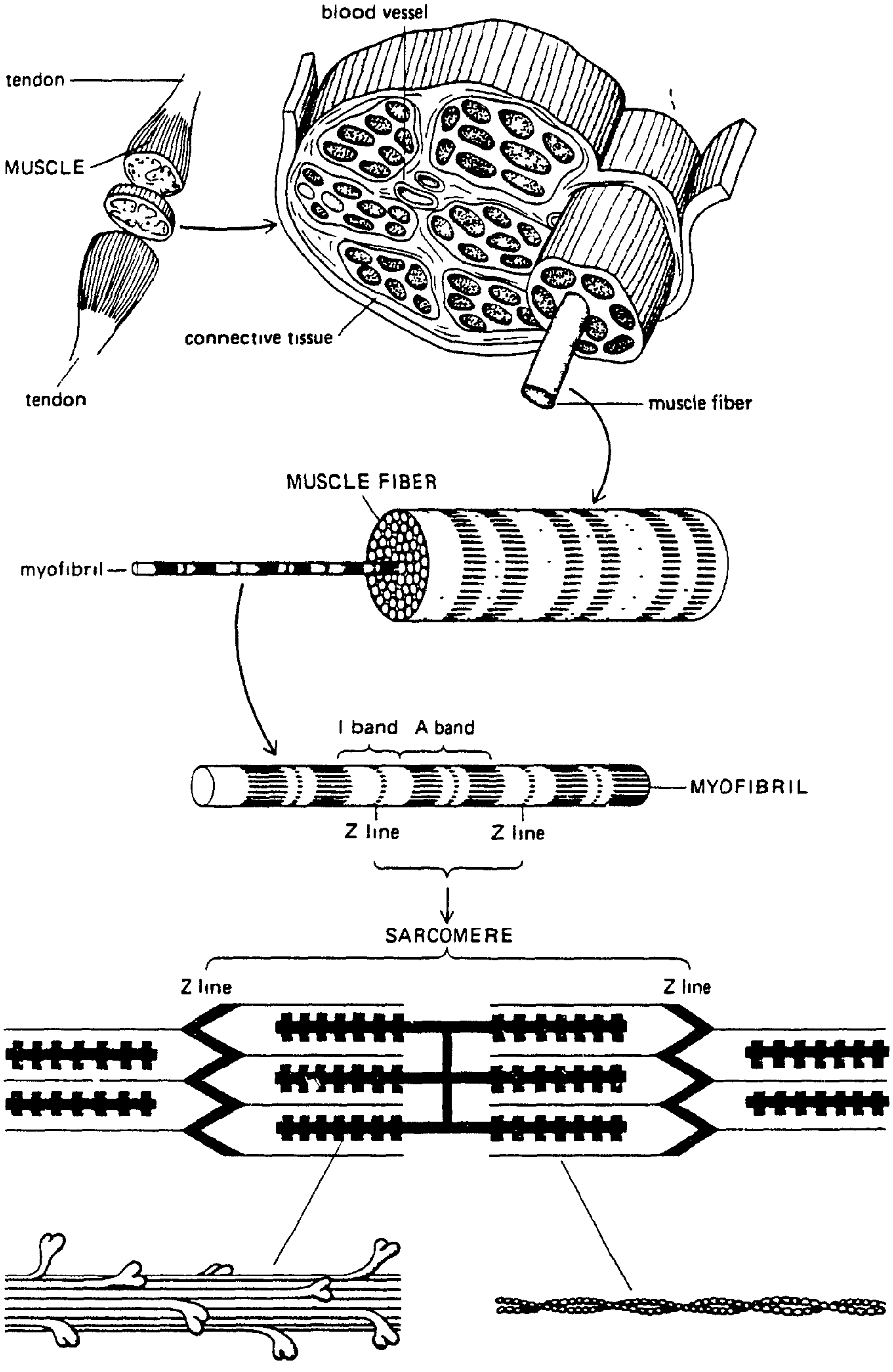

Figure 2 2 The structural organization of muscle (from Vander, 1985).

THE LENGTH-TENSION RELATIONSHIP OF ISOLATED MUSCLE FIBRE

The force generated by active muscle is a nonlinear function of muscle length (Gordon *et al.*, 1966), as shown in Figure 2 3, which presents the variation of maximum isometric tension developed in an isolated muscle fibre with muscle fibre length Note that a muscle fibre also has passive mechanical properties, the length-tension curve of passive muscle is nonlinear and exhibits behaviour much like a hard spring (McMahon, 1984) This is not shown in the figure The tensions developed due to active and passive properties are additive, so the total length-tension curve is somewhat different (Aubert *et al* , 1951) However, this section is only concerned with active contractile mechanisms, so Figure 2 3 is illustrative The crossbridge and sliding filament theories have been used to explain this relationship The premise is that muscle force is dependent on the number of crossbridges in operation When a muscle fibre is stretched, the degree of overlap of the fibres decreases, so that fewer crossbridge attachments are possible, thus diminishing the potential for force generation Conversely, if muscle shortens beyond a certain length, the force-generating ability of the fibre will be hampered because the thin filaments will begin to over-

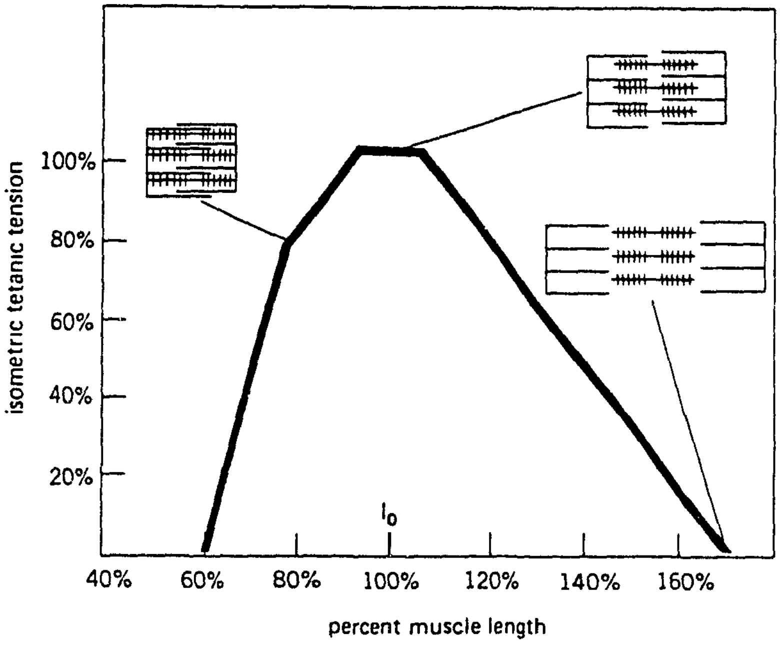

Figure 2 3 The nonlinear length-tension relationship of isolated muscle fibre (from Vander, 1985) lap, and the thick filaments will begin to butt against the ends of the sarcomere (González-Serratos, 1971) This is illustrated in the figure by the schematic depictions of the thick and thin fibres of a sarcomere in a muscle fibre at various elongations Note however, that the range of length changes that occur *in vivo* is smaller than the range encompassed by the curve of Figure 2 3 The *in vivo* range is between 70 and 130 percent of the length at which a muscle fibre develops maximum tension (labelled l_0 in the figure)

THE FORCE-VELOCITY RELATIONSHIP OF ISOLATED MUSCLE FIBRE

The velocity of shortening of muscle fibre is a nonlinear function of the load on the muscle Shortening velocity is greatest when the load is zero, and decreases with increasing load, until the load is equal to the maximum possible force of the muscle, at which point the velocity is zero This is shown in Figure 2 4

The length-tension and force-velocity relationships for isolated muscle are not entirely representative of the situation encountered *in vivo*. The length and velocity dependence of the force generated by intact muscle *in vivo* has been determined for different levels of muscular activity (Wilkie, 1950; Joyce *et al.*, 1969; Joyce and Rack, 1969, Rack and Westbury, 1969) An example of the results of these studies is shown in Figure 2 5 These curves provide an estimate of the space of possible operating points for the neuromuscular system

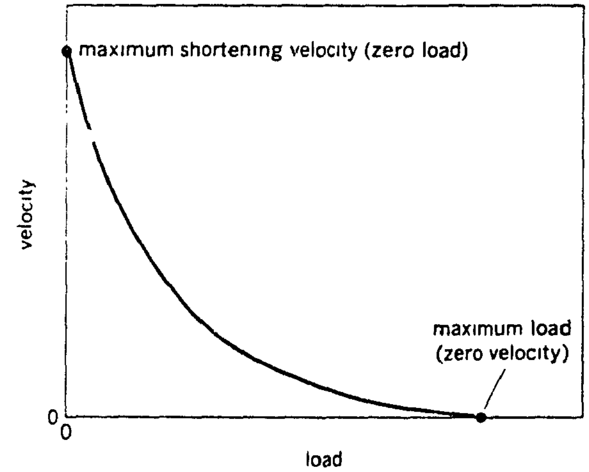

Figure 2 4 The force-velocity curve for isolated muscle fibre (from Vander, 1985)

As would be expected from the nonlinear nature of the length-tension and force-velocity relationships, contractile mechanisms for isolated muscle are a nonlinear function of displacement amplitude and direction, velocity of displacement, and other factors (Stein, 1974) Work is underway to model the dynamics of the contractile mechanisms of isolated

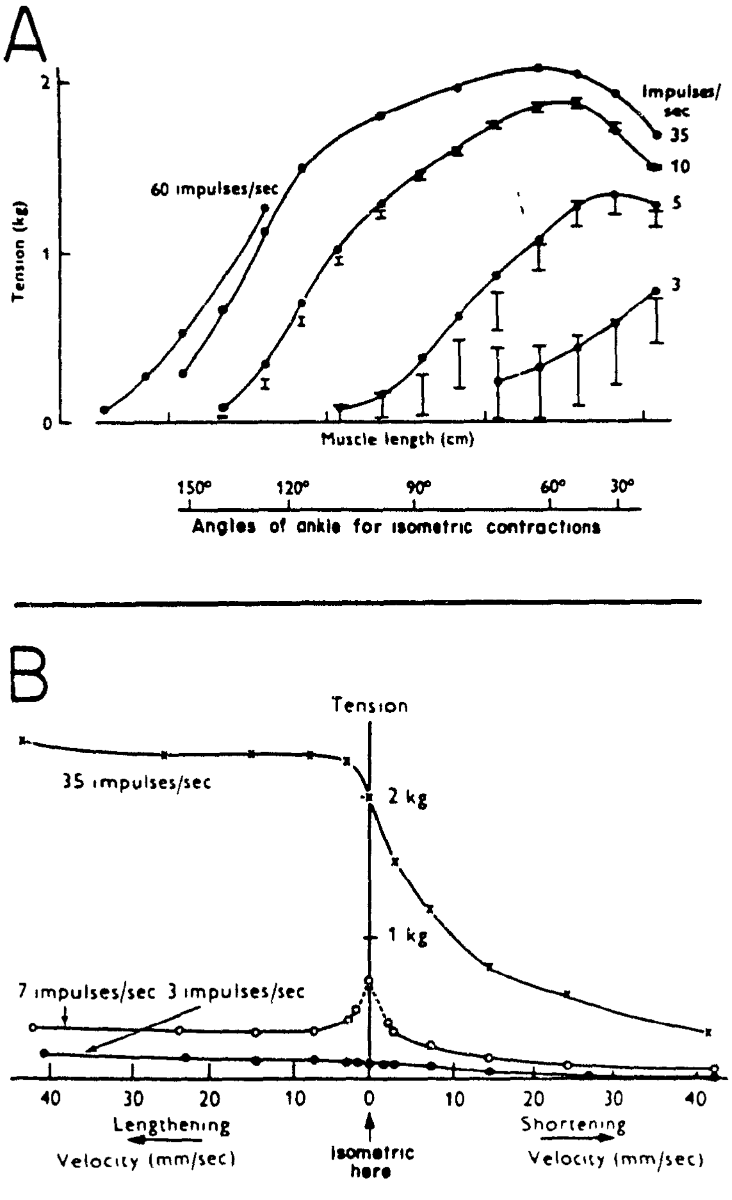

Figure 2 5 The dependence of contractile muscle force on limb position, its rate of change, and direction A) Length-tension curves for isometric cat soleus muscle at various rates of nonsynchronous supramaximal stimulation B) Muscle force generated during different lengthening and shortening velocities (from Brooks, 1986) muscle using nonlinear system identification methods (Hunter, 1986), however a comprehensive model has yet to be developed

ACTIVATION DYNAMICS

Activation dynamics describe how electrical signals from the neuromuscular system relate to the force generated by muscle As with contractile mechanics, activation dynamics are the result of the underlying physiology

THE MOTOR UNIT

Muscle fibres are controlled by motoneurons (also known as α-motoneurons) residing in the anterior horn of the spinal grey matter Each motoneuron innervates a number of muscle fibres, (e g , from 2 in human laryngeal muscles to over 2000 in the medial head of gastrocnemius (Basmajian and DeLuca,1985)), but each fibre receives neural input from only one motoneuron Each time the motoneuron fires, the action potential descending the nerve axon results in the nearly simultaneous contraction of all fibres on which it terminates The motoneuron and the muscle fibres it supplies therefore act as a single entity This entity is called a motor unit, and is shown schematically in Figure 2 6

All muscle fibres in a muscle are not identical; their properties span a broad spectrum, from highly vascularised, nonfatiguing fibres having slowly rising long twitch contractions to sparsely vascularised, easily fatigued ones with fast, short twitches However, the fibres of a single motor unit have nearly identical properties

Motor units in a single muscle have varied numbers of fibres, units with relatively few fibres have smaller, slower conducting axons, produce slow, low force contractions, and fatigue slowly Large units have faster conducting axons, and can produce large contractions but fatigue rapidly

RATE CODING

The neuromuscular system controls the force output of whole muscle by two mechanisms, rate coding and recruitment Rate coding refers to the adjustment of the firing rate of motoneurons For single action potentials, a motor unit will respond with a twitch, in which a rapid increase in force is followed by a slower decrease For multiple action poten-

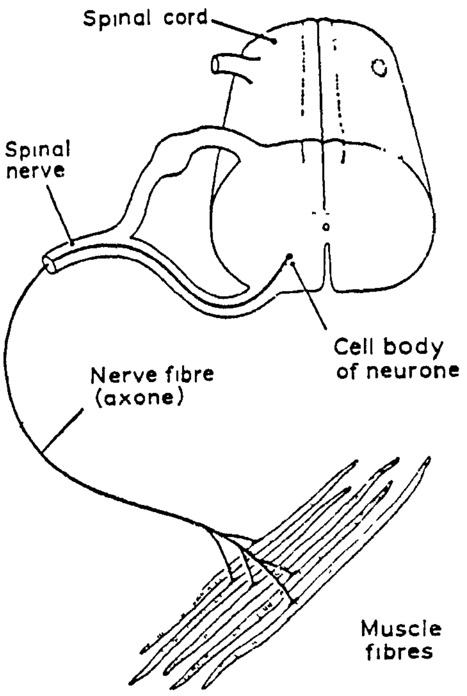

Figure 2 6 The structure of the motor unit (from Basmajian, 1978)

tials, if the period between action potentials is less than the time for the muscle to relax, there will be superposition of the twitches, resulting in increased muscular tension When the firing frequency reaches a critical value, the contributions of the individual action potentials overlap completely, resulting in a smooth sustained tension, called tetanus, as illustrated in Figure 2 7

The dynamic response of muscle force to changes of stimulus frequency has been modelled as a low-pass system with corner frequency near 2 Hz (Mannard and Stein, 1973, Bawa and Stein, 1976) In addition, there is a static nonlinear relation between stimulus frequency and muscle force under conditions of repetitive stimulation at constant rate (Rack and Westbury, 1969)

RECRUITMENT

Muscle force is also controlled by alterations of the number of active motor units The majority of investigations have found that motor units are recruited according to the size principle (Henneman and Olson, 1965) At low levels of contraction, the small, fatigue

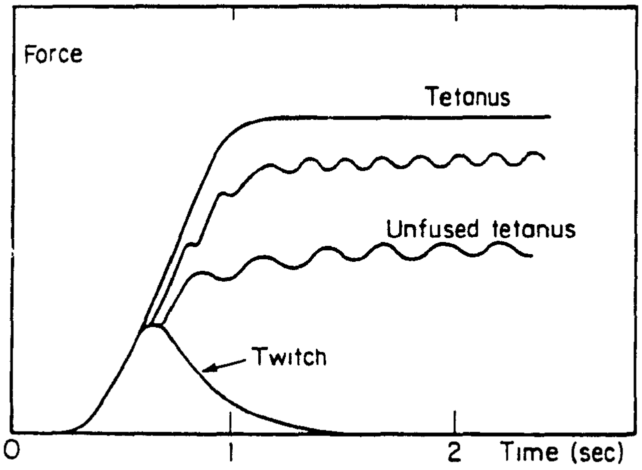

Figure 2 7 The effect of firing frequency on muscle force (from McMahon, 1984)

resistant units are activated first As contraction level increases, the recruitment strategy proceeds from the small, low force units to larger, faster units until all motor units have been recruited

Rate coding and recruitment work in concert, with the relative contributions depending on the muscle and level of contraction (Brooks, 1986) It has been reported for some muscles that recruitment is the primary mechanism at low levels of contraction, at medium levels of contraction both mechanisms play nearly equal roles, and rate coding dominates at levels above around 70% of maximum (Basmajian, 1978)

EMG

When muscle contracts, its fibres are activated by a wave of depolarization called a motor unit action potential (MUAP) which travels along their external membrane, and can be detected as a change of voltage, either in a single fibre or on the skin above a muscle This measure, known as the electromyogram (EMG), gives an indirect measure of muscular activity A convenient way to detect the electrical activity of muscle is by using an electrode on the skin surface The EMG signal recorded in this way represents the activity of a number of fibres in a finite volume under the electrode, and is the result of the activity of a large number of motor units The recorded signal will be the spatio-temporal summation of the electrical activity of the muscle fibres in the volume from which the electrode is able to detect voltage The voltage recorded at the electrode will also be an altered version of the original myoelectric activity due to filtering by the intervening skin and muscle fibres

The recorded voltages are low amplitude, typically in the microVolt range, so the signal must be considerably amplified Because background noise will have power comparable to that of the surface EMG, it is common to record using two electrodes in a bipolar configuration oriented parallel to the direction of the fibres in the muscle The signals from the electrodes are differentially amplified, so that any signals picked up simultaneously by both electrodes are rejected The noise removal performance of differential amplifiers is evaluated in terms of their ability to remove the signal content common to both channels, and is called the common mode rejection ratio (CMRR) CMRR is defined as the ratio of the differential gain to the common gain A CMRR between 100 and 120 dB is effective for removal of most background noise in the majority of EMG applications (Basmajian and DeLuca, 1985) However, the bipolar recording scheme distorts the EMG signal further, because the MUAP will travel under the electrodes at different times This introduces a constant lag between the signals picked up by the two electrodes which is a function of inter-electrode distance and conduction velocity (the velocity of the MUAP) The distortion will have a high-pass frequency response similar to a comb filter, having frequencies of attenuation occurring at intervals proportional to the ratio of the conduction velocity of the MUAP and the inter-electrode distance (Lindström, 1970) Thus the recorded signal will be an altered version of the true EMG due to the spatial and temporal filtering caused by the bipolar recording scheme

The EMG signal is typically further processed after recording by high-pass filtering the signal with a corner frequency in the neighborhood of 10 Hz to remove movement and other low frequency artifacts In many applications this is followed by full-wave rectification and change of polarity to distinguish between agonist and antagonist EMG and low-pass filtering at high frequency to remove the high frequency components of the signal introduced by other noise sources

It is evident that the electrical signal that is the final result of recording and processing the surface EMG is very different from the electrical activity of a single muscle fibre, or a group of fibres from a single motor unit Still, the surface EMG signal is useful, and is typically interpreted as a noise signal whose amplitude is modulated by the number of active motor units in the volume under the electrode, and the rate at which they fire A signal to noise ratio of less than 30 dB is common for surface EMG (Parker and Scott, 1984, Basmajian and DeLuca, 1985, Zhang *et al.*, 1989) therefore is it is difficult to extract meaningful amplitude information from a single EMG trace In practice EMG is recorded for a number of repetitions of the same task and the traces ensemble averaged to diminish the effects of atypical variations in amplitude Under time-invariant conditions, mean rectified EMG increases monotonically with level of contraction (Milner-Brown and Stein, 1975) For isometric contractions, the relationship between voluntary force levels and rectified EMG has been found to be well modelled by a linear, second-order transfer function (e g Genadry *et al* , 1988)

CO-CONTRACTION

In order to provide force in flexion and extension, muscles have an agonist - antagonist orientation, contraction of one muscle group will oppose contraction of a muscle group on the opposite side of the joint (Smith, 1981) The dynamics of a joint will therefore depend upon the level of contraction of agonist and antagonist muscles When the opposing muscle groups co-contract, the mean torque developed at the ankle will be the vector sum of the two torques, and therefore will be diminished Stiffness, however, increases with force under static conditions, and adds in parallel on opposite sides of a joint, so the overall stiffness of the joint will increase during co-contraction This has important ramifications in this experiment If during the course of the increase of contraction of the calf muscles there is co-contraction of tibialis anterior, then the observed dynamics will reflect this change

INTERACTION OF CONTRACTILE MECHANICS AND ACTIVATION DYNAMICS

In order to effect limb motion, or to compensate for load disturbances, changes in firing rate and recruitment of motoneurons are regulated by the motor control system to provide appropriate muscular forces The behaviour of the muscles of a joint will be determined by the joint's position, as well as the direction and rate of change of position because muscle has length-tension and force-velocity relationships that change with the firing rate and recruitment pattern (Brooks, 1986). During the development of the motion or regulating force, the mechanical characteristics of the muscle will change This is illustrated in Figure 2.5 for different levels of stimulation of cat soleus muscle Thus, the dynamics of a joint will depend upon the motion or load compensation being performed

2.1.2. PERIPHERAL CONTROL DYNAMICS

The peripheral nervous system utilizes feedback signals of joint position and its derivatives as well as muscle force to control the dynamic response of a joint to external disturbances. Each mechanism of this system has its own receptor and neural pathway as shown in Figure 2 8.

MUSCLE SPIN

Joint pos d its derivatives are sensed via spindle receptors They are small, spindle-shaped capsules situated parallel to the muscle fibres, attached at both ends to the muscle, they therefore experience the same changes in length as the muscle Inside the spindle are intrafusal muscle fibres, differentiated into bag and chain fibres according

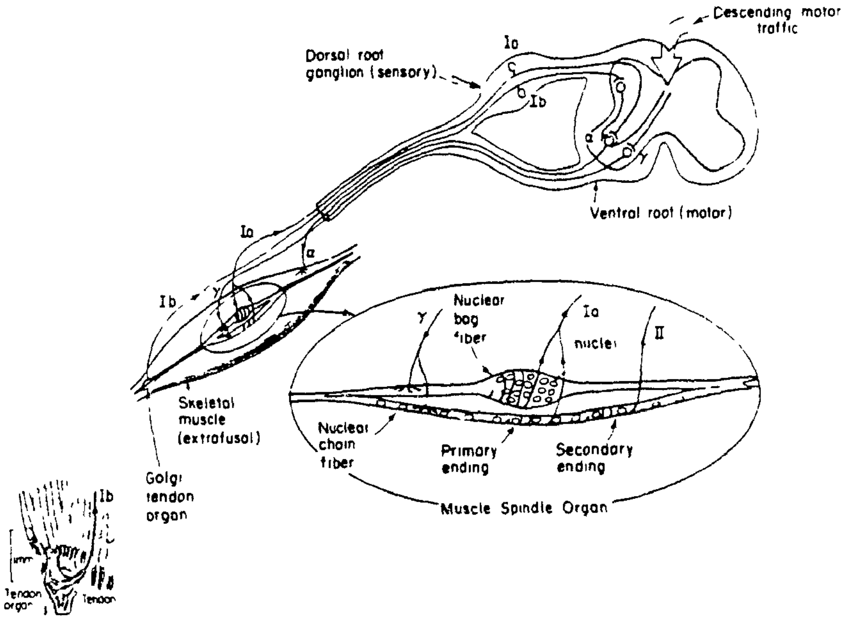

Figure 2 8 The anatomy of the reflex system (from McMahon, 1984) to the arrangement of their nuclei Nuclear bag fibres, the longer and larger of the two, have closely packed nuclei grouped near the centre of the fibre Nuclear chain fibres are half the diameter and length of the bag fibres, and have a single row of nuclei The fibres are oriented parallel to each other, with the ends of the nuclear chain fibres attached to the bag fibre Typically, spindles have a length of 2 to 3 mm, are about 0 15 mm in diameter, and contain two nuclear chain fibres and three to five nuclear bag fibres (McMahon, 1984)

Spindles receive both afferent and efferent innervation. The term afferent fibre is synonymous with sensory fibre, and therefore applies to neurons which carry information from the spindle to the spinal cord There are two types of afferent fibres primary and secondary Primary fibres have large group Ia myelinated axons which, after losing their myelin sheath, coil around the intrafusal fibres Secondary endings are comprised of smaller group II fibres which terminate mainly on the chain fibres Elongation of the spindle is thought to result in distortion of the endings of the fibres, generating action potentials (Houk and Henneman, 1974)

Linear system identification techniques have been applied to determine the dynamic response of the primary and secondary endings to position inputs (Jansen and Matthews, 1962, Alnaes, 1967, Matthews and Stein, 1969, Poppele and Bowman, 1970) These studies have found that the responses are high-pass, having a corner frequency at approximately 1 Hz, but that spindle primary afferents are more sensitive to small displacements, and have a smaller linear range of amplitude than secondary fibres Primary afferents also exhibit acceleration sensitivity at high frequencies, whereas secondary afferents do not.

Intrafusal fibres are innervated by γ-motoneurons, as opposed to the larger α-motoneurons which supply extrafusal muscle fibres These cause contraction of the intrafusal fibres, and may have the purpose of adjusting the stiffness of the intrafusal fibres, which in effect would alter the sensitivity of the spindle endings to displacements When γ-motoneurons are stimulated electrically, two different effects are observed, related to their influence on the sensitivity of the spindle to ramp displacements Stimulation of dynamic γ-motoneurons increases the response of the primary afferents to the velocity component of ramp stretches Static γ-motoneurons increase the response of primary and secondary spindle afferents at a constant length (Crowe and Matthews, 1964)

GOLGI TENDON ORGANS

Located in tendons are small capsules, called Golgi tendon organs, which transduce muscle force A large Ib afferent fibre terminating in many small branches within the capsule senses distortions in the capsule due to stretching of the tendon, caused by forces exerted by the muscle fibres to which it attaches Tendon organs attach to relatively few muscle fibres, and are therefore extremely sensitive to active contraction of muscle, but relatively insensitive to passive forces on the muscle, which are divided throughout the numerous fibres comprising the whole muscle

The response of tendon organs to sinusoidal stretch has been observed *in situ* (Alnaes, 1967, Houk and Simon, 1967, Rosenthal *et al* , 1970, and Anderson, 1974) and in isolated preparations (Wilkinson and Fukami, 1983) The majority of these studies have found the dynamic response of Golgi tendon organs to have high-pass characteristics with corner frequency at approximately 1 Hz

PERIPHERAL REFLEX EFFECTS

Signals from spindle afferents have an excitatory effect on motoneurons belonging to the same muscle Spindle primary afferents are the only receptor to have a monosynaptic connection with α-motoneurons The majority of primary afferents synapse with motoneurons of the same muscle, fewer have monosynaptic pathways to synergist muscles Secondary spindle afferents have fewer monosynaptic connections than primary afferents, and have less of a depolarizing effect on the motoneuron (30 μV compared to 65 μV, Stein, 1980) Both primary and secondary afferents have inhibitory influences on antagonist muscles via interneurons, therefore they cause reciprocal inhibition, i e , they excite synergistic contraction while inhibiting antagonistic contraction

Signals from the Ib afferents of Golgi tendon organs have an excitatory effect on small interneurons in the spinal grey matter These interneurons have an inhibitory connection with α-motoneurons of the same muscle Thus there is negative feedback of the muscular force signal As mentioned previously, Golgi tendon organs are very sensitive to small increases in force generated by small numbers of muscle fibres, therefore they may play an important role in regulation of muscle force at all levels of contraction

A block diagram of the peripheral control system is presented in Figure 2 9. A central command signal to generate muscular force is transmitted to the motoneuron pool, whereas by the size principle, the smallest motor units are recruited first In the soma of the α-motoneuron there is an integration of the collective influences of the central command signal, excitatory signals from the spindle primary afferents, inhibitory signals from the golgi tendon organs of the motor unit as well as influences from more complex polysynaptic pathways If the sum total of the signals exceeds the motoneuron's threshold, an efferent signal is transmitted, causing the muscle fibres in the motor unit to contract (Houk and Henneman, 1967)

The contributions of the various neural pathways to the excitement or inhibition of the α-motoneurons is influenced by the central nervous system via pathways from higher centres which synapse directly on α-motoneurons, γ-motoneurons, or interneurons in reflex loops There are a number of centres which have descending projections onto α-motoneurons in the spinal column It is postulated that they control voluntary actions, but may also be involved in altering the sensitivity of the motoneuron to reflex signals (Baldissera *et al* , 1981) Granit and Kaada (1952) found that stimulation of many areas of the reticular

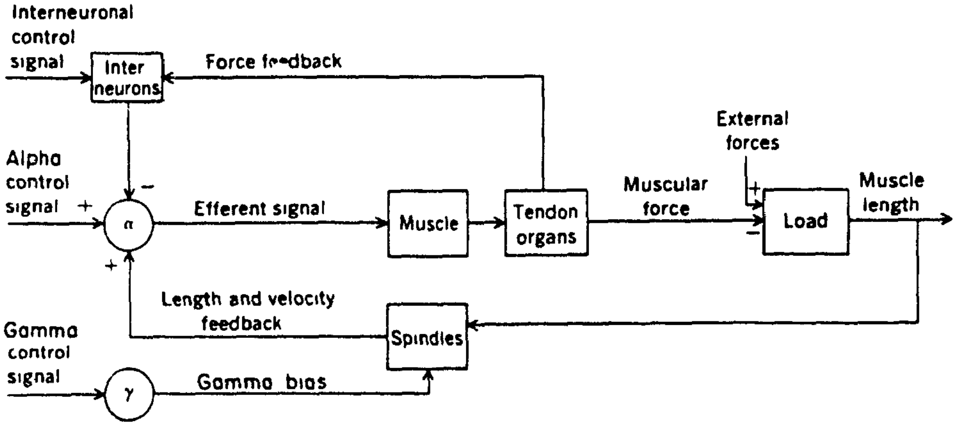

Figure 2 9 Block diagram representation of the peripheral control system (from Brooks, 1986) formation in the brainstem of cats activated γ-motoneurons, providing evidence that sensitivity of spindles is determined supraspinally Stein and colleagues have observed the magnitude of spindle-mediated responses to be modulated considerably during different phases of locomotion (Akazawa *et al*, 1982, Capaday and Stein, 1986) These researchers have proposed that the modulation is due to γ-motoneuron drive or changes in the state of spinal interneurons, leading to alterations of the gain of the position feedback loop

Central control of the effect of signals from Golgi tendon organs via interneurons has been observed by many groups (e g , Eccles and Lundberg, 1959, Hongo *et al*, 1969, Houk *et al*, 1970, Rymer and Hasan, 1979) There are monosynaptic connections from the brainstem to γ-motoneurons which have been proposed to be closely linked to the actions of the same regions on α-motoneurons (Grillner *et al*, 1969) These factors make it apparent that peripheral reflex pathways are under direct control of the central nervous system, via direct projections of descending pathways to α-motoneurons, spinal interneurons, and γ-motoneurons

INFLUENCE ON JOINT DYNAMICS

The dynamics of a joint may therefore strongly depend on the strength of the peripheral feedback signals received by the α-motoneurons controlling the joint's muscles, however this remains to be seen It is possible that joint stiffness may increase when the signals from the position feedback pathways become stronger, and joint stiffness may decrease when signals from the force sensing pathway increase in strength

The strength of these signals depends upon the potency of the stimulus received by the receptors, and can also be adjusted through the influence of higher centres Thus peripheral control mechanisms may potentially be important contributors to the changes in joint dynamics that may occur during changes in muscular contraction

2.1.3. ARTICULAR MECHANICS

The structures associated with the articulation, namely viscoelastic properties of the joint surface, ligaments and other connective tissue will contribute to the overall joint dynamics However, in the middle of the joint's range of motion, these effects are small in comparison to the other contributors, but are more important near the limits of the range (Gottlieb and Agarwal, 1978, Weiss *et al* , 1986a)

2.1.4. LIMB DYNAMICS

The limb can be considered to be a rigid body rotating about the joint, and can therefore be modelled as a pure rotational inertia It should be noted, however, that the rotation of the limb about the joint is unlike the classical revolute joint of mechanics, there is usually sliding of the joint surfaces, causing the centre of rotation to vary with joint position (e g Sammarco *et al* , 1973)

2.1.5. JOINT KINEMATICS

The length of a muscle at a given joint position is governed by the kinematics of the joint, i e , the insertion and origin points of the muscle and the geometry of the articulation In addition, the contribution of the tendon to overall muscle length must be considered Muscle and tendon are connected in series, so that length changes between origin and insertion are the result of the cascade of muscle and tendon stiffness properties This interaction is complex, tendon has a nonlinear stress-strain relation (Rack and Westbury, 1984, Proske and Morgan, 1987) and the mechanical properties of muscle are nonlinear and time-varying (Hunter and Kearney,1987)

2.1.6. ACTUATOR AND FIXATION DYNAMICS

In experiments investigating joint dynamics using system identification techniques, the joint is perturbed in a controlled fashion, and the subsequent response of the joint recorded Typically, the mechanical actuating device used to impart the perturbations will have dynamics which will determine the character of the perturbations For system identification purposes, the perturbation must contain power over the bandwidth of the system being investigated Skeletal muscle has dynamics that are low-pass, with a corner frequency in the neighborhood of 2 Hz (Stein, 1974, Baratta and Solomonow, 1990), however ankle joint stiffness is high-pass with a corner frequency as high as 25 Hz (Hunter and Kearney, 1982) Thus ankle dynamics will have significant components to rather high frequencies In order to resolve the important features of the stiffness responses (i e , the corner frequency) from the effects of background noise, an actuator for identification of ankle dynamics should provide a position signal with power resolvable from background noise for frequencies up to at least 50 Hz

To impart perturbations to the joint, one of its segments must be attached to the actuator. The ideal fixation device would have infinite stiffness, zero inertia, and provide a secure attachment between the actuator and limb However, in reality no fixation device has these properties, and its effects on the observed dynamics must be considered Finite stiffness and non-zero inertia of the fixation will introduce additional dynamic effects to the observed joint dynamics

In order to avoid corruption of the results by the dynamics of the actuator and fixation, their effects are generally removed from the output data prior to analysis by subtraction of their contribution to the observed output (Doeblin, 1983) The effects of relative motion between the limb and actuator are less quantifiable, therefore fixation devices should be designed to provide as uncompromising a hold as possible

2.2. ANATOMY

The gross skeletal and muscular structure of the ankle joint are shown in Figure 2 10. The ankle joint connects three bones the tibia, the fibula, and the talus This study is concerned with movements of the ankle in flexion-extension (i e , in the saggital plane) There are two muscle groups responsible for these movements The gastrocnemius and soleus muscles comprise the triceps-soleus group (TS) which causes plantarflexion (rotation of foot away from the head), and the tibialis anterior (TA) causes dorsiflexion (rotation of foot upward) By convention, all recorded variables (position, torque, EMG) associated with dorsiflexion are positive, while those associated with plantarflexion are negative

2.3. VARIATION OF JOINT DYNAMICS WITH MEAN JOINT TORQUE

Joint dynamics are known to be influenced by a number of factors, including mean joint torque (Agarwal and Gottlieb, 1977, Hunter and Kearney, 1982), joint position (Gottlieb and Agarwal, 1978, Weiss *et al.*, 1986a, b), and amplitude of perturbation (Kearney and

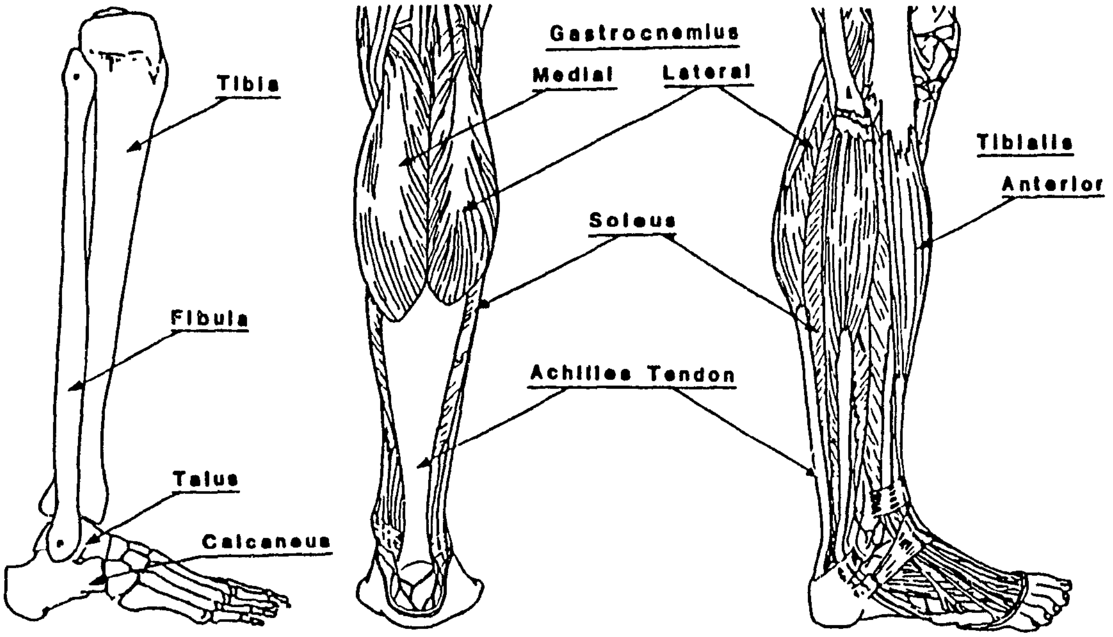

Figure 2.10. Major skeletal and muscular anatomical features of the lower limb.

Hunter, 1982) This study is concerned with the changes in joint dynamics that occur while the level of mean joint torque increases due to voluntary contraction The perturbations used in this study were small, centred about a constant mean position, and of uniform amplitude probability distribution Therefore, the effects related to changes of mean position and perturbation amplitude were likely small in this experiment, so that any changes in dynamics were related to the increase of mean joint torque

Numerous studies have observed changes in joint dynamics with changes in the level of muscular contraction Transient perturbations of either torque or position have been imparted to joints to measure their elastic and viscous parameters at different levels of muscular contraction Allum (1975) used ramp torque disturbances having 100 ms duration to investigate the stretch reflex response of human shoulder muscles The static stiffness of the joint was estimated by calculating the slope of the force response at maximum arm displacement (with inertial effects removed) versus the size of the disturbance The viscous parameter was also estimated as the slope of the force response in its first constant velocity phase (where the response was assumed to be due to passive muscle properties) The static stiffness was found to increase linearly with muscle force, while the viscous parameter varied nonlinearly

Akazawa and colleagues (1983) performed similar experiments on the human thumb, applying transient torque stimuli, and measuring the subsequent change in thumb position for three different kinds of voluntary contraction: force control, position control, and position control of an unstable load Different amplitudes of stretch were applied for various discrete levels of voluntary contraction Thumb stiffness was found to linearly increase with level of contraction

Direct measurement of the dynamics in terms of frequency response has also been accomplished. Agarwal and Gottlieb (1977a, b) investigated ankle joint compliance at different levels of voluntary contraction of the muscles associated with the ankle using sinusoidal (1977a) and stochastic (1977b) torque inputs In both studies joint compliance was found to behave as a second order underdamped system having different static stiffness and viscous parameters (or equivalently, gain and natural frequency) at the different levels of contraction They found the elastic and viscous parameters to increase linearly with muscular activation in the stochastic input study, and in the sinusoidal input study found resonant frequency and gain to increase monotonically Similar results for stochastic perturbations have been reported for the forearm (Cannon and Zahalak, 1982) and ankle joint (Hunter and Kearney, 1982; Weiss *et al* , 1988), and for sinusoidal perturbations of the thumb (Brown *et al* , 1982) and ankle (Evans *et al* , 1983)

All these studies have taken a quasi-time-invariant approach to obtain piece-wise stationary representations of joint stiffness at distinct levels of muscular activity Unfortunately, these models provide no insight to the time course of stiffness changes as the level of muscular contraction changes This is an important consideration for studies of joint dynamics which endeavor to characterize neuromuscular control of movement or other functional activity Levels of muscular contraction change considerably and rapidly during many functional actions, identification of the subsequent changes in joint dynamics may provide a greater understanding of the underlying neural control mechanisms Therefore, it is essential that an analysis method capable of tracking rapid changes in joint dynamics be employed

One possible means of determining the changes of dynamics is to employ a time-varying system identification approach In the next section, an overview of the different methods of time-varying system identification is given

2.4. TIME-VARYING IDENTIFICATION

How joint dynamics vary throughout a continuous change of muscular contraction is unknown The dynamics may change significantly over short periods of time in a complex manner Any method suitable for studies of joint dynamics must be capable of tracking rapid changes in dynamics without *a priori* assumptions regarding the form the dynamics may take (e g , the form and order of an analytical model) or the manner in which the dynamics change with time With these criteria established, the different methods available for time-varying identification will be evaluated in terms of their applicability to the study of joint dynamics

Methods for identification of time-varying systems can be divided into four main classes (Marmarelis, 1987a)

2.4.1. QUASI-TIME-INVARIANT METHODS

These methods apply time-invariant identification techniques over finite record segments under the assumption that the system's dynamics do not change substantially in this period Many researchers have employed this approach, for example, Hunter and Kearney (1982) and Weiss *et al* (1988), who used it to characterize ankle joint dynamics for a range of constant levels of muscular activation. These methods provide representations of the system at discrete operating points, thus they cannot identify a system whose operating point changes significantly in a period of time comparable to the duration of the system's impulse response function (up to 200 ms in the case of ankle compliance impulse response functions (e g , Weiss *et al* , 1986a))

2.4.2. ADAPTIVE METHODS

Adaptive methods use recursive algorithms to minimize the output error of a parametric system model whose parameters change with time (Kalman, 1960, Mayne, 1963, Ljung and Sòderstrom,1983, Lai and Wei,1986, Moser and Graupe,1989a) These methods have been used extensively in process control and target tracking applications, and have been used in neuromuscular research, for example, to develop myoelectric prosthetic controllers (Moser and Graupe, 1989b) However, adaptive methods are inappropriate for identification of systems whose structure cannot be assumed *a priori*, severely limiting the method's applicability for identification of systems having unknown structure For example, the method proposed by Moser and Graupe (1989a) to identify the time-varying coefficients of an ARMA (autoregressive, moving average) model through the use of Kalman filtering requires the order of the model to be selected prior to identification Another scheme presented by Chen and Guo (1989) requires only the upper bound of the model be specified, but the model is still restricted to be of one particular form

2.4.3. TEMPORAL EXPANSION METHODS

Temporal expansion methods describe the time-varying characteristics of a system by a series expansion whose coefficients are treated as additional parameters to be estimated (Hall *et al* ,1977, Marmarelis,1981 and 1987b, Grenier, 1983, Sharman and Friedlander, 1984) The various implementations of this method can only be successfully applied if the system's time-variations are known in advance, or are periodic, or almost periodic (Gardner, 1983), thus rendering them incapable of identifying systems whose changes with respect to time are unknown

2.4.4. ENSEMBLE METHODS

Ensemble methods evaluate time-varying system behaviour from ensembles of responses, each of which exhibits the same time-varying behaviour In general, ensemble methods use standard time-invariant system identification techniques, but the data used for input and output are chosen across the ensemble of responses at the same point in the time-varying behaviour, rather than over the time course of a single response These methods have the advantage of not requiring *a priori* knowledge of the system's behaviour or its form of time-variation, and can be used where the changes in dynamics are of the same time scale as the dynamics themselves

2.4.5. DISCUSSION

The quasi-time-invariant, adaptive and temporal expansion methods are widely applied in situations where only a single sample path of data is available However, they can only be used successfully in situations where the variation of the system's dynamics with time is slow, periodic, or of a known form Consequently, these methods are not appropriate for the study of the neuromuscular system, whose dynamics are not only unknown, but can also undergo rapid unpredictable changes

The most promising of the four techniques for studies of joint dynamics is therefore the ensemble method Nevertheless, it has not been used extensively, most likely because general purpose algorithms for this approach have not yet been formulated, and due to difficulties associated with acquiring, storing, and analysing multiple repetitions of an experiment Many system identification experiments can be designed to record numerous input - output realizations of the system in question under statistically similar conditions Consequently this method has potential for identification of time-varying systems encountered in a broad spectrum of applications, one in particular is the study of the neuromuscular system

Lawrence and Dawson (1977) first used a correlation-based ensemble method to identify the time-varying dynamics of a rotating naval antenna A similar method was subsequently used by Soechting and co-workers to evaluate the time-varying myotactic response (Soechting *et al* , 1981) and dynamic compliance (Lacquaniti *et al* , 1982) of the human elbow Both methods are limited in their applicability because of the assumptions necessary for proper application of correlation functions to identify time-varying systems

First, the method requires that strict timing exist between input and output, to ensure that the occurrence of the system's time variation is shifted by one sampling interval with respect to the input for successive realizations If this is possible the input - output temporal characteristics at any time across the ensemble and along a given realization will be the same This essentially freezes time by enabling the input - output crosscorrelation function to be calculated across the ensemble at a particular instant Crosscorrelation will only provide an accurate estimate of the impulse response function of the system at the instant in time if two conditions are met The input must be a repetitive pseudorandom binary sequence shifted by one sample for consecutive realizations, and the time-varying impulse response must be periodic with a period one sample increment greater than the duration of one repetition of the input sequence

There are many situations where secure timing between input and output cannot be ensured, and non-stereotypical time-variations are commonplace in many experiments In these cases, if the realizations are arranged in ensemble form according to the temporal requirements of the correlation-based technique, there will not be the same time-varying behaviour across the ensemble This will result in inaccurate estimates of the dynamics because the timing of the variations between repetitions will not be consistent For example, aperiodic variations will occur in experiments requiring voluntary actions of a subject, because jitter will be introduced by randomness of the subject's reaction time Also, some of the time-variations will not have the required trajectory In these cases, it is desirable to be able to remove atypical time-variations, and to align the realizations so that the time-variation occurs over the same interval with respect to the ensemble The inflexible structure imposed by correlation-based methods does not allow these operations to be performed, thereby rendering them inapplicable to experiments where the above-mentioned situations arise (Hunter and Kearney, 1986)

Second, a white input spectrum is necessary for correlation functions to provide accurate estimates of the dynamics In practical conditions, this is not always possible An actuator used to impart perturbations to the system will have limited bandwidth over which its input can be considered white For example, the hydraulic actuator used in this study has a flat position frequency response to 20 Hz, followed by a third- or higher-order attenuation of frequencies above 20 Hz Non-white input will have a non-impulsive autocorrelation, so that the contribution of the input will be convolved with the dynamics estimated by correlation methods (Eykhoff, 1974)

Third, the correlation-based method is founded on the assumption that the system being identified is linear This is certainly not the case for many systems, especially those encountered in physiology (Marmarelis and Marmarelis, 1978) It is essential that a tool for analysis of physiological systems be able to identify nonlinear systems, unfortunately, correlation-based methods cannot do so

2.4.6. APPLICATION TO JOINT DYNAMICS

There have been three previous studies of time-varying joint dynamics which have employed ensemble methods Two have been performed by Soechting and associates, the one most relevant to this thesis is the one conducted by Laquaniti *et al.* (1982), in which the compliance of the elbow was identified during a change in contraction level of the muscles of the upper arm In addition to having questionable results due to the use of the correlation method, this study suffered from the use of a linear second-order parametric model to characterize the compliance dynamics, thereby ignoring the possibility of other dynamic behaviour This caused unreliable estimates of the dynamics during the time-variation, where the dynamics were of the greatest interest

A new approach to ensemble identification has been developed which employs singular value decomposition (SVD) of a matrix equation relating input and output via convolution to provide models of time-varying systems (Kearney and Hunter, 1987) The SVD-based method does not restrict the input to be of a specific structure, thus it avoids the problems of the correlation-based scheme This study has used this method to identify the changes in ankle joint dynamics during an increase of muscular contraction The details of the method are presented in the next chapter.

The other study of time-varying joint dynamics to use an ensemble method (Bennett *et al.*, 1990) has employed SVD to identify the time-varying compliance of the human elbow during a voluntary movement However, the same difficulty encountered by Laquaniti *et al.* (1982) arises in this study, because a linear second-order ARMA model was used to represent the time-varying dynamics in terms of the changes of the three parameters of the model

In the present study, the SVD method has been formulated to provide nonparametric models of time-varying joint dynamics Thus, this version of the SVD method has the advantage of not requiring *a priori* assumptions regarding the form the dynamics may have. The use of this method may therefore allow more faithful representation of joint dynamics under time-varying conditions Thus it has the potential to be a powerful tool for studying the neuromuscular system during functional activity

3. THEORY

This chapter describes the theory and implementation of a new method for identification of time-varying systems This method uses an ensemble identification approach, and therefore requires the collection of a number of input - output realizations, each realization representing the system's response as it undergoes an identical time-variation Singular value decomposition (SVD) is used to find a series of nonparametric models of a system's dynamics at discrete instances throughout the system's time-variation

3.1. DERIVATION OF THE SVD METHOD FOR ENSEMBLE IDENTIFICATION

The following derivation is for linear time-varying systems It should be noted that this method can deal with nonlinear time-varying systems by replacing the linear convolution of equation (3 1) below by the more general Volterra functional series (Neilsen *et al.*, 1989) However, the nonlinear identification algorithm requires an enormous amount of data, and is extremely computationally intensive, therefore it was not employed in this investigation

The output y(t) of a linear, time-varying system can be represented by the convolution of a time dependent impulse response function (IRF, kernel, filter, or weighting function), h(t,τ) with an input x(t) (Bendat and Piersol, 1986)

$$y(t) = \int_{-\infty}^{\infty} h(t,\tau)\ x(t-\tau)d\tau \tag{3 1}$$

The ensemble method requires the collection of a number of input-output realizations, each realization representing the dynamics of the system as it undergoes a similar variation with time For a single realization in the ensemble, denoted as realization k, input and output are related by the convolution integral

$$y_k(t) = \int_{-\infty}^{\infty} h(t,\tau)\ x_k(t-\tau)d\tau \tag{3.2}$$

Under the assumption that the system's impulse response is finite and two-sided, equation (3.2) becomes

$$y_k(t) = \int_{-\tau_o}^{\tau_o} h(t,\tau)\ x_k(t-\tau)d\tau \qquad , \qquad (3\ 3)$$

where $h(t,\tau) \approx 0$ for $\tau > |\ \tau_o\ |$ For digital data with sampling interval Δt, equation (3 3) can be approximated by the discrete convolution sum (Hunter and Kearney, 1983)

$$y(i,k) = \Delta t \sum_{j=-n}^{n} h(i,j)\ x(i-j,k) \qquad , \qquad (3\ 4)$$

where i is the index of discrete time, and $n = \tau_o/\Delta t$

Therefore, the IRF will be $2n+1$ points long For convenience, let the length of the IRF be denoted by q If there are m realizations in the ensemble, there will be a system of m linear equations, each relating input and output for a particular trial in the ensemble

$$\begin{array}{c} y(i,1) = \Delta t\ [h(i,-n)\ x(i+n,1) + \ldots + h(i,n)\ x(i-n,1)] \\ \cdot \\ \cdot \\ \cdot \\ y(i,m) = \Delta t\ [h(i,-n)\ x(i+n,m) + \ldots + h(i,n)\ x(i-n,m)] \end{array} \qquad (3\ 5)$$

which may be expressed in matrix notation as

$$\mathbf{Y}_i = \Delta t\ \ \mathbf{X}_i\mathbf{H}_i \qquad , \qquad (3\ 6)$$

where

$\mathbf{Y}_i$ is a vector of length m with k^{th} element y(i,k),

$\mathbf{H}_i$ is a vector of length q with j^{th} element h(i,j),

and $\mathbf{X}_i$ is an $q \times m$ matrix with j,k^{th} element x(i-j,k)

Therefore, the IRF at cross-sectional time i ($\mathbf{H}_i$), may be found by solving (3 6), knowing the system input and output ($\mathbf{X}_i$ and $\mathbf{Y}_i$ respectively) Under ideal conditions, this can be accomplished by choosing the number of realizations (m) to be equal to the length of the IRF (q) **H**$_i$ could then be determined by standard methods (e.g , by Gaussian elimination (Strang, 1980)) In practice, however, noise will be introduced to the system's output, therefore it will be desirable to record more realizations than points in the IRF (m > q), so that the matrix **X**$_i$ will be overdetermined, and a unique solution of (3 6) will not exist

One solution of Equation (3.6) can be found by minimizing the squared error between the observed and predicted outputs

$$s^2 = \sum_{r=1}^{m} \left[y(i,r) - \Delta t \sum_{p=-n}^{n} x(i-p,r)\ \hat{h}(i,p) \right]^2 \quad , \tag{3.7}$$

where $\hat{h}(i,p)$ represents the coefficients of the IRF estimated for time i In matrix notation, for each time increment we wish to find the IRF estimate, $\hat{\mathbf{H}}_i$, which minimizes

$$\| \mathbf{Y}_i - \Delta t \mathbf{X}_i \hat{\mathbf{H}}_i \| \tag{3 8}$$

The vector minimizing (3 8) in the least-squares sense may be found by performing the singular value decomposition (SVD) (Strang, 1980) of **X**$_i$ Thus,

$$\mathbf{X}_i = \mathbf{U}_i \mathbf{D}_i \mathbf{V}_i^{T} \quad , \tag{3 9}$$

where

U$_i$ is an m × q column-orthogonal matrix corresponding to time i,

V$_i$ is a q × q column-orthogonal matrix corresponding to time i, and

D$_i$ is a q × q diagonal matrix of the singular values of **X**$_i$

These matrices are orthogonal in the sense that their columns are orthonormal, i.e ,

$$\mathbf{U}^{T}\mathbf{U} = \mathbf{I} \quad , \tag{3 10}$$

$$\mathbf{V}^{T}\mathbf{V} = \mathbf{I} \quad , \tag{3 11}$$

and, since **V** is square, it is also row-orthonormal, i e.,

$$\mathbf{V}\mathbf{V}^{T} = \mathbf{I} \tag{3 12}$$

Continuing with the derivation substitution of (3 9) into (3 8) gives

$$\| \mathbf{Y}_i - \Delta t \mathbf{U}_i \mathbf{D}_i \mathbf{V}_i^{T} \hat{\mathbf{H}}_i \| \tag{3 13}$$

This has a minimum value in the least-squares sense when

$$\mathbf{Y}_i = \Delta t \mathbf{U}_i \mathbf{D}_i \mathbf{V}_i^{T} \hat{\mathbf{H}}_{ls_i} \tag{3 14}$$

where the subscript ls denotes the least-squares solution Rearranging

$$\hat{\mathbf{H}}_{ls_i} = \frac{1}{\Delta t} \left[\mathbf{U}_i \mathbf{D}_i \mathbf{V}_i^{T} \right]^{-1} \mathbf{Y}_i \tag{3 15}$$

The quantity $\left[\mathbf{U}_i \mathbf{D}_i \mathbf{V}_i^{T} \right]^{-1}$ is known as the pseudoinverse of the rectangular matrix $\mathbf{X}_i$, and is denoted $\mathbf{X}_i^{+}$ Therefore,

$$\mathbf{X}_i^{+} = \mathbf{V}_i \mathbf{D}_i^{+} \mathbf{U}_i^{T} \tag{3 16}$$

The matrix $\mathbf{D}_i^{+}$ is a diagonal matrix whose diagonal elements are assigned values according to the following

for i = j

$$d_{ij}^{+} = \frac{1}{d_{ij}} \quad \text{if} \quad d_{ij} \neq 0 \tag{3 17}$$

$$d_{ij}^{+} = 0 \quad \text{if} \quad d_{ij} = 0 \tag{3 18}$$

for i ≠ j

$$d_{ij}^{+} = 0 \tag{3 19}$$

Therefore, for a particular time i in the input - output ensemble, the least-squares approximation of the system's instantaneous impulse response function is

$$\hat{\mathbf{H}}_{ls_i} = \frac{1}{\Delta t} \mathbf{X}_i^{+} \mathbf{Y}_i \tag{3 20}$$

3.2. IMPLEMENTATION

An algorithm employing the theory of the SVD method has been implemented in the operator TVFIL in NEXUS, a language for signal and system analysis (Hunter and Kearney, 1984) This operator requires three channels of data the input and output data, constructed as concatenations of the individual input and output realizations, and a third channel consisting of the indices representing the times when the system's dynamics correspond to the same operating point in the time-variation for each realization The third channel provides the means to generate uniform input and output ensembles by aligning the individual realizations, as well as enabling the user to effectively eliminate unwanted trials from the original ensembles For a particular ensemble cross-sectional time, the analysis proceeds by generating the input matrix $\mathbf{X}_i$ and output vector $\mathbf{Y}_i$, with ensemble average removed to remove offset bias and linear trends The estimated IRF is then determined using the NAG singular value decomposition subroutine F04JGF (Numerical Algorithms Group Limited, 1988) The code for the implementation is provided in Appendix A

3.3. DISCUSSION

Ensemble methods can identify rapidly time-varying systems because they identify the dynamics in terms of the input - output response across an ensemble of realizations By performing the cross-ensemble identification over the time-span of the variation of the dynamics, a series of representations is obtained which describes the variation of the system's dynamics with time.

The SVD method is a very powerful tool for ensemble identification of time-varying systems It provides nonparametric models of the time-varying dynamics of a system, therefore it does not require assumptions regarding the form of the system's dynamics. Furthermore, the time-variation of the system can be of any form, and is not required to occur in regular intervals In addition, as mentioned at the onset of this chapter, the method can be formulated to identify nonlinear time-varying systems

Singular value decomposition of a matrix is always possible and is not affected by the matrix' singularity or overdetermination In the case of an overdetermined set of equations, the solution found via SVD will be the most accurate one in the least-squares sense (Press *et al.*, 1986) For least-squares applications, the only requirement imposed by SVD on the input matrix is that its rows be independent for best results (Eykhoff, 1974, Strang, 1980). The solution is not dependent upon the input sequence having a white frequency spectrum, thus the SVD method is not hindered by the dynamic limitations of actuators used to input test signals to the system being investigated

The SVD method offers a significant advantage over the correlation-based methods used by Lawrence and Dawson and Soechting and colleagues by virtue of its less strict input requirements The SVD method does not require an input ensemble having a special structure, therefore it enables alignment of the realizations with respect to a cross-ensemble reference point to reduce the effects of variability of the onset time of the time-variation By the same token, the SVD method allows the removal of trials which do not conform to the desired trajectory, thereby providing the facility for identification using an ensemble of records having as uniform a time-variation as desired Nevertheless the method is adversely affected if the variation between trials is large Thus, a considerable number of input - output realizations may be required by the SVD method to obtain accurate estimates from noisy data The effects of additive output noise on the performance of the SVD method were evaluated by applying it to identify the time-varying dynamics of a simulated system in the presence of different output signal to noise ratios The results of the simulation study are given in the next chapter

4. TIME-VARYING ANKLE DYNAMICS: SIMULATION STUDY

This chapter describes a simulation of human ankle joint dynamics undergoing a time-variation of the level of contraction of the calf muscles, and the subsequent identification of the time-varying dynamics through the use of the SVD method for various levels of additive output noise The results indicate the new method to be capable of tracking changes in system dynamics on a time-scale comparable to that expected in the physiological situation, and to be robust in the presence of the additive output noise

4.1. METHOD OF SIMULATION

The strategy used for the simulation is presented schematically in Figure 4 1 In this study, an experiment was simulated in which a stochastic torque signal was imparted to a hypothetical human ankle during repeated contractions of the calf muscles, induced by periodic neural activation The position output signal was generated by convolving the torque signal with a second-order low-pass filter whose parameters changed with time, representing the time-varying ankle compliance dynamics during the contraction The parameters of the filter varied as a function of the mean torque produced by the calf muscles, in agreement with the observations of previous studies using quasi-time-invariant methods The mean torque was considered to be the result of the convolution of the neural activation signal and a filter representing the activation dynamics of skeletal muscle

One technical note the simulation has been generated with joint dynamics described in the low-pass compliance formulation as opposed to the high-pass stiffness formulation used in the experimental study A low-pass system is much easier to simulate than a high-pass system because simulation of a high-pass second order system involves two numerical differentiations, which will lead to an artificial amplification of any noise present in the original input signal, thus corrupting the estimates of the dynamics

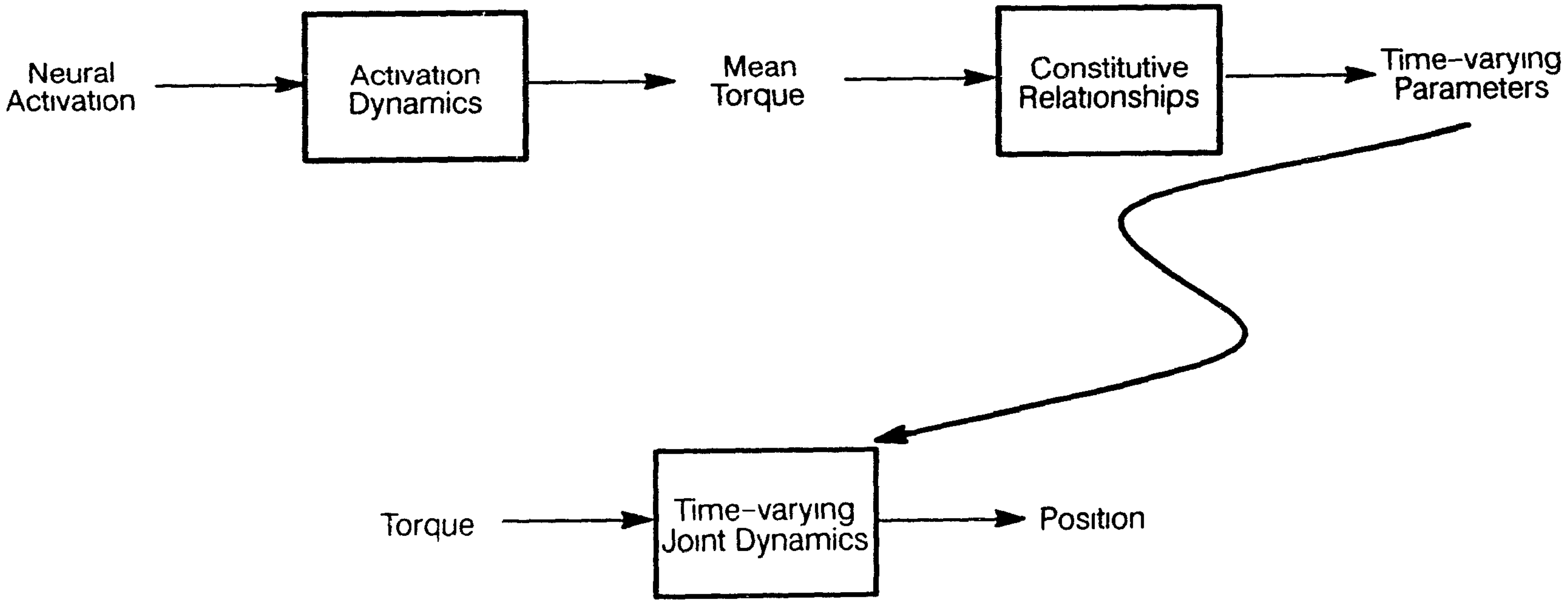

Figure 4 1 Schematic diagram of the strategy used to simulate time-varying ankle dynamics

4.1.1. JOINT DYNAMICS

Joint dynamics were modelled as a linear, second-order, time-varying system having the transfer function

$$\frac{\Theta(s)}{TQ(s)} = \frac{G(\alpha)\omega_n^2(\alpha)}{s^2 + 2\zeta(\alpha)\omega_n(\alpha)s + \omega_n^2(\alpha)} , \qquad (4\ 1)$$

where

$TQ(s)$ is a wide-sense stationary, controlled input torque signal,

$\Theta(s)$ is a nonstationary position output,

$G(\alpha)$ is the compliance gain,

$\zeta(\alpha)$ is the damping parameter,

the parameter $\omega_n(\alpha)$ is the natural frequency, and

the variable α represents the time over which the change in dynamics occurs

This model of time-varying joint dynamics is based on the results of previous investigations using quasi-time-invariant methods (Agarwal and Gottlieb, 1977a, b, Hunter and Kearney, 1982, Weiss *et al*, 1988) These studies have shown that joint dynamics are well modelled by a second-order dynamic system for constant levels of contraction. For the sake of simplicity, the piece-wise time-invariant results of the quasi-time-invariant studies have been assumed to be representative of the manner in which joint dynamics change during a continuous change in level of muscular contraction

The time-varying dynamics were simulated by varying the parameters G, ζ, and ω_n as a function of α The variation of these parameters was chosen to agree with the results of previous investigations of the human ankle (Hunter and Kearney, 1982; Weiss *et al.*, 1988) These studies revealed that at distinct levels of muscular contraction,compliance gain was proportional to the inverse of the resultant mean torque, and natural frequency varied in such a way as to maintain a constant damping parameter

The time-varying mean joint torque signal was a function of a square wave generated to simulate a series of periodic step increases of neural activation The square wave had a period of 2.00 s, and was modulated between 0 and 1 arbitrary units of activation. This neural activation signal was convolved with a filter with characteristics similar to the dynamic EMG – torque relationship of the human ankle observed by Genadry *et al.* (1988), i.e., a second-order low-pass filter with a corner frequency of 2 Hz, and a damping parameter of 0.4. The result of the convolution was the mean joint torque signal used to generate the time-varying parameters of equation (4.1). The resulting time variations of the parameters over one cycle of contraction are shown in Figure 4.2.

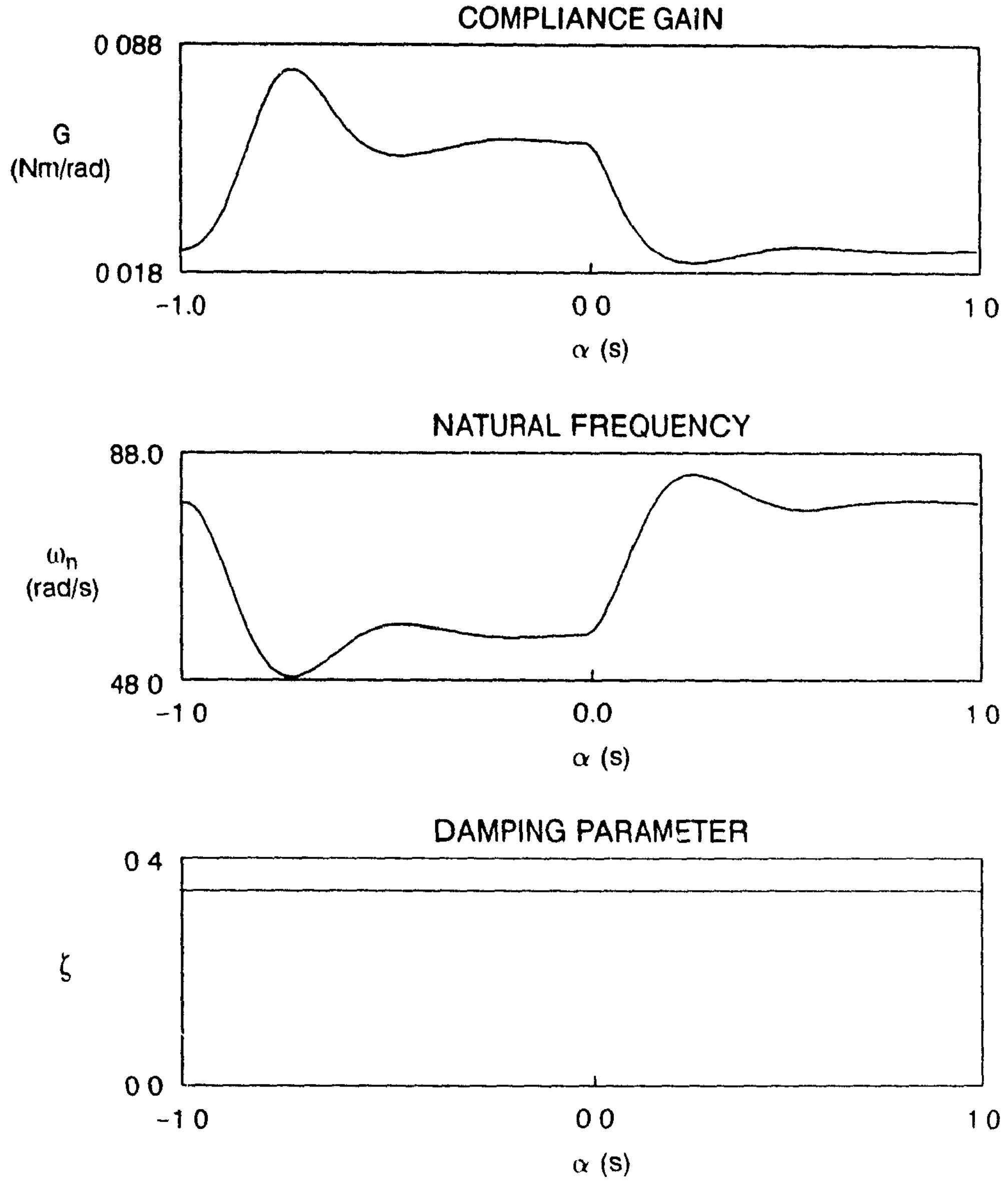

Figure 4.2 Variation of the parameters of the simulated time-varying system for a single contraction cycle. Independent variable α represents the ensemble time, $\alpha = 0.0$ is the time at which the step increase in neural activation occurred.

The torque input signal was a pseudo-random binary sequence (PRBS) having peak to peak amplitude of 10 0 Nm, zero mean, and 0 01 s sampling interval This sequence was composed of individual realizations having 2 00 s duration, each realization being independent of the others to ensure the nonsingularity of the input matrix, thus providing the best situation for the least-squares SVD algorithm to operate

The position signal was generated by the discrete convolution of the torque perturbation input with the time-varying convolution kernel representing ankle compliance

$$\theta(i) = \Delta t \sum_{j=0}^{n} h(i,j)\ tq(i-j) \quad , \qquad (4\ 2)$$

where the limits of summation are for a causal kernel because of the compliance formulation used in the simulation

The kernel h(i,j) was generated for each discrete time using the appropriate values of G, ζ, and ω_n The convolution of the input with the time-varying kernel resulted in a nonstationary output signal whose statistics were a function of α The input and output records for a single sample path are shown in Figure 4 3, for zero additive noise

4.1.2. EFFECT OF ADDITIVE OUTPUT NOISE

In practice, inherent noise in the recorded signals and variability between trials will corrupt the data The least-squares solution obtained by SVD will depend on the number of observations of the time-variations of the system, which will determine the degree of overdetermination of the system of equations to be solved The higher the degree of overdetermination is, the greater the possibility that the least-squares solution will be an accurate representation of the dynamics

To determine the robustness of the SVD algorithm in the presence of additive Gaussian, white, output noise, ensembles of input and output were generated for different output signal to noise ratios (S/N), ranging from infinite S/N (no additive noise) to a S/N of 1 (variance of additive noise equal to that of the output) For each data set, the dynamics were identified using different ratios of ensemble width to IRF length, i.e , the degree of overde-

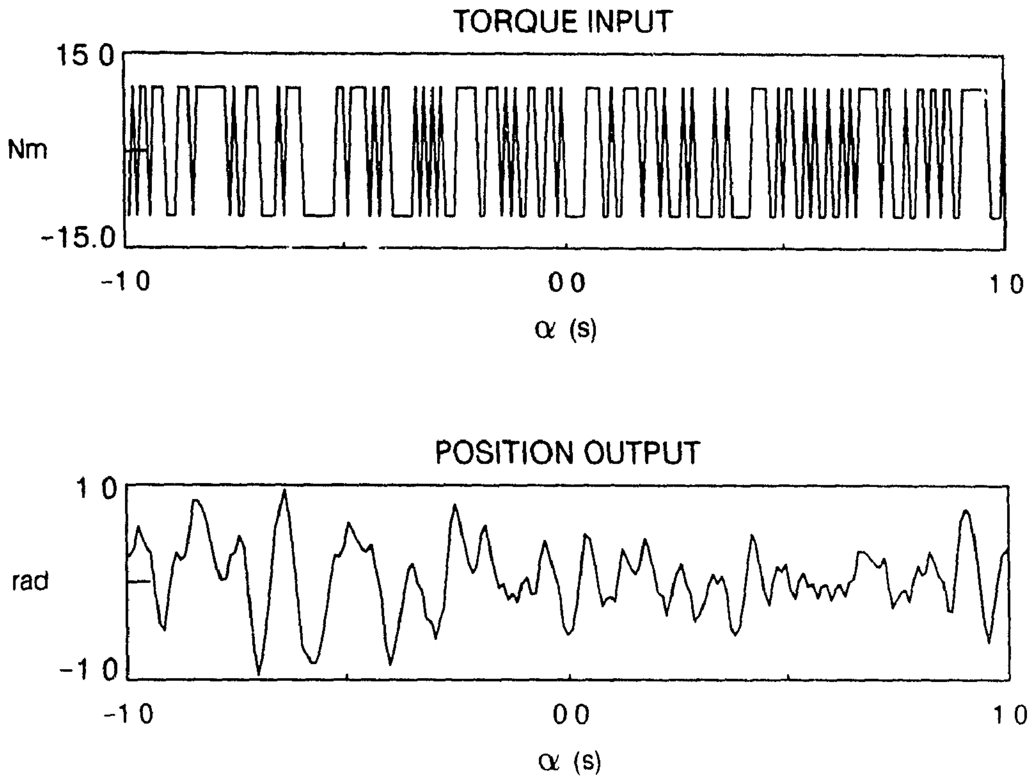

Figure 4 3 Simulated input and output records representing the time-variation of ankle joint dynamics for a single realization with no additive output noise.

termination of the system of equations (ρ) The IRF length was held constant at 50 points, i e , the IRFs had a support spanning 500 ms, which was sufficient for the response to die out to zero The number of trials in the ensemble ranged from 100 to 500, so that the degree of overdetermination of the system of equations varied from 2 to 10

4.2. RESULTS

For each simulated condition, the series of input-output realizations was arranged in ensemble form, with each realization aligned so that the step increase of neural activation occurred at the same time across the ensemble A series of impulse response functions representing the change in system dynamics was determined in 10 ms intervals over the period from 1 0 s before the step increase in neural activation to 1 0 s after Figure 4 4 shows IRF estimates obtained for a data set with infinite signal to noise ratio The variations of gain and natural frequency of the simulated joint with contraction level are reflected in the changes in the amplitude of the first peak and the lag of the first overshoot of the IRFs

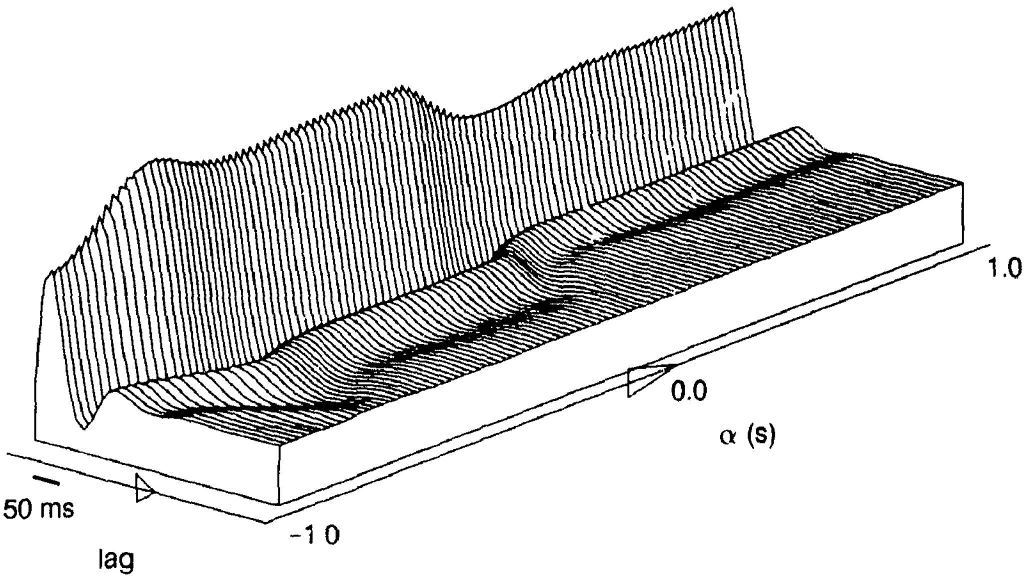

Figure 4 4 Series of compliance impulse response functions (IRF) estimated for simulated data with no additive noise Each IRF represents the dynamics of the simulated system at an instant in the time-course of its variation with time

The accuracy of the estimated IRFs was quantified in terms of the percentage of the variance of the actual system output predicted by convolving the system input with the series of estimated IRFs This quantity is called the variance accounted for (VAF) of the series of estimated IRFs, and is formulated as

$$\mathrm{VAF} = \left[1 - \frac{\sum_{i} (y_i - \hat{y}_i)^2}{\sum_{i} y_i^2} \right] \qquad (4\ 3)$$

where y is the actual system output caused by a given input signal, and $\hat{y}$ is the output predicted by the convolution of the input signal with the series of IRFs This measure does not reflect the accuracy of the individual IRFs, but it is still useful for evaluation of differences in accuracy between whole series of IRFs This issue will be addressed further in the discussion section of the next chapter Figure 4 5 shows the VAF as a function of signal to noise ratio (S/N) and degree of overdetermination (ρ) The accuracy of the estimates increased proportionally with signal to noise ratio and degree of overdetermination Accurate estimates were obtained in the presence of considerable additive output noise provided that the degree of overdetermination was suitably large For example, for a signal to noise ratio of 1, the method provided estimates having greater than 80% VAF for ρ greater than 5 5

4.3. DISCUSSION

Although the simulated system was chosen to have properties similar to those observed for the ankle join under quasi-time-invariant conditions (Hunter and Kearney, 1982, Weiss, *et al.*, 1988), this should not be interpreted as an accurate representation of the dynamics of the joint The simulation does not address the influence of factors such as the properties of the central command signal, reflex mediated effects, motor unit recruitment, or cross-bridge related effects, which have profound influence on joint dynamics It does, however, demonstrate the power and robustness of the analytical technique

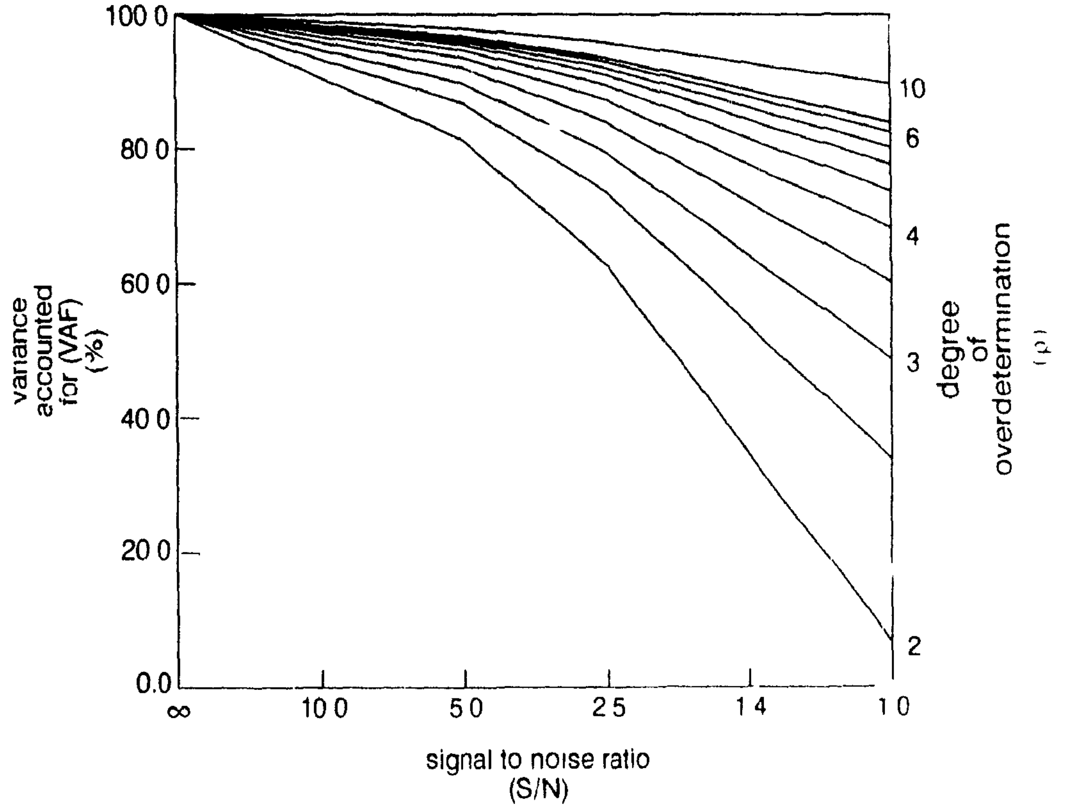

Figure 4 5 Variance accounted for (VAF) by the estimated impulse response functions as a function of degree of overdetermination (ρ), and output signal to noise ratio (S/N)

The simulation does not explicitly take the effects of inter-trial variability in the change of level of contraction's trajectory or onset time into account Because the SVD method affords the ability to remove nonuniform contractions from the ensemble and to align trials in the ensemble so that the change in level of contraction is uniform across the ensemble, it has been assumed that these two effects can be minimized by a preprocessing procedure prior to the analysis This preprocessing technique will be detailed in the next chapter Nevertheless, some degree of variability between trials will exist after the preprocessing, which will lead to decreased accuracy of the estimates As a first approximation, this simulation has been formulated under the assumption that the effect of onset time variability can be made negligible by alignment of the ensemble prior to analysis Therefore, in the simulation study, the factors most liable to introduce poor estimation quality will be poor signal to noise properties of the recorded signals, and variability between trials

The noise signal was created to be independent between trials, so that the probability distribution of the noise was similar across the ensemble and along a single realization Thus the additive output noise signal can be considered to represent the combined effects of cross-ensemble variation and the inherent signal to noise characteristics of the output signal The contribution of these two effects to the variability of the ensemble data will depend upon the system being investigated If, for example, the data recorded in an identification experiment has high signal to noise quality, then the largest source of variability in the ensemble will be across the ensemble, in terms of deviations of the individual realizations from an ideal trajectory On the other hand, it is conceivable that the system being identified may produce an output signal with poor signal to noise qualities, e g , an EMG signal (see the treatment on EMG in the background) In this situation, the inherent noise of the output signal may dominate the variability of the output

This simulation study has shown the SVD method to be a viable method for identification of systems whose dynamics change under conditions comparable to those encountered in joint dynamics In light of the success of the method's application to simulated data, it was used to analyze experimental data obtained under conditions similar to those used in the simulation study This work is presented in the next chapter

5. TIME-VARYING ANKLE DYNAMICS: EXPERIMENTAL RESULTS

This experiment was designed to investigate the changes in dynamics of the ankle during a rapid increase of contraction of the calf muscles,corresponding to a change in mean joint torque from 10% to 25% of the subject's maximal plantarflexion torque The human ankle was investigated in this study because it plays an important role in posture and locomotion, and may be representative of the dynamics of other joints under similar conditions Also, from a practical standpoint, the ankle is easily constrained to rotation in a single plane, and, being the most distal joint in the limb, it can be studied independently of other limb segments

In the experiment, subjects executed a large number of contractions of triceps-surae while the ankle was stochastically displaced about a mean position The SVD method was used to determine the dynamic stiffness of the ankle throughout the time-variation of contraction level The results, in terms of a series of stiffness impulse response functions representing ankle dynamics at 2 ms intervals, provide a nonparametric representation of the changes in joint dynamics that accompany a change in level of muscular activation They reveal that during the transition of contraction level, ankle dynamics deviate from the second-order dynamic behaviour reported by previous studies employing quasi-time-invariant approaches

5.1. APPARATUS

During the experiment, the subject and all the apparatus associated with input and recording of the experimental responses were located on an experimental table (Kearney *et al.*, 1983) Subjects lay supine on the table with their left foot attached to an electrohydraulic rotary actuator (Rotac Model RN-32-IV) by means of a custom-fitted fibreglass boot (Morier *et al.*, 1990) The subject was held in place by wide straps over the waist and left knee Ankle position was determined by the actuator, which was controlled via a servo valve (Moog Model 73-104) operating under position feedback control In this configuration, a position reference signal was generated digitally (DEC VAXStation II/GPX) and converted to analog form by a 12 bit D/A converter (DEC, model AAV11-A) Actuator position was transduced by a rotary potentiometer (Beckman Helipot, Model 6263-R5K-L 50) located on the axis of the actuator The signal from the potentiometer was used both to close the control loop, and to represent joint position This control system had a frequency response that was flat to 25 Hz, and was capable of applying suitable power for system identification purposes to greater than 50 Hz

The torque resulting from rotary displacements of the foot, its boot, and the actuator was recorded via a torque transducer (Lebow, Model 2110-5k, stiffness = 50 000 Nm/rad) located on the shaft of the actuator between the actuator and the foot fixation device

Disposable Ag-AgCl surface electrodes (Hewlett-Packard, Model 14445a), mounted in a bipolar configuration oriented parallel to the muscle fibre direction, were used to detect EMG activity from the soleus (TS) and tibialis anterior (TA) muscle groups of the left leg The bipolar signal was differentially amplified by custom-built preamplifiers incorporating an instrumentation amplifier (Burr-Brown, Model 3620, common mode rejection ratio of 100 dB at 100 Hz, 80 dB at 1000 Hz), variable gain and offset control, and current isolation switches (Ohmic Instruments Model IS-100) The resulting signals were high-pass filtered (corner frequency 10 Hz, 2-pole Butterworth filters (Frequency Devices, Model 772BT-2)), full wave rectified (TA EMG positive, TS EMG negative), and low-pass filtered (cutoff frequency 1 kHz, 4-pole Bessel filters (Datel Systems, Model FLT-LP4L5K))

The position, torque, TS EMG and TA EMG signals were anti-alias filtered at 100 Hz by 8-pole Bessel filters (Frequency Devices, Model 902 LPF) prior to sampling at 500 Hz by a 16 bit A/D converter having ± 10 V dynamic range (Data Translation, Model DT2757)

5.2. METHODS

5.2.1. MAXIMUM VOLUNTARY CONTRACTION

Dorsiflexion and plantarflexion maximum voluntary contraction (MVC) were recorded prior to the experimental trials With the ankle held in its rest position by the actuator, the subject was required to execute a maximal contraction in response to a step change in a tracking stimulus displayed on the oscilloscope A dorsiflexor MVC was executed for 5 s followed by a 5 s plantarflexor MVC after a period of 120 s The 5 s interval of maximal contraction was divided into five 1 s partitions, the largest torque averaged over a single partition was designated the maximum torque

5.2.2. POSITION PERTURBATION

A 2000 point pseudo-random binary sequence (PRBS) was repeatedly displayed at 500 Hz by the D/A converter This signal drove the actuator's servo valve, resulting in stochastic displacements having peak to peak amplitude of 0 05 rad about the ankle's rest position, with power suitable for system identification up to 50 Hz

5.2.3. PARADIGM

The paradigm was chosen because the task required of the subject was relatively simple and stereotyped, while at the same time representative of the rapid and significant changes in joint dynamics that occur during natural limb motion In order to initiate the desired time-varying behaviour, two signals were displayed on an oscilloscope (Kikusui, Model COS5020) mounted above the subject's head One was a square wave target signal calibrated to represent the torque required to elicit a change of plantarflexor contraction from 10% to 25% MVC The other was a low-pass filtered version of the signal from the torque transducer which provided visual feedback of the torque generated by the subject

While the ankle was stochastically perturbed by the actuator, the subject was trained to track the target signal by changing the level of TS contraction using the feedback signal as a guide After the subject became adept at this task, the sets of input - output trials were recorded Each set of trials consisted of 32 contractions occurring at approximately 4 s intervals (the contractions were not initiated at the same time with respect to the target signal due to variations in the subject's reaction time) Up to 28 sets were collected, with a five minute rest between sets In addition, the subject was allowed a longer rest near the midway point of the experiment, during which the restraining belts were released and the subject given the opportunity to sit up During this time the subject's foot remained in the fibreglass cast, attached to the actuator, so that the ankle's position relative to the actuator was not compromised The experiment was continued until the subject began to experience discomfort or slight fatigue Input an output records for a single realization from the data of one of the subjects are presented in Figure 5 1

5.2.4. SUBJECTS

Three healthy male subjects, denoted S1, S2, and S3, were studied They ranged in age from 23 to 43, and had no known abnormalities.

5.3. ANALYSIS

5.3.1. REMOVAL OF ACTUATOR AND BOOT DYNAMICS

The observed torque was not only due to dynamics associated with the ankle, but also the result of the dynamics of the actuator and the foot fixation device In order to determine the torque solely due to ankle dynamics, the other non-ankle influences were identified and removed in the following manner. After completion of the trials, the subject was released from the apparatus, and a calibration was performed to identify the dynamics of

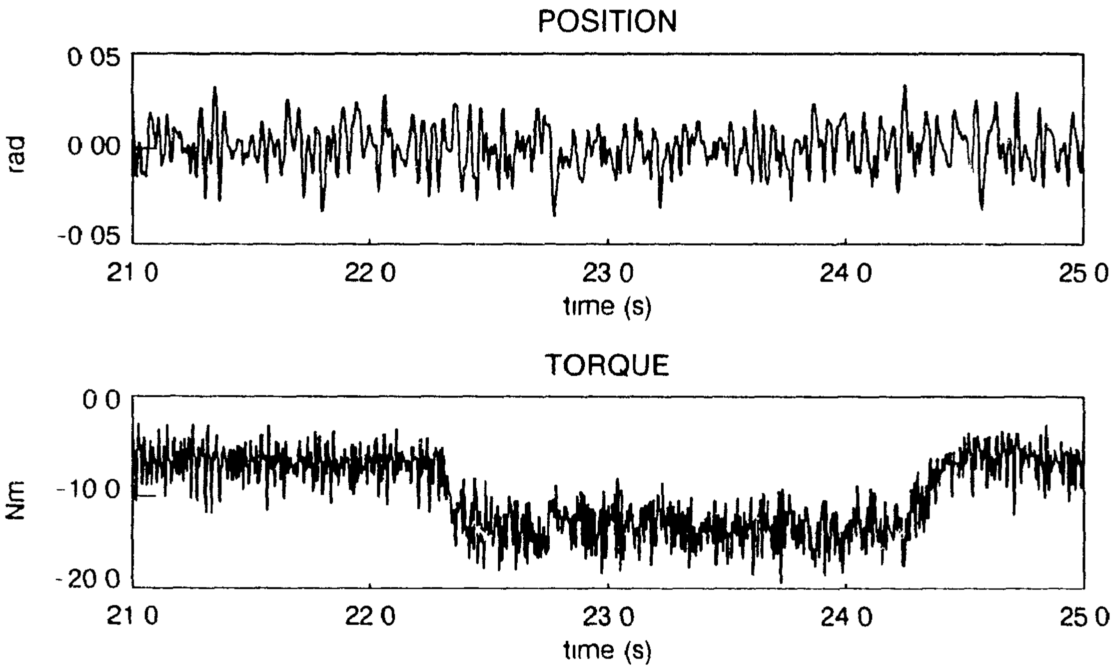

Figure 5 1 Position input and torque output records for a single realization from the ensemble of subject S2 the apparatus with the boot attached to the actuator A PRBS test signal of the same amplitude and frequency content as the experimental input was used to obtain an IRF representing these dynamics The position record obtained during the entire course of the trials was then convolved with this IRF, and the resulting estimate of the contribution of the apparatus was subtracted from the observed torque, resulting in a corrected torque signal, representing the contribution of the ankle alone In the following text, all references to torque are to this corrected torque

5.3.2. ALIGNMENT OF TRIALS

In order for proper application of the SVD method, it was necessary for each of the individual realizations in the ensembles of input and output to be the result of identical time-variations Therefore, the subject was required to execute the contractions exactly in the same manner for each experimental trial In practice, however, this was difficult to achieve for two reasons First, there was variation in the latency between the onset of the target signal and the initiation of the change in level of voluntary contraction Second, although most contractions demonstrated a stereotyped trajectory, there were occasional anomalous contractions Prior to the application of the identification procedure, these effects were minimized by processing the torque records in the following manner

1 The torque record was low-pass filtered (511 point FIR filter, Hamming window, 2 Hz cutoff) to remove the torque variations associated with the PRBS position input

2 A reference point was defined for each torque realization, indicating the time at which the level of torque was half-way between the two target levels The trials were aligned to this reference point which was assigned the cross-ensemble time $\alpha = 0 0$ s

3 The ensemble mean and standard deviation were determined with respect to the reference point

4 Individual trials whose trajectories lay outside one standard deviation of the ensemble mean were rejected

Figure 5 2 illustrates the results of the application of this procedure to data for one of the subjects Part A of the figure shows the unfiltered torque ensemble prior to processing The filtered, unaligned ensemble is presented in part B In part C, the ensemble has been aligned to the mid-way point between the two target levels of torque The final screened ensemble is presented in part D The unfiltered version of this ensemble was used in the identification

The results of the screening procedure are tabulated for the three subjects in Table 5 1 Note that in all cases, more than half the original number of trials were rejected by the screening procedure

Subject	Initial Number of Trials	Number of Trials After Screening Procedure
S1	960	337
S2	800	297
S3	800	258

Table 5 1 Change in number of trials in the ensemble as a result of the application of the screening procedure to the data for the three subjects

5.3.3. ESTIMATION OF TIME-VARYING DYNAMICS

For each subject, the SVD method was applied to the preprocessed ensemble data Two sided, 47 point linear impulse response functions representing joint stiffness were estimated for each sample interval in the time spanning ± 0 4 s relative to the midway point in the increase in torque Therefore, a series of 401 IRFs was obtained in which each individual IRF represented the dynamics at instances in time separated by 0 002 s The series of IRFs as a whole represented the time-variation of the dynamics of the ankle throughout the increase of muscular contraction

5.4. RESULTS

5.4.1. ENSEMBLE AVERAGE TORQUE

The range over which the dynamics were identified is indicated by the dotted lines in Figure 5 3, which presents the ensemble average torque for the three subjects over a

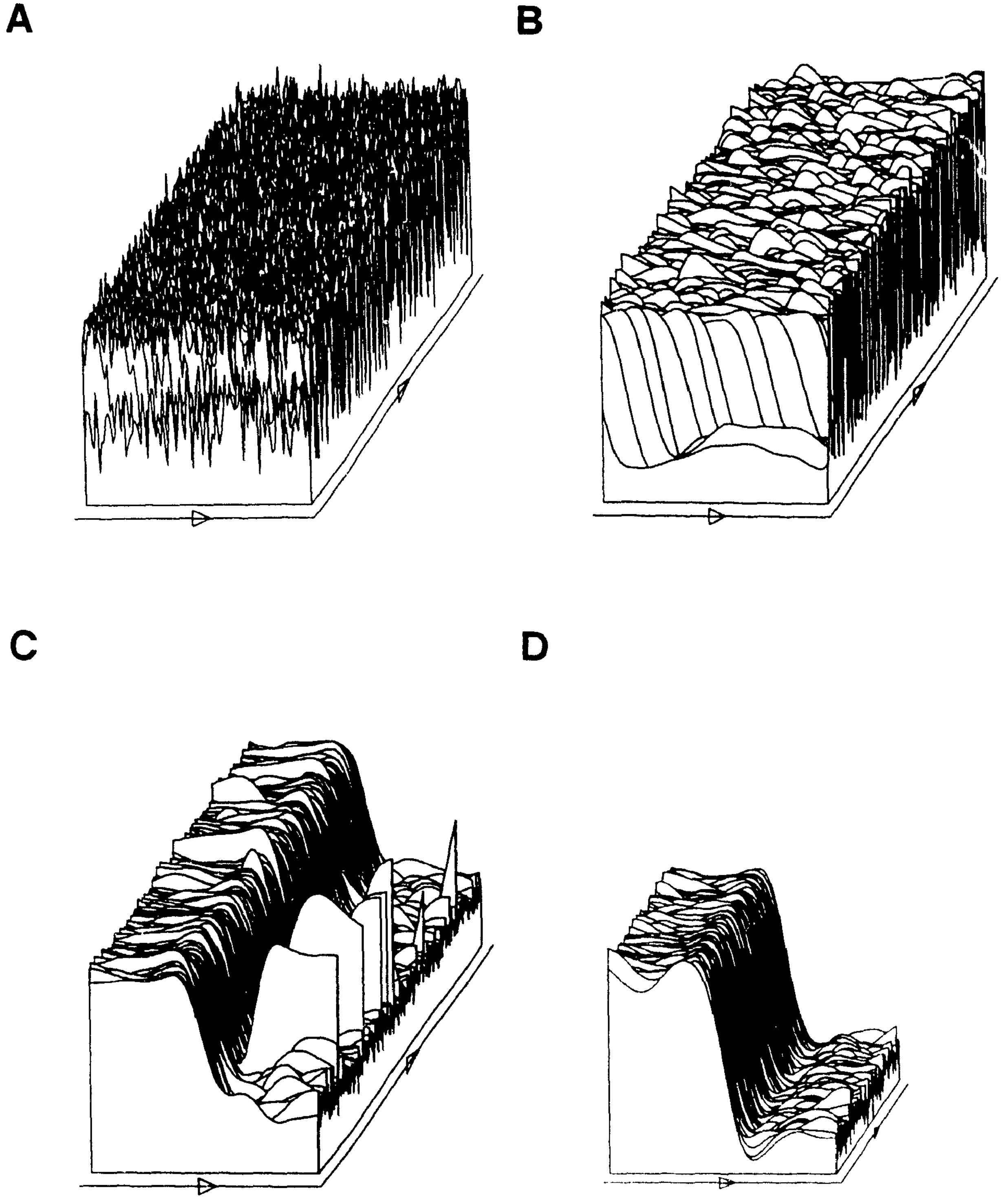

Figure 5 2 Stages of preprocessing for the torque ensemble of one of the subjects A) Unfiltered, unaligned torque ensemble B) Low-pass filtered version of the unaligned torque ensemble C) Ensemble in B after alignment D) Ensemble after removal of trials outside of one standard deviation of the ensemble mean time spanning ±1 0 s of the reference point It is evident that this time-span encompasses the dynamics of the ankle from before to after the increase in contraction Also indicated in Figure 5 3 is the variability of the torque records used in the analysis, in terms of a ±1 0 ensemble standard deviation envelope

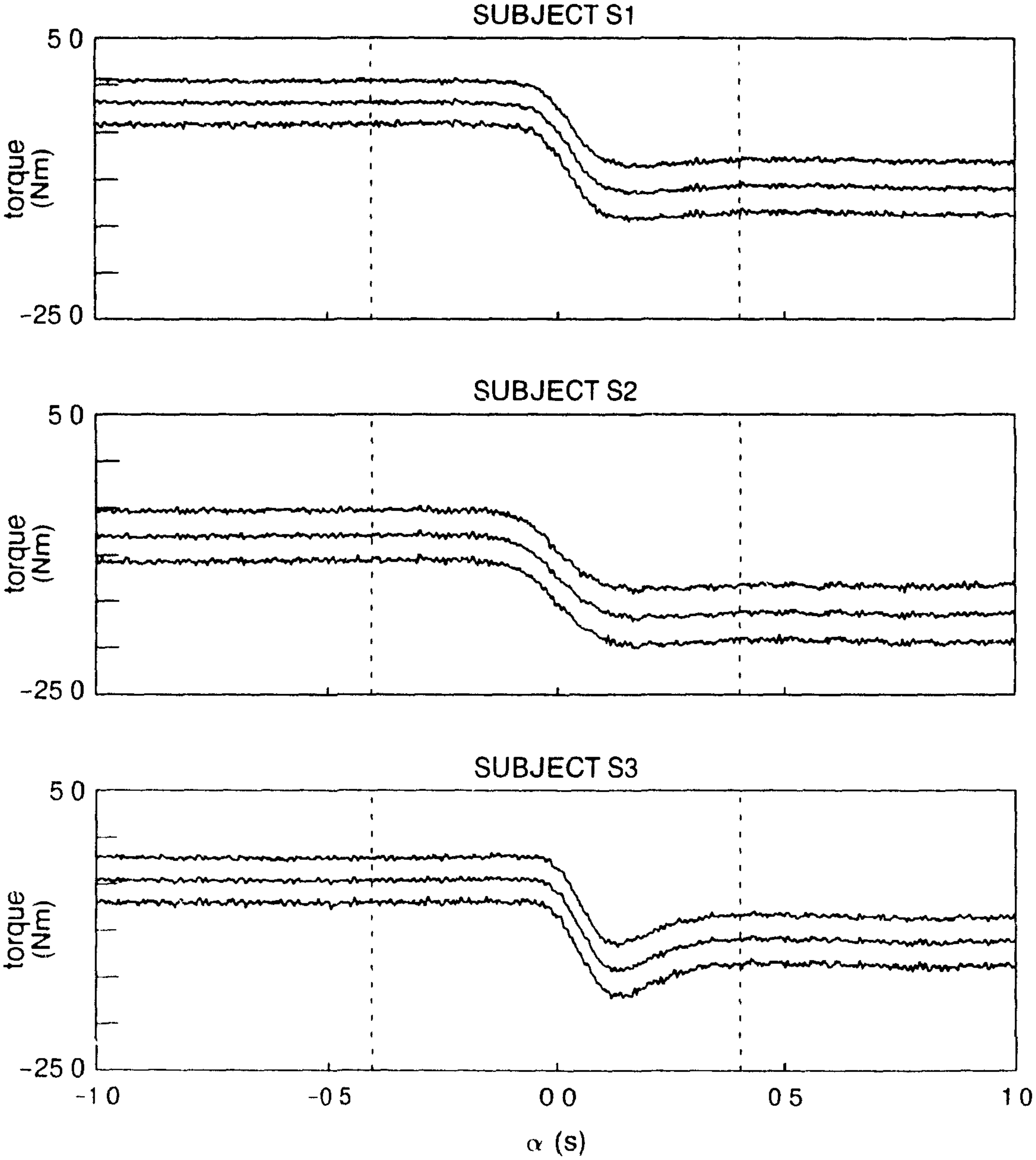

Figure 5 3 Ensemble average torque records ± 1 0 standard deviation for each subject The dotted lines indicate the time-span over which the dynamics were identified

The reference point $\alpha = 0\ 0$ s denotes the midway point in the change of level of contraction, negative values of α correspond to pre-mid-transition, and positive to post-mid-transition This convention will be used to present the results throughout this chapter

5.4.2. ACCURACY OF RESULTS

A good measure of how well the results of an identification procedure represent the actual dynamics is the extent to which they can account for variation of the output given the actual system input This quantity is known as variance accounted for, or VAF In this study, VAF has been calculated in terms of the ability of the individual impulse response functions to predict the cross-ensemble output corresponding to the time in the ensemble represented by the IRF In this way, the time-varying model's ability to represent the dynamics is quantified for each sampling interval in the time-span of the identification

Consider the other possible means of assessment of the model's accuracy, i e , in terms of the ability of the entire series of IRFs to predict the output of a single realization given the realization's input In this measure, the presence of poor estimates of the dynamics over a small segment of the time-span of the realization (e g., the transition phase of contraction in this experiment) may be masked by better estimates of the dynamics elsewhere in the course of the realization For this reason, it is advisable to evaluate the accuracy of estimates resulting from ensemble time-varying identification by determining the cross-ensemble VAF of individual estimates as opposed to calculating the VAF by considering the series of estimates as a whole

The variance accounted for (VAF) by the stiffness IRFs determined for the three subjects is shown in Figure 5 4 Each point in the VAF records represents the ability of the individual IRF corresponding to that time to predict the cross-ensemble output at that instant It is evident that in all cases the linear IRFs provide an excellent representation of ankle dynamics throughout the variation of muscular activity, for two of the three subjects (S1 and S3) the VAF exceeded 80% across the time-span, while the VAF of subject S2 had a minimum value of 73 4% Possible reasons for the lower VAF of S2 will be discussed later in this chapter

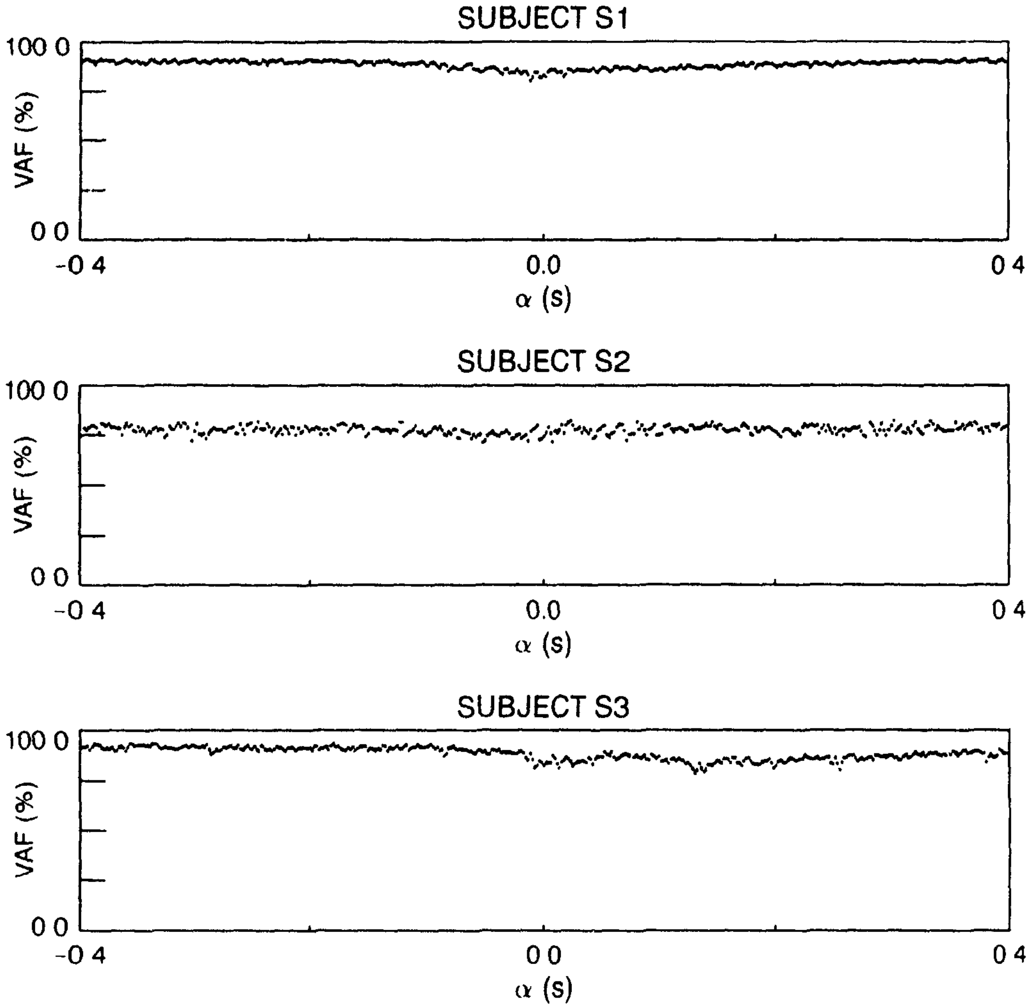

Figure 5 4 VAF of the linear stiffness IRFs for the three subjects studied

5.4.3. STIFFNESS IMPULSE RESPONSE FUNCTIONS

The ensemble of stiffness IRFs for subject S1 is presented in Figure 5 5 The sampling rate of this experiment was 500 Hz, with an anti-alias cutoff frequency of 100 Hz, however the input signal only had resolvable power for frequencies up to 50 Hz Thus, the estimated IRFs had frequency components above 50 Hz which did not contribute significant information regarding the dynamics of the ankle For presentation purposes, these effects were removed by low-pass filtering the series of IRFs (3 point FIR, 3 dB point at 125 Hz), resulting in the series of IRFs shown in the figure Both sides of the the filtered IRFs die out to zero in the 0 094 s (47 point) support, thus all the significant dynamics of the ankle occur in the time span of the filters

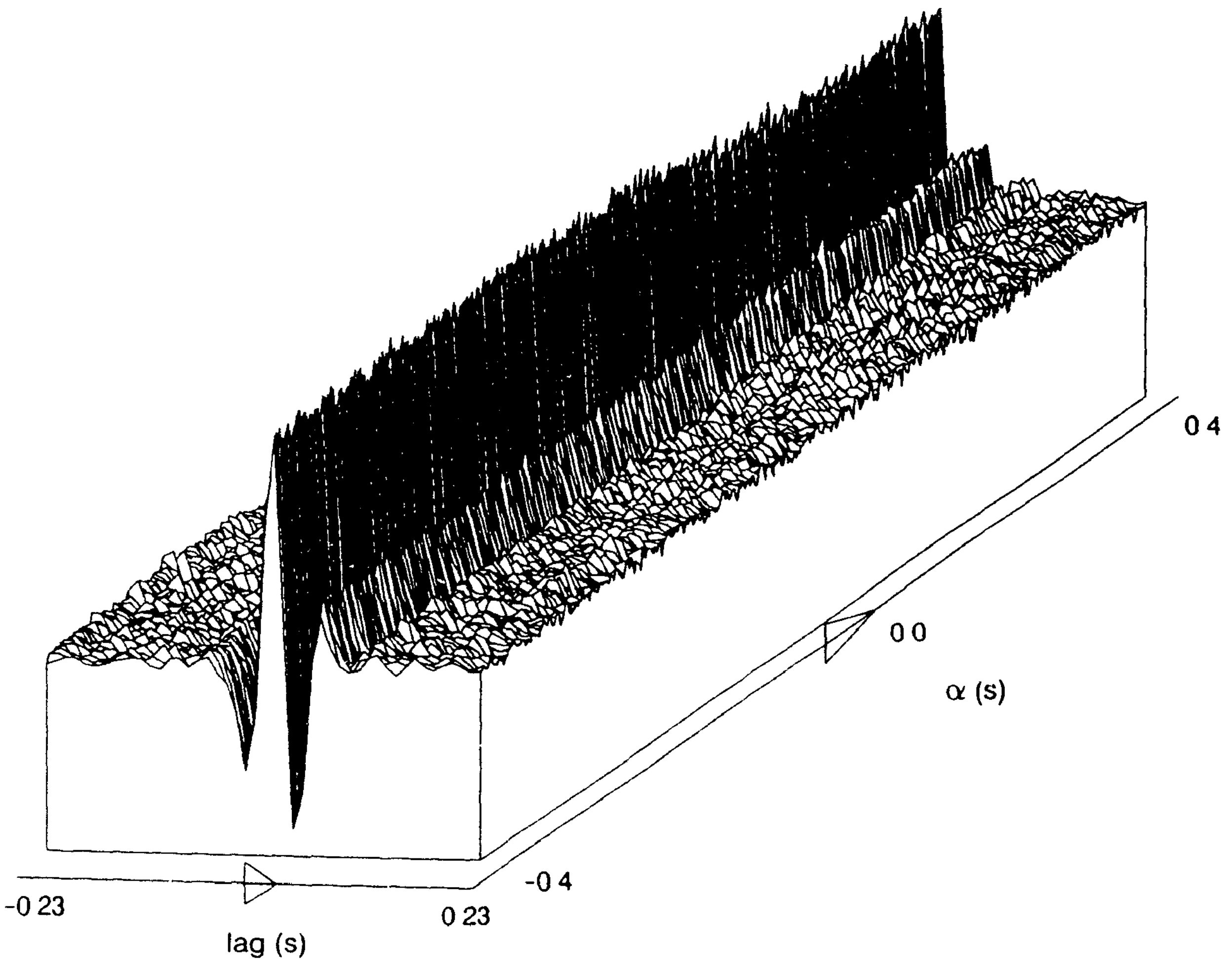

Figure 5 5 Series of numerically smoothed linear stiffness impulse response functions representing ankle dynamics of subject S1 in 2 ms intervals before, during and after the increase in level of contraction Time α = 0 0s denotes the time in the ensemble where the level of muscular activity was half-way between the two target levels Negative α denotes dynamics prior to the mid-point and positive α denotes dynamics after the mid-point

5.4.4. FREQUENCY RESPONSES

Stiffness IRFs, being representative of a high-pass, non-causal system, are difficult to interpret visually However, when presented in terms of their frequency domain representations, a clearer picture of the changes in dynamics results Figures 5 6a, b and c show the gain and phase parts of the stiffness frequency response obtained by Fourier transformation of zero-padded versions of the stiffness IRFs for the three subjects (zero padding provides an interpolated transform having a smoother appearance, however it does not improve the inherent resolution (Marple, 1987))

These results show a smooth change of ankle dynamics from the pre-transition phase to the post-transition phase The variations in the shape of the frequency responses reflect changes in ankle dynamics that occur as the subjects increased the level of torque developed at the ankle In each case, it is evident from the responses that the dynamics during the transition behave differently than those observed in the pre- and post-transition phases The responses before and after transition were similar to those of an underdamped second-order high-pass system, the gain response was flat at low frequencies, with an attenuated response at frequencies near resonance, followed by monotonically increasing gain at frequencies above resonance Similarly, the phase part of the frequency responses exhibited a rapid increase in phase lead centred about the resonant frequency which asymptotically approached a lead of 180° greater than at low frequencies

During transition, the dynamic behaviour exhibited a marked deviation from second-order behaviour At low frequencies, the gain response was not flat, but was attenuated, the degree of attenuation decreasing as the frequency increased Also, the phase response demonstrated a larger phase lead than would be expected for a second-order system At higher frequencies the responses during the increase in contraction exhibited a behaviour much like the responses before and after the increase The differences between the dynamic behaviour of the ankle before during and after the increase are shown in Figure 5 7, which presents the gain and phase responses of subject S1 in the three regimes

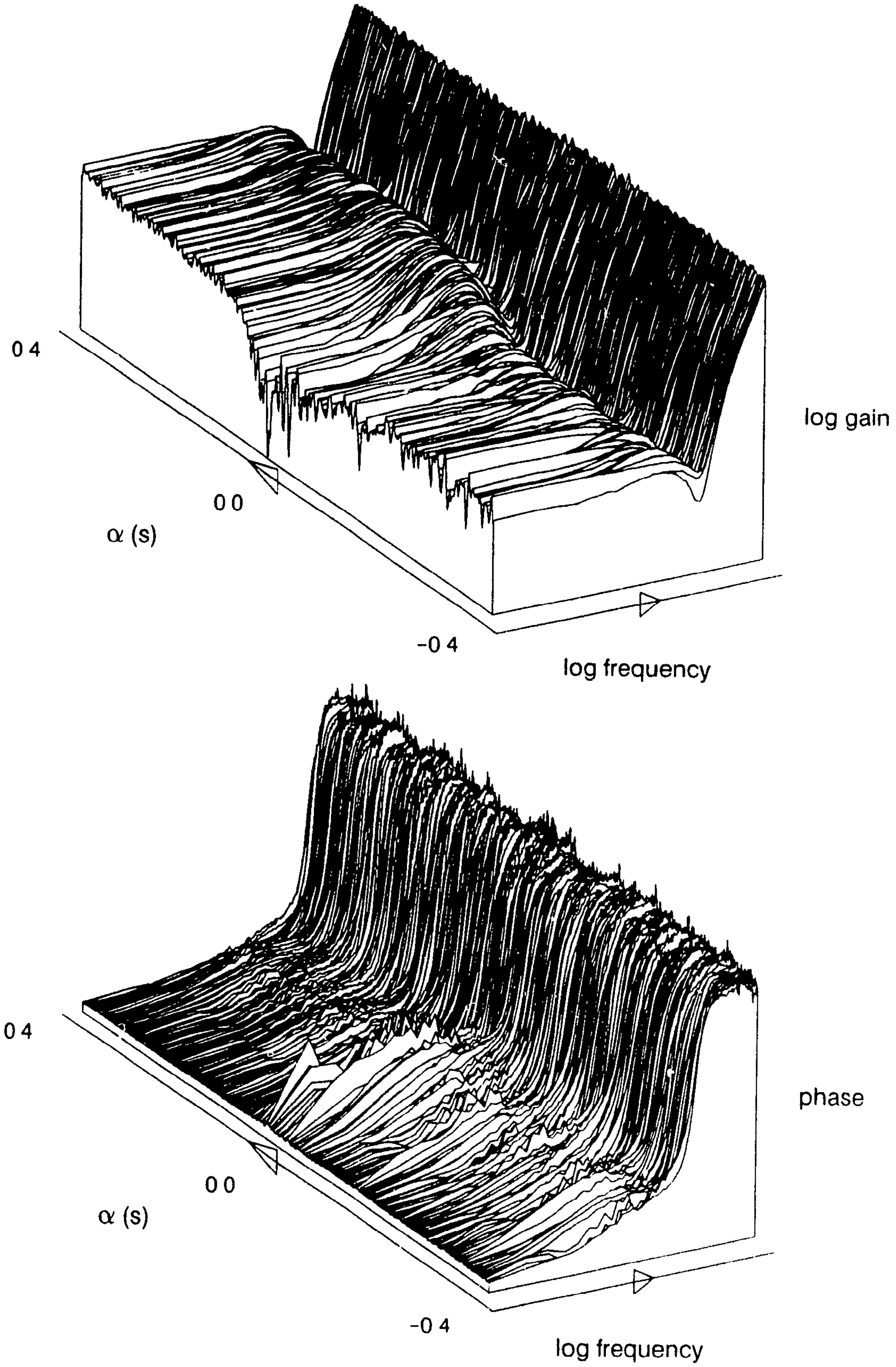

Figure 5.6a Gain and phase parts of the Fourier transformation of the stiffness IRFs of subject S1

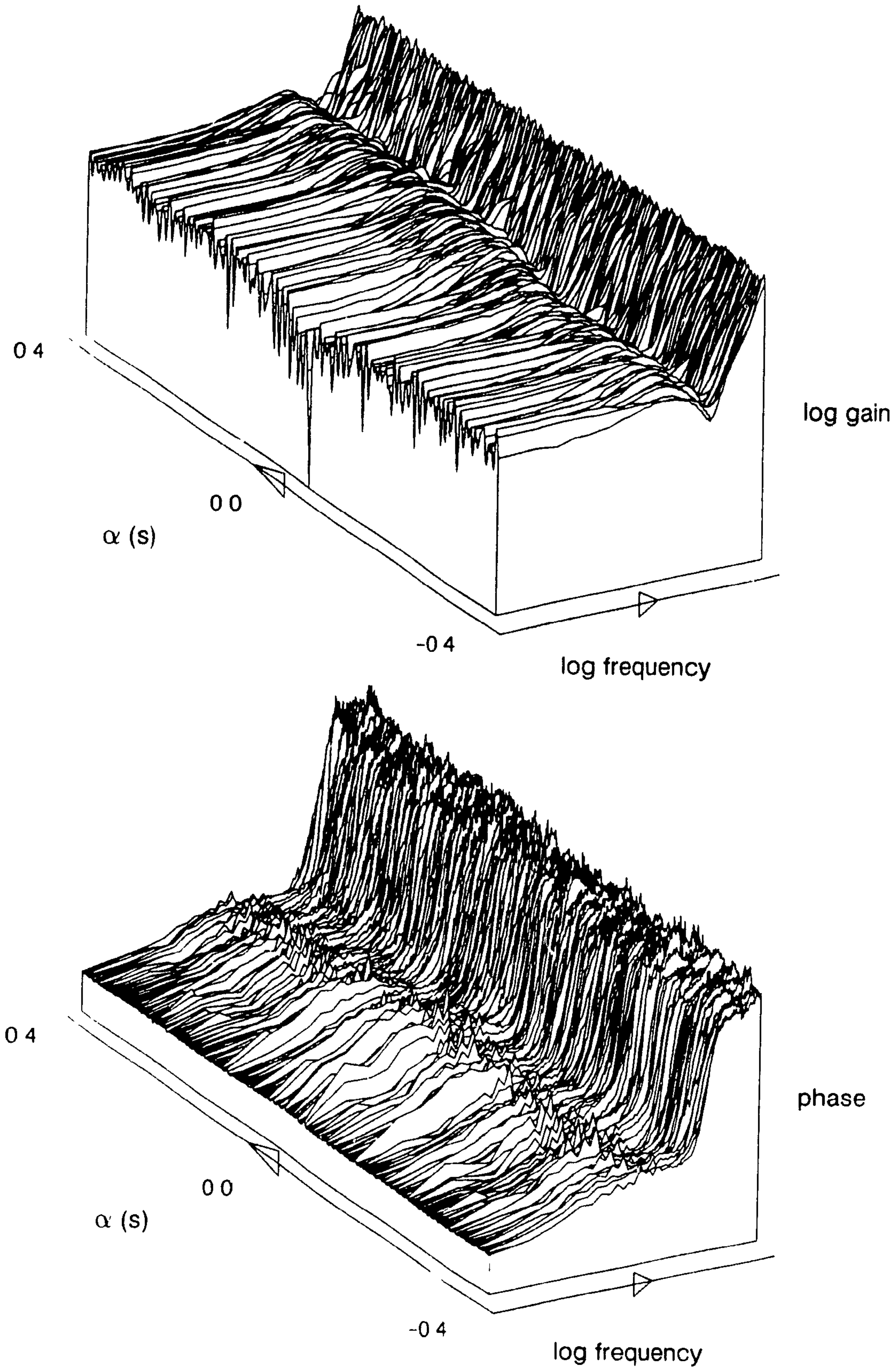

Figure 5 6b Gain and phase parts of the Fourier transformation of the stiffness IRFs of subject S2

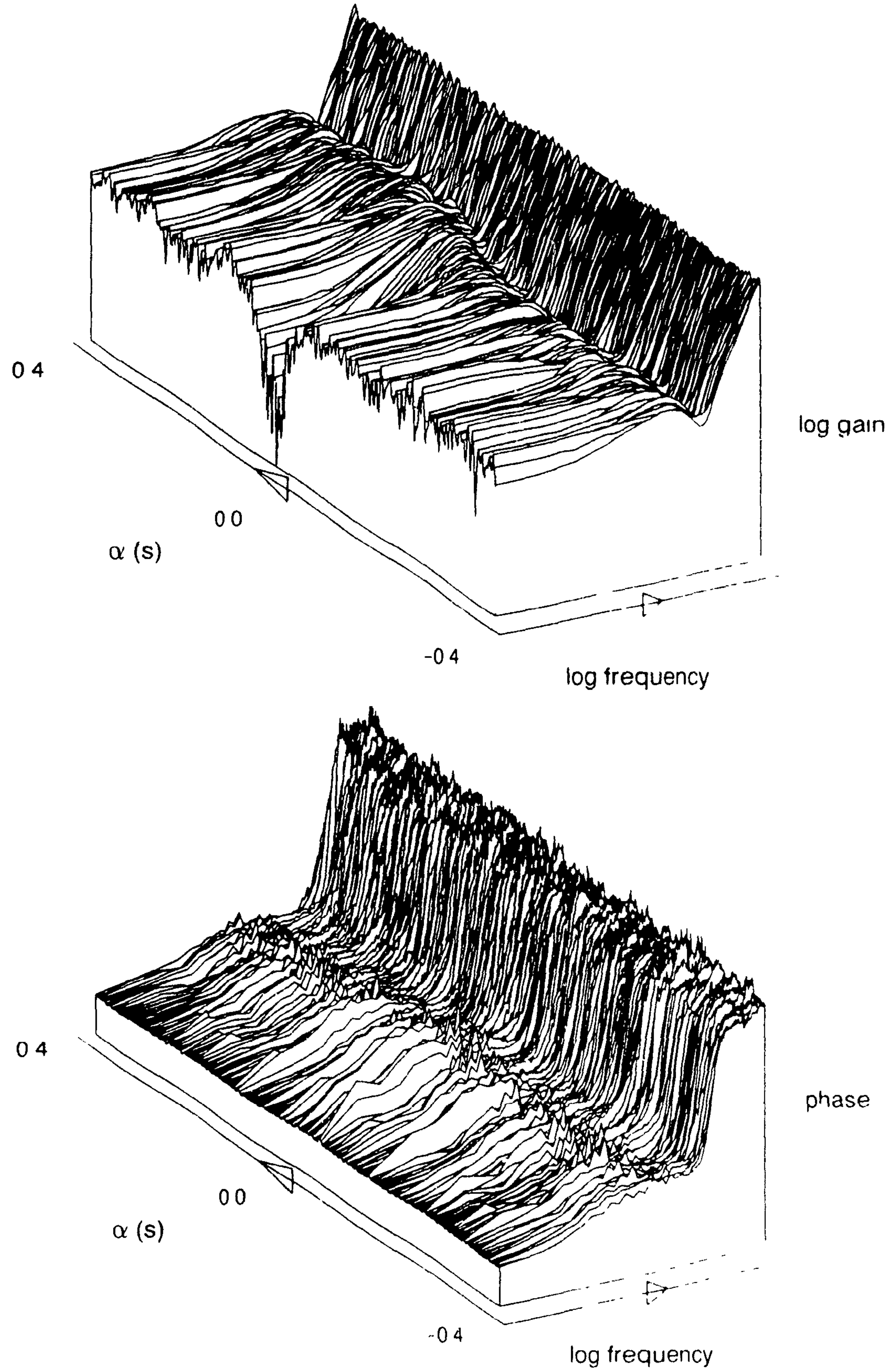

Figure 5 6c Gain and phase parts of the Fourier transformation of the stiffness IRFs of subject S3

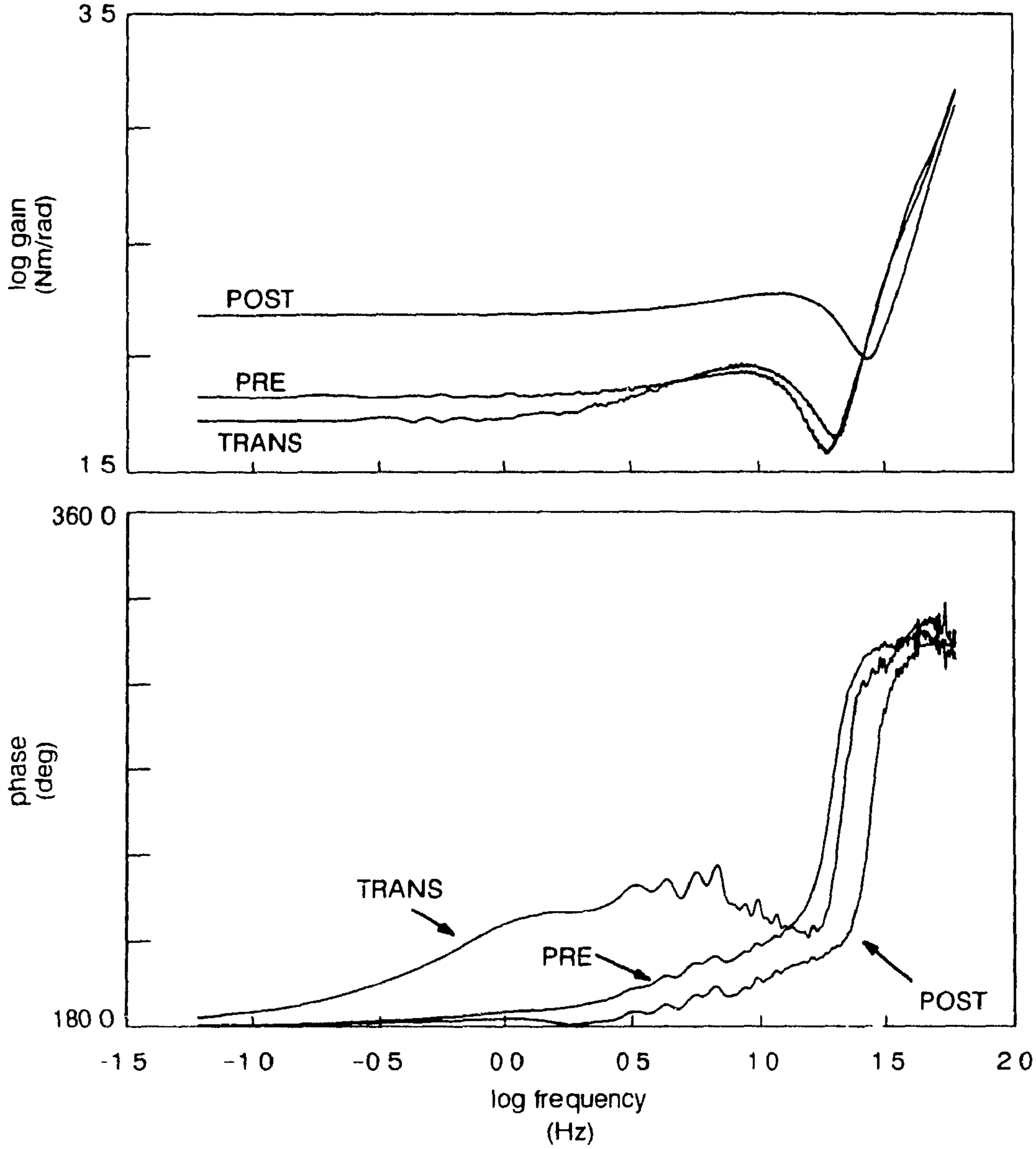

Figure 5 7 Gain and phase responses of subject S1 for the pre-, transition, and post- regimes of the change of level of contraction

5.4.5. SECOND-ORDER MODEL

In order to determine the change in dynamic behaviour during the transition phase in a more quantitative manner, a second-order dynamic model of the form shown below was fit to each of the stiffness IRFs

$$\frac{TQ(s)}{\Theta(s)} = \frac{s^2 + 2\zeta\omega_n s + \omega_n^2}{G\omega_n^2} \tag{5 1}$$

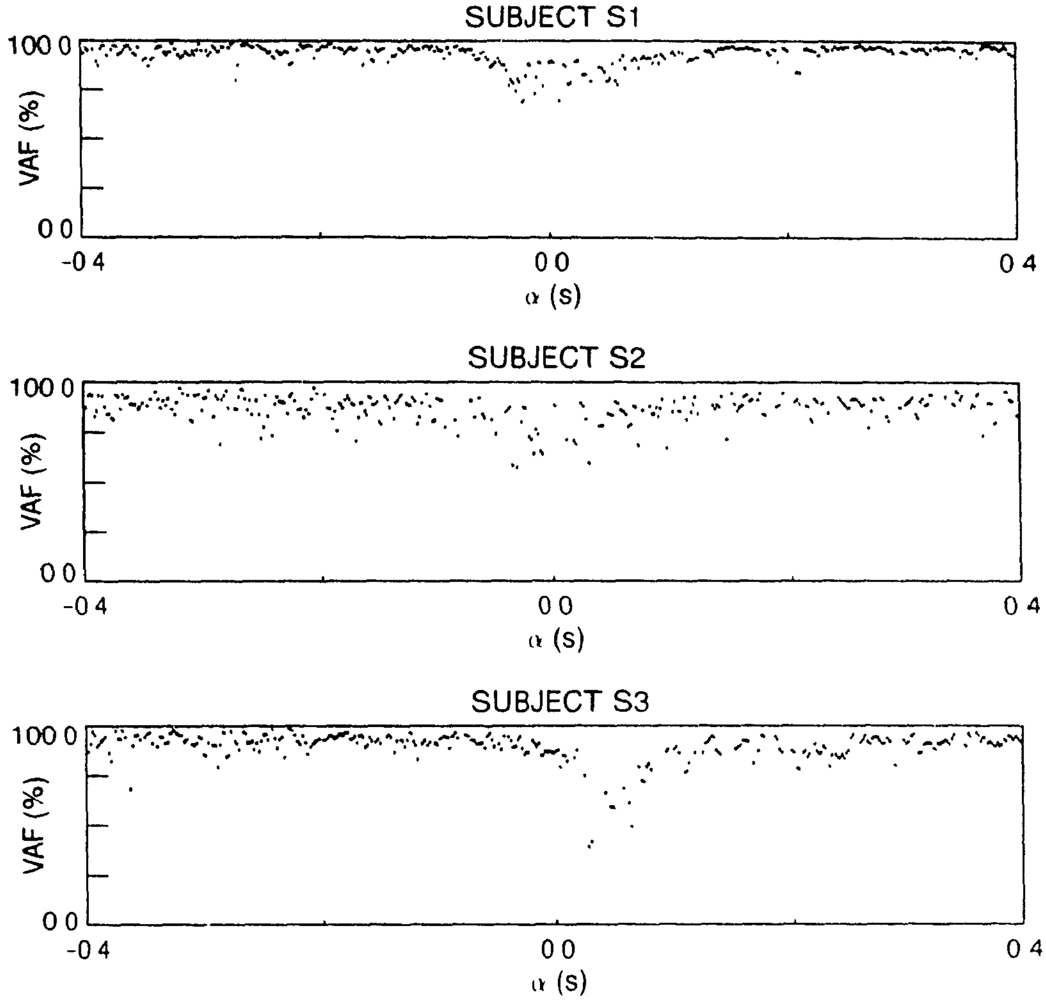

Figure 5 8 VAF by second-order fits to the series of stiffness IRFs obtained for each subject

The results, shown in Figure 5 8, reinforce the observations from the frequency responses before and after the transition phase, the dynamics are well described by the second-order parametric model The dynamics during the transition do not have a second-order behaviour, indicated by the low VAFs of the fits during those periods

5.4.6. CHANGES IN LOW FREQUENCY GAIN AND RESONANT FREQUENCY

Had the dynamics behaved in a second-order manner throughout the change of level of contraction, they could have been presented as variations in the parameters of the analytical representation given above However this is not the case Therefore in order to represent the changes of dynamics more parsimoniously two salient features were extracted from the frequency responses the system's gain at low frequency, and resonant frequency The resonant frequency was considered to be the frequency at which the gain part of the frequency response was minimum (in the neighborhood of the resonant dip, apparent in Figure 5 7) The gain at low frequency was taken to be the value of the gain part of each of the frequency responses at 0 6 Hz The variation of these parameters with the change of contraction level is presented in Figures 5 9 and 5 10 The resonant frequency increases monotonically as the level of activation increases, while the low frequency gain decreases significantly during the transition

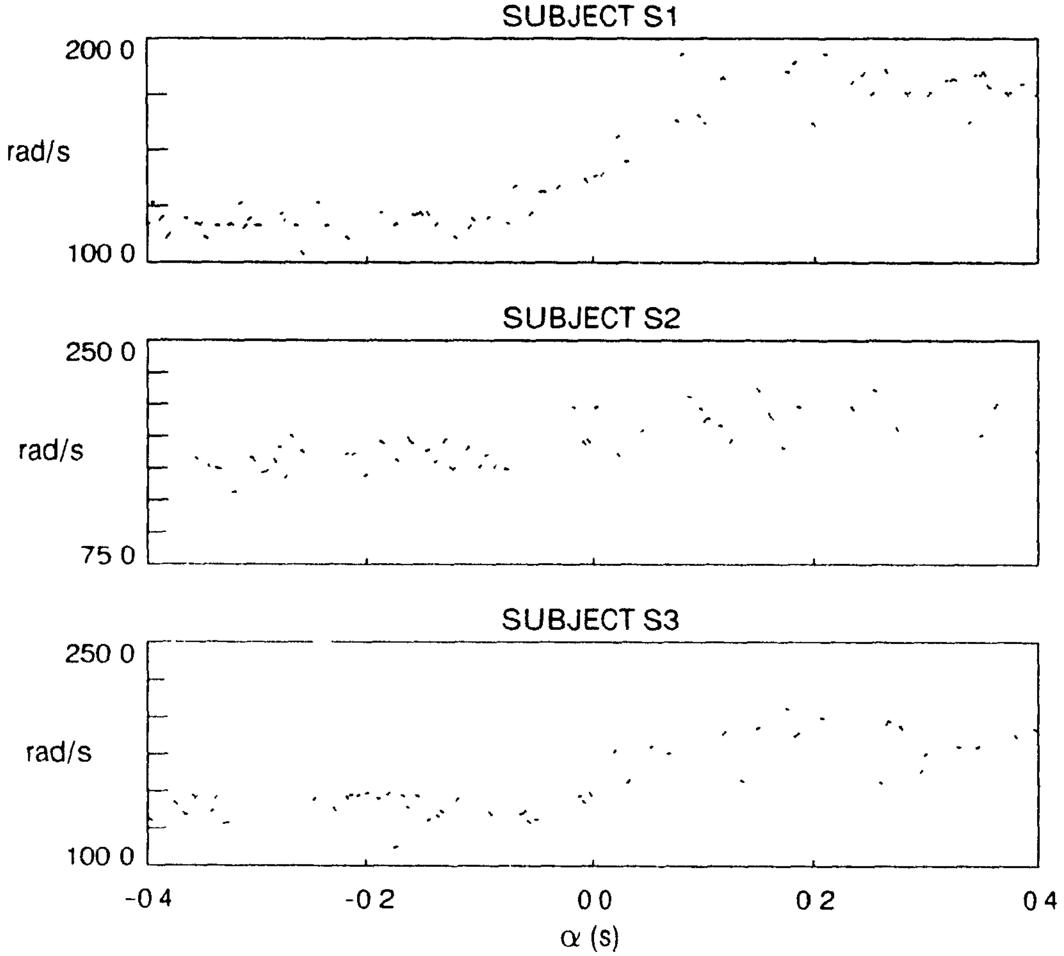

Figure 5 9 Variation of resonant frequency (ω) of ankle stiffness with change of level of contraction for the three subjects

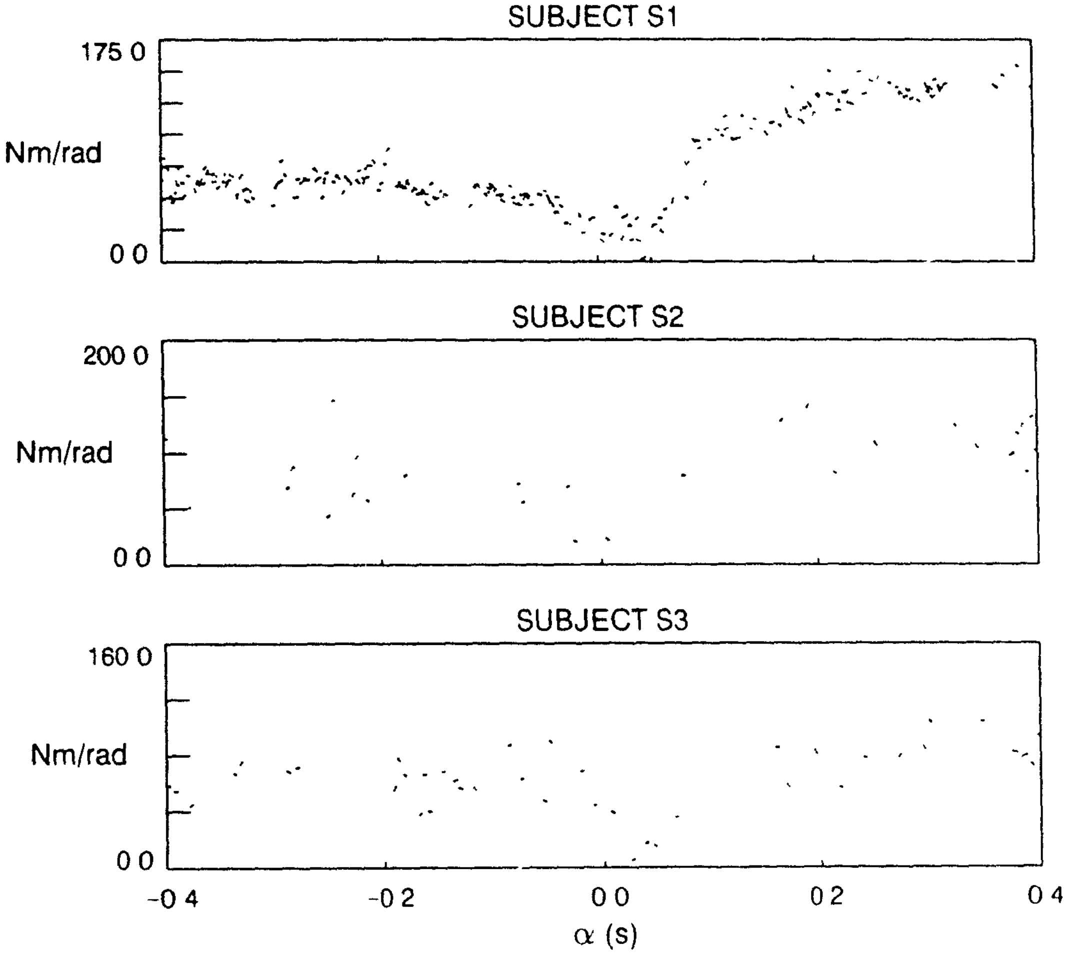

Figure 5 10 Variation of low frequency gain (G_{LF})of ankle stiffness over the change of level of contraction for the three subjects

5.4.7. EMG RESULTS

The ensemble average EMGs representing mean TS and TA activity are presented in Figure 5 11 The TA EMG record for subject S1 was not available due to problems encountered during sampling The ensemble average EMGs disclose the presence of a large increase of TS activity, and negligible change of TA activity, corresponding to the change in level of contraction

5.4.8. SUMMARY

Figures 5 12a, b, and c provide a summary of the results for the three subjects The ensemble average torque, as well as its rate of change (obtained by numerical differentiation of a highly smoothed version of the ensemble average torque), are presented with

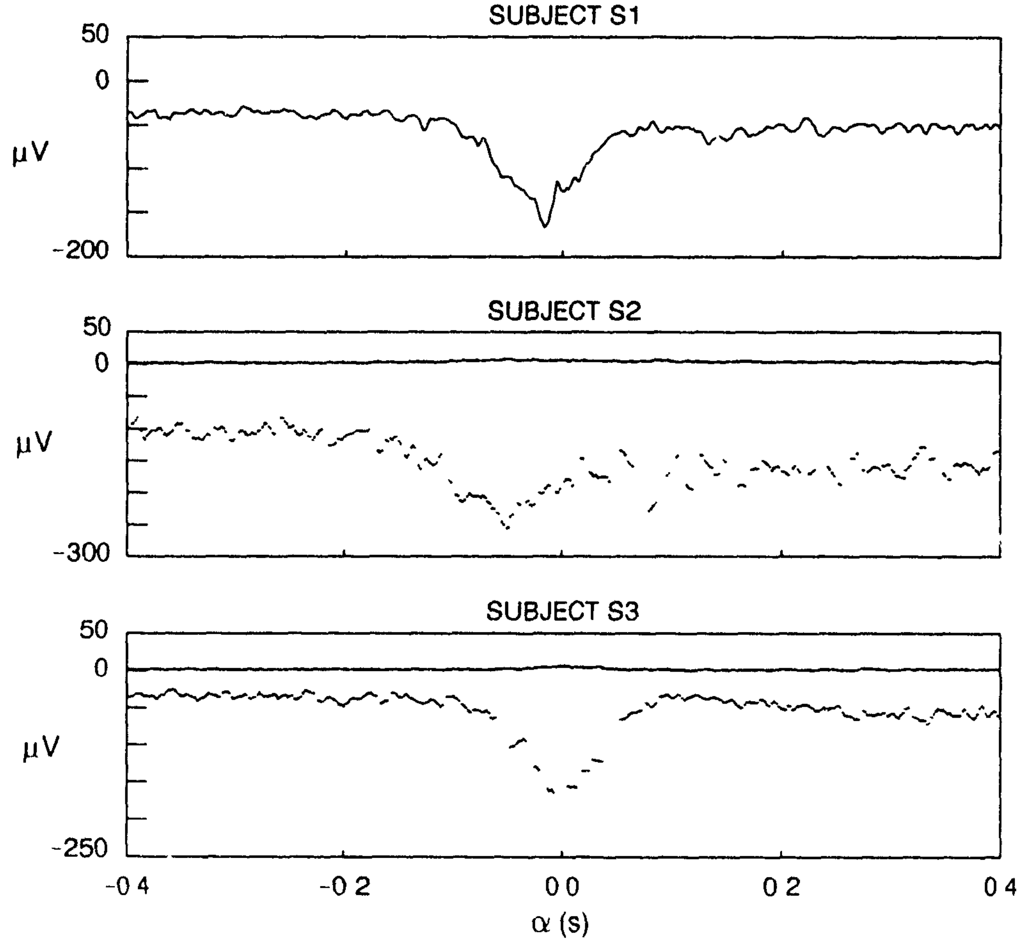

Figure 5 11 Ensemble average EMG for the three subjects The top trace is TA EMG, the bottom trace is TS EMG By convention, TA EMG was positively rectified, and GS EMG was negatively rectified The TA EMG record for subject S1 was not recorded

the other features of the results, on a subject by subject basis The timing of the events during the contraction can be inferred from the figures For each of the subjects, the increase of TS EMG activity preceded the onset of the increase of contraction level by approximately 50 ms This is likely due to the low-pass nature of activation dynamics, as discussed in the background chapter The changes in low frequency stiffness and resonant frequency began at approximately the same time as the increase of joint torque The non-second-order behaviour and the decrease in low frequency stiffness occurred during the transient phase of contraction, when the rate of change of the ensemble average torque was near maximum

The records of ensemble average torque and its rate of change show that subjects used different strategies to accomplish the increase of contraction The ensemble average torque of S2 had the lowest maximum rate of change, and the longest time to attain the higher torque level, in contrast to the record of S3, which had the greatest maximum rate of change, but exhibited an overshoot before finally settling at the target level Subject S1 used a moderate rate of change of contraction to attain the final torque level without overshooting the target

The differences in strategy correlate well with the different patterns of changes in low frequency stiffness and TS EMG observed for the three subjects The low frequency gain trace of S3 showed the deepest modulation in terms of a decrease during transition, concurrent with the maximum rate of increase of torque In addition, there was an increase of low frequency stiffness above the final stiffness coincident with the overshoot of the target level Subject S2 exhibited the slowest increase in torque, and the smallest decrease of low frequency gain of the three subjects The ensemble average TS EMG trace of subject S2 differed from the traces of S1 and S3 The increased TS activity in S1 and S3 occurred in single bursts, while the increase in TS activity of S2 was of longer duration, and displayed a second peak approximately 150 ms after the maximum of the first burst of activity This may be indicative of an extra effort exerted by S2 to attain the target level of torque, and is supported by the tentative manner in which S2 reached the higher level of contraction shown in the traces of ensemble average torque and its derivative

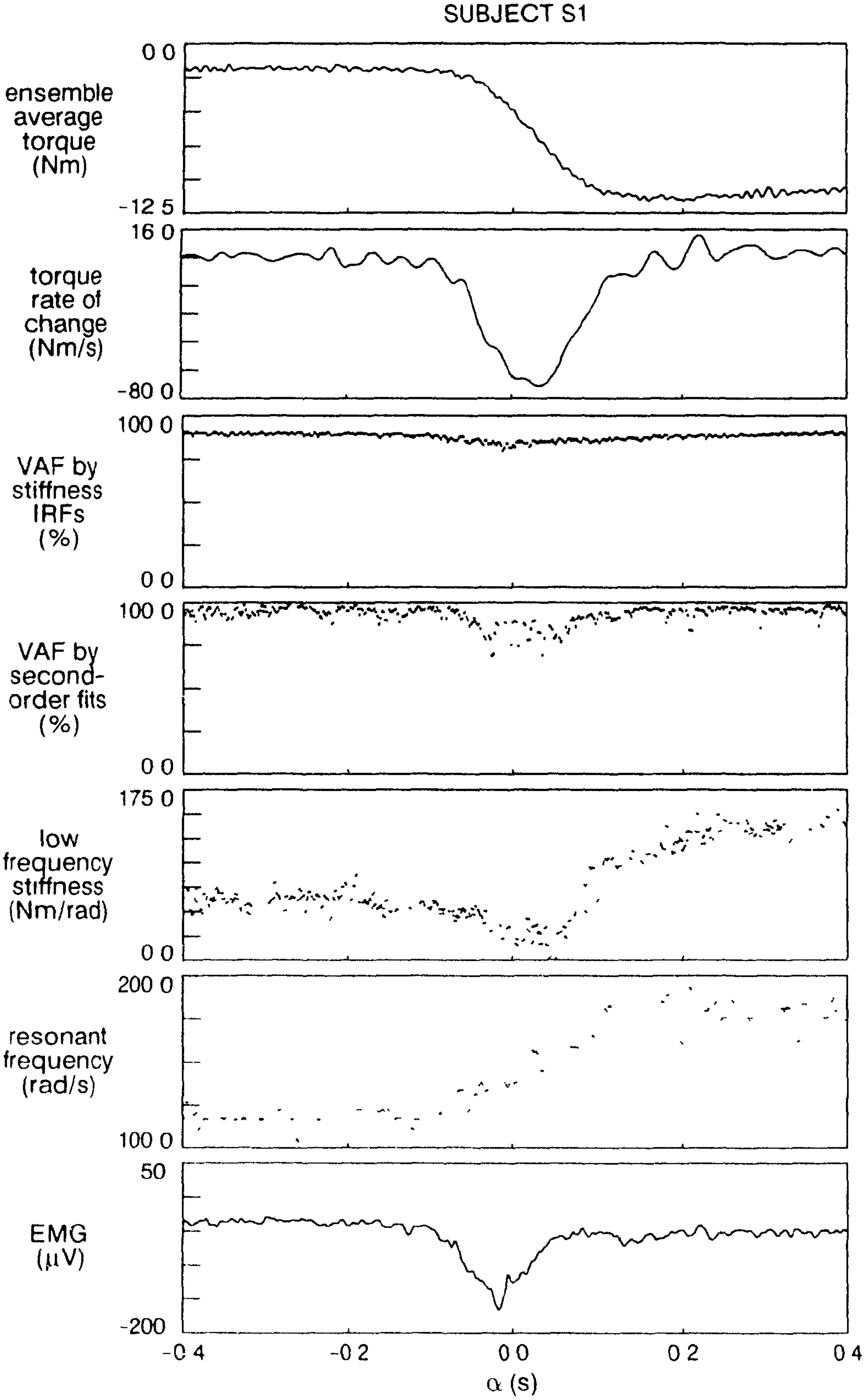

Figure 5 12a Summary of results of subject S1

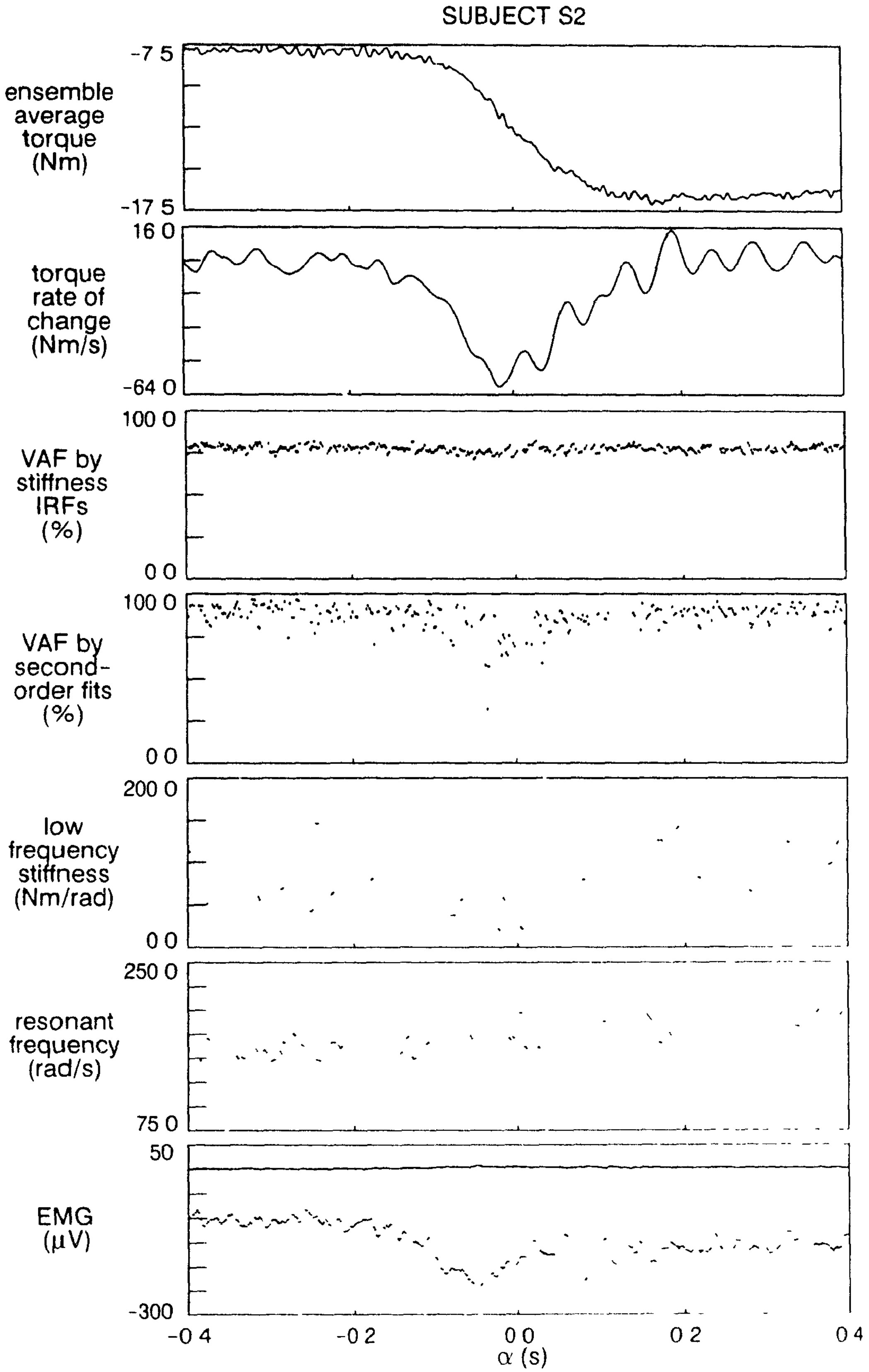

Figure 5.12b Summary of the results of subject S2

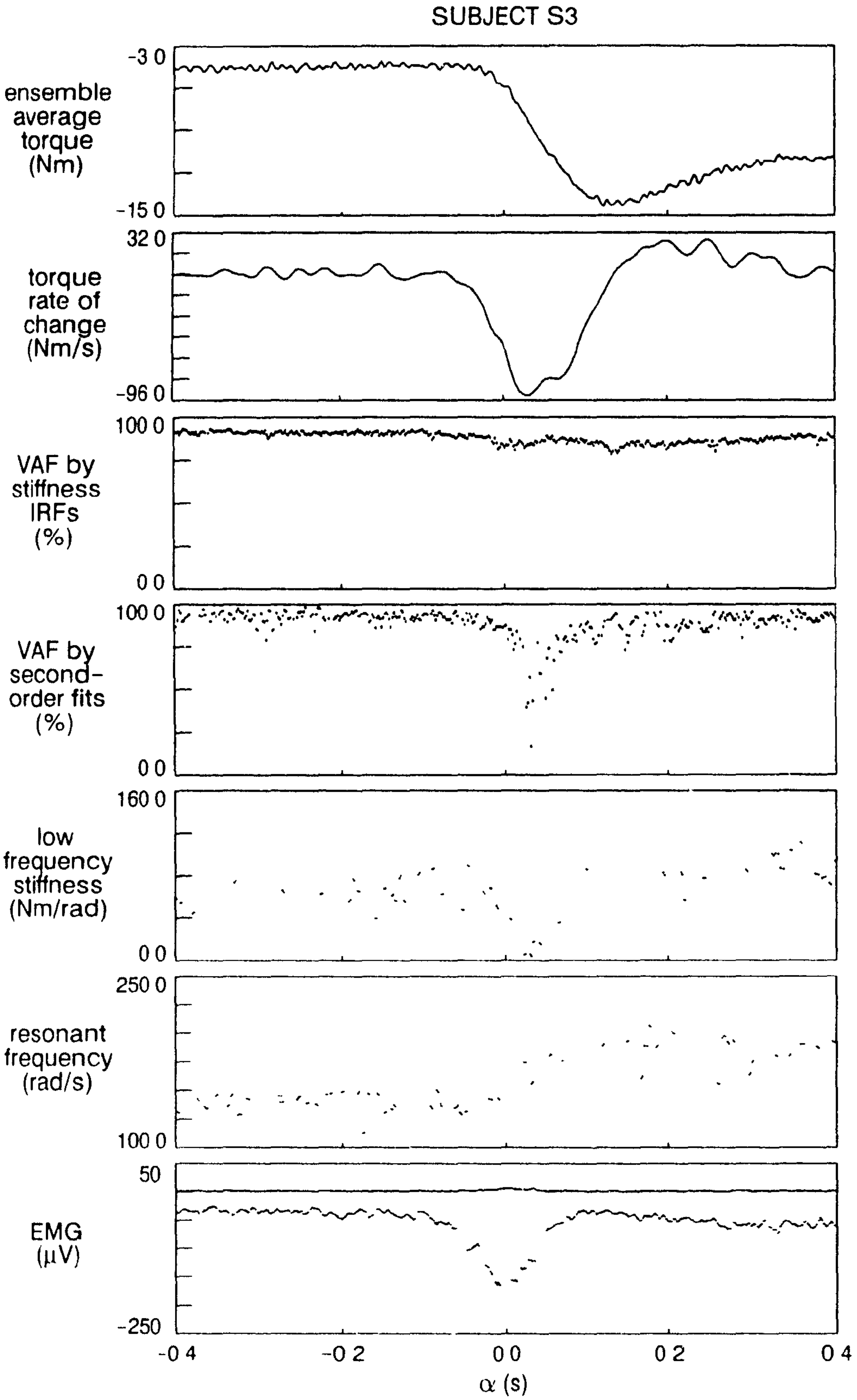

Figure 5 12c Summary of the results of subject S3

5.5. DISCUSSION

The phenomena of non-second-order behaviour and decreased joint stiffness at low frequencies during increasing muscular contraction have not been previously reported However, this study has employed a relatively unused time-varying identification method, which has allowed accurate measurement of joint dynamics throughout the change Additionally, the phenomena have been observed in all three subjects studied Thus it seems probable that the phenomena are real However, before discussing the implications the results of this experiment may have on the study of joint dynamics, their validity must be addressed

5.5.1. ACCURACY OF RESULTS

MODEL VALIDITY

Examination of Figures 5 12a, b, and c reveals that the non-second-order behaviour and decreased stiffness at low frequencies was closely linked to the phase in which the rate of change of muscular contraction is highest This suggests the possibility that the identification method may not have been able to track the most rapid variations of the dynamics It is evident from the simulation study that the SVD method can track changes of dynamics of the same magnitude and time-scale as the ones encountered in the experimental study, even in the presence of considerable output noise, but this may not be true under more realistic conditions However, in the experimental study, the VAF records of the estimated IRFs remained high during the epoch of increased torque rate of change Thus the estimates of the dynamics are valid representations of the variation of the data, and the SVD procedure itself can be ruled out as a possible source of the observed dynamics

A more likely possibility is that the observed change in dynamics was somehow related to an artifact caused by the alignment procedure The trials were aligned so that the time at which the change in mean joint torque was at its midpoint coincided across the ensembles of input and output This may have affected the cross-ensemble data in such a way as to introduce low frequency attenuation of the torque with respect to the position resulting in reduced stiffness at low frequencies This possibility was investigated by performing a second analysis of the data of subject S1 after realignment of the ensembles to a reference point 75 ms prior to the original one If the alignment procedure was the cause of the decreased stiffness phenomenon, then significant differences between the results of the two analyses would occur In order to compare the results of the two analyses, the low frequency stiffness records from the two were examined The results are presented in Figure 5 13, in which the traces have been aligned so that the reference point of the second analysis occurs 75 ms prior to the reference point of the first analysis The two records are nearly identical, the small differences between the two results are likely due to differences in inter-trial variability between the two analyses This result strongly suggests that the alignment procedure was not the cause of the observed attenuation of stiffness and concomitant non-second-order behaviour

Subject	Minimum VAF (%)
S1	83 4
S2	73 4
S3	79 5

Table 5 2 Minimum VAF in the series of stiffness impulse response functions for the three subjects

Table 5 2 shows the minimum VAF across the time span of the identification of the three subjects tested Examination of Table 5 2 and the VAF traces for the stiffness IRFs indicates that the results of subjects S1 and S3 account for at least 80% of the output variance, while the estimated dynamics for subject S2 are not as accurate This may be because S2 was required to produce a larger absolute torque than the other two subjects, which may have led to greater difficulty in tracking the target stimulus. Indeed, S2 reported experiencing fatigue near the midway point in the experiment, while the other two subjects did not The presence of fatigue may be the cause of the higher ensemble standard deviation of the torque recorded for S2 (see Figure 5 3).

LINEARITY OF DYNAMICS

The time-varying dynamics were well described by a linear nonparametric model, as evidenced by the high VAF obtained for the stiffness IRFs. The linear approach was valid in this investigation because conditions of isometric contraction and invariant amplitude

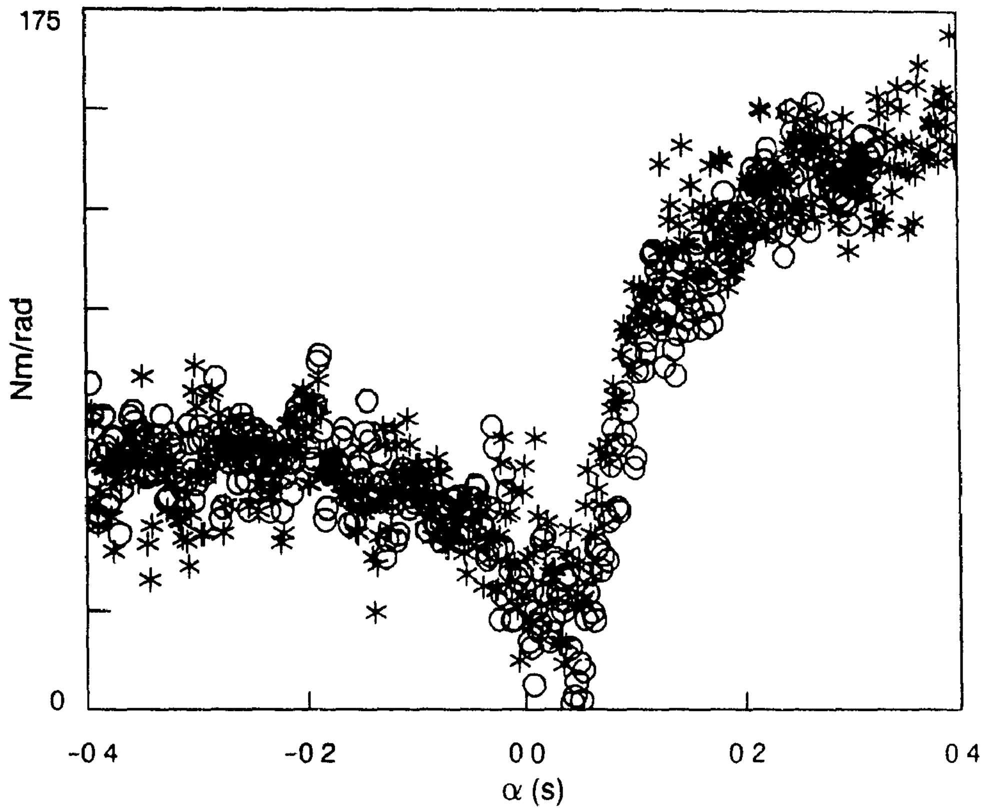

Figure 5 13 Low frequency stiffness records obtained from two analyses of the data of subject S1 Points marked by asterisks represent the results of the original analysis Points marked by circles are the result of an analysis in which the reference point for alignment of the ensemble data was 0 075 s prior to the reference point of the original analysis

probability distribution were imposed, thereby eliminating changes in mean joint position, the cause of significant nonlinearities In addition, the range of contraction level may have fallen within a linear range of the generally nonlinear contraction - stiffness relationship This may be an explanation for the lower VAF of the estimates of the dynamics of S2, whose tracking task was more intensive in terms of the absolute torque that was required of him, and therefore may have caused the dynamics of S2 to be in a more nonlinear region of the relationship than S1 or S3

5.5.2. COMPARISON WITH PREVIOUS STUDIES

QUASI-TIME-INVARIANT STUDIES

This study has shown that during a change of muscular activation, joint stiffness has a behaviour that is more complex than second-order, characterized by a decrease in joint stiffness at low frequencies These results are somewhat surprising in light of the results of previous studies in which the influence of muscular activation on ankle dynamics was investigated using a quasi-time-invariant approach These studies have reported the dynamics to be consistently second-order, and that joint stiffness increases monotonically as the level of muscular contraction increases (e g , Agarwal and Gottlieb, 1977b, Hunter and Kearney, 1982, Weiss *et al.*, 1988) This difference is due to the limitation of quasi-time-invariant methods to step-wise invariant models to represent the change in dynamics The dynamics of the joint change on far too rapid a time scale for the piece-wise models to be able to depict the changes, because they can only represent the dynamics of the joint at a number of distinct operating points Therefore, they are unable to identify the dynamics as they change between static operating points Through the use of a time-varying identification scheme, the dynamics of the ankle have been tracked as they change, thereby providing information regarding aspects of ankle dynamic behaviour unattainable by quasi-time-invariant methods

TIME-VARYING STUDIES

There are two opposing schools of thought that can be followed when identifying the dynamics of an unknown system One choice is to assume a parametric model of the system *a priori*, thereby reducing analysis requirements by restricting the model to be of a single dynamic form, or at best a limited number of forms, which can be described by a relatively small number of parameters For example, a number of studies of joint dynamics have assumed joint dynamics to be of a second-order dynamic form, and have identified the dynamics in terms of three parameters The other choice is to allow the model to assume any dynamic form by formulating the identification algorithm to identify nonparametric models of the dynamics This approach is more computationally intensive because it involves the solution of equations having a large number of unknowns, e g the points in an impulse response function, as compared to parametric identification but it has the advantage of being able to identify systems having any dynamic form Most importantly for this study, it also enables the identification of systems whose dynamic form changes during the identification

Two studies of the dynamics of a joint under time-varying conditions have been performed using parametric techniques In the study of time-varying compliance of the human forearm conducted by Lacquaniti and co-workers (1982), linear time-varying models of joint compliance were estimated using the correlation-based technique described in chapters 2 and 3 Along with the difficulties associated with this method, the authors compromised the effectiveness of their analysis by assuming the model to be a valid description of the dynamics, and fit second-order parametric models to the impulse response functions they obtained The authors do not state explicitly the accuracy with which the parametric models represented the dynamics, but plots showing both the original IRFs and IRFs representing the second-order model at selected instances are presented The second-order model does not compare favorably with the actual dynamics in five of the eight cases shown Therefore the reliability of the second-order parametric models in this case must be questioned

The other study was conducted by Bennett *et al* , (1990), who used SVD to obtain the time-varying parameters of an ARMA model from ensemble data This study used an SVD-based ensemble method to identify the compliance of the human elbow during a repeated motion The task was executed with aperiodic and nonuniform time-variations thus the SVD method was well-suited to this problem However, by assuming a second-order parametric model *a priori*, the models obtained for the dynamics may not have accurately represented joint compliance

Consider the ramifications the assumption of a second-order parametric model would have on the results of the investigation presented in this report In Figure 5 8, the variance accounted for by second-order fits to the nonparametric impulse response functions obtained in this study show that a second-order model would not be able to accurately identify the dynamics of the joint during the time period where the dynamics are changing with the level of muscular contraction This is precisely the time period of interest, however Obviously, the results obtained from such a parametric approach would be uninformative, and probably misleading

5.5.3. POSSIBLE MECHANISMS RESPONSIBLE FOR THE OBSERVED DYNAMICS

The results of this study have revealed a higher-order dynamic response of a joint than previously seen during an increase of muscular contraction It is evident that the results are not due to an artifact of the analysis, and that the results of this study are a valid depiction of the changes in joint dynamics that occur during an increase of isometric contraction Thus, it appears that changes in the underlying physiological mechanisms are the cause of the changes in dynamics All the elements of the neuromuscular system have dynamic responses. Presumably a change in the torque generated at a joint could lead to higher-order dynamics because of the sensitivity of the components to factors associated with the rate of change of joint torque However, the experimental and analytical procedures used in this investigation do not permit the individual factors influencing joint dynamics to be determined Nonetheless, a few speculative explanations regarding the mechanisms underlying the results of this investigation may be appropriate

CO-CONTRACTION

One physiological mechanism that could cause the decreased static stiffness during the increase of contraction is decreased coactivation of agonist and antagonist muscles Recall from the background chapter that co-contraction can lead to an increase of joint stiffness for a given level of mean joint torque. If TA was initially activated and then deactivated during the increase in TS level of contraction, there would be a high stiffness prior to the increase of contraction, followed by a decrease during the transition phase and return to a higher stiffness afterwards due to increased TS activity However the ensemble average EMG traces shown in Figure 5 11 do not support this TA activity is negligible compared to TS for the two subjects whose TA traces were available Indeed, if anything, there was a slight increase in TA activity during the transition phase, providing further argument against the possibility of co-contraction as a potential mechanism

MUSCLE MECHANICS

The processes underlying muscular contraction may influence joint dynamics during changes in level of activation A difference has been observed between the time course of muscle force and static stiffness in studies of isolated and intact whole muscle (Stein and Parmiggiani, 1979, Bressler and Dusik, 1984, Stein and Gordon, 1986, Bagni *et al* . 1988) None of these studies has reported static stiffness decreasing during an increase in muscle contraction, however Therefore it is improbable that contractile mechanisms are solely responsible for the decrease in low frequency stiffness observed during the increase of torque at the ankle Note that these studies investigated the force - stiffness relation for electrically stimulated muscle, and therefore do not give an indication of the degree to which reflex and higher neural centres influence muscular contraction

REFLEX MEDIATED EFFECTS

PERIPHERAL MECHANISMS

Despite the intensive effort to investigate the regulation of motor function by the peripheral nervous system, the role of reflex mechanisms in the control movement remains unclear Nevertheless, reflexes may be involved in the changes in dynamics during an increase of isometric contraction The tendon organ and spindle transducers are dynamic systems (Jansen and Mathews, 1962, Alnaes, 1967) but their interactions have not been satisfactorily characterized as yet It is conceivable that during voluntary increases of muscular activity, these two systems may have an effect on the dynamics of a joint that could lead to the observation of non-second-order behaviour accompanied by a decrease in low frequency stiffness

Supraspinal centres may also influence the behaviour of the peripheral nervous system to bring about the phenomena The sensitivity of the reflex pathways may be altered during voluntary contraction via changes of the state of interneurons However, whether peripheral mechanisms can cause joint stiffness to decrease during an increase of muscular force remains unclear

MUSCLE TENDON INTERACTIONS

Both muscle and tendon have different nonlinear elastic properties Thus, when a joint is displaced, the two structures absorb different amounts of the length change The relative distribution will be a function of the displacement amplitude and its derivatives, as well as the displacement frequency and the mean level of muscular force Also, the structures may vibrate at frequencies other than those of the perturbation It is possible that at certain perturbation frequencies, some frequency components of the vibrations of part of one of the structures will be matched to the loop delay of its constituent proprioceptive transducers Thus the reflex force elicited by the receptor would be timed such that it would not resist imposed movements at those frequencies, but in fact would assist them

This scenario has been proposed by Rack *et al* (1983) to explain decreased stiffness to sinusoidal stretch of the ankle observed in the 6-8 Hz range In that study, this behaviour was only found in subjects with a highly sensitive stretch reflex, and primarily during changes in stretch frequency

This may provide an explanation for the observation of the present study that the stiffness of the ankle at low frequencies is attenuated only during the change of contraction level It is possible that during the change of contraction, the reflex gain increased to a level sufficient for the proprioceptive signal to induce a low frequency modulation of force that was somewhat in phase with the low frequency components of the imposed movements It follows from this argument that during the transition phase a decreased resistance to the low frequency components of the position perturbation would have resulted, but during periods of invariant contraction the reflex gain would not have been as enhanced, so that the decreased resistance to low frequency movements would not occur

Reflex mediation therefore appears to be the most probable cause underlying the changes in dynamics Identification of the changes in reflex dynamics (torque - EMG relationship) accompanying a change in level of contraction could allow evaluation of this hypothesis However, considerably more trials than the number recorded in this experiment are necessary to obtain accurate estimates of reflex dynamics As mentioned in the discussion of the results of the simulation study, the muscular activity information obtained from surface EMG is contained in the modulations of signal that is highly corrupted with noise (signal to noise ratio of less than 30 dB) In contrast, the position and torque signals recorded in this experiment had very low levels of noise associated with them (signal to noise ratio approaching 90 dB) The degree of overdetermination of the ensemble data needed for accurate estimation in the present study was therefore determined by the variability between trials However, the poor signal to noise qualities of the EMG signal will add considerably more noise to the ensemble than merely the inter-trial variability that existed in this study, thus significantly decreasing the accuracy of the estimation procedure for a given degree of overdetermination

5.5.4. CLOSING COMMENTS

The observations of this study have provided new information regarding the control of muscular contraction However, the mechanisms responsible for the observed changes in joint dynamics are not obvious It is probable that there are several additional factors influencing joint dynamics that have not been mentioned The interactions between the mechanisms underlying joint dynamics have not been explicitly studied Therefore, further investigation of the processes underlying joint dynamics must be undertaken to determine the cause of the phenomena Some of these issues will be addressed in the directions for future research section of the next chapter

6. CONCLUSIONS

6.1. SUMMARY

A method for identification of linear time-varying systems from ensemble data using singular value decomposition has been presented in this thesis This technique, which provides a series of nonparametric impulse response function representations of the system as it varies with time, is capable of tracking rapid changes in dynamics without *a priori* assumptions regarding the system's dynamic structure, or the nature of its time-varying behavior The results of the application of this method to simulated and experimental data have shown it to be robust in the presence of additive output noise, and to be a viable method for accurately representing the time-varying dynamics of the neuromuscular system This technique may allow a major advance in the study of the neuromuscular system, in which the most interesting behaviour, i e , the transition from one state to another, has been previously beyond the capabilities of quantitative study

By virtue of the linear, nonparametric, time-varying models provided by the SVD method, this study has accurately tracked the changes in joint dynamics that occur during a voluntary isometric contraction. The results have revealed two phenomena During a transition of contraction level, the ankle joint does not behave as a second order dynamic system, and the joint's resistance to low frequency perturbations decreases These effects were not foreseen, and additional work is required to understand their origin and significance

6.2. DIRECTIONS FOR FUTURE RESEARCH

This investigation has generated a number of questions regarding the physiological mechanisms responsible for the changes in joint dynamics observed in this study There are four factors which are most likely to be at the root of the dynamics· central control mechanisms, reflex control mechanisms, intrinsic muscle mechanics and muscle-tendon interactions It may be feasible to investigate the influences of these mechanisms through careful experimental design as follows

The effect of voluntary control on joint dynamics during changes in level of contraction can be removed by electrical stimulation of muscle to elicit contraction A two-part experiment in which similar muscular contractions are first brought about by electrical stimulation and subsequently under voluntary control could be performed The differences between the time-varying dynamics observed for the two paradigms may provide insight to some of the centrally mediated influences on *in vivo* muscular contraction

The nonlinear formulation of the SVD method has other potential areas of application The nonlinear time-varying dynamics of isolated single muscle fibres and whole muscle, as well as intact muscle preparations can be identified and compared, thereby establishing the contributions of muscle contractile mechanics, activation dynamics and reflex dynamics to the dynamics of muscle

The hypothesis that muscle-tendon interaction is the source of the observed dynamics might be evaluated by performing tests on isolated whole muscle using preparations which include intact tendon However, it will be difficult to quantify the interaction of the two structures because of the intimate relationship between the active and passive components of muscle as a whole The structures contributing to the passive mechanical properties of tendon and muscle tissue are widely dispersed to varying degrees within whole muscle, and the state of activity of the crossbridges will vary spatially and temporally Therefore the muscle-tendon complex must be considered to be a distributed, time-varying, nonlinear system In order to obtain a qualitative appraisal of the interactions of the components of this system, a finite element investigation could be performed However, a study of this type will require very accurate models of the dynamics of the constituents as well as the histology of whole muscle to be valid

The experiment performed in this work can be readily adapted to investigate time-varying reflex dynamics (the torque - EMG relationship) under the same conditions as this study, as well as for electrical stimulation and movement studies The results of these experiments may provide concrete evidence regarding the role of reflex mechanisms in movement

Other investigations of the time-variations of joint dynamics under various operating conditions will also provide important contributions to the understanding of motor control. An investigation in which joint dynamics are identified during contractions having different variations of level of contraction may give an indication of the existence of a force-dependent nonlinearity. If the existence of a nonlinearity was established, a more formal identification of the nonlinear time-varying dynamics could be performed using the nonlinear formulation of the SVD method (Nielsen *et al.*, 1989). The hypothesis that different strategies exist in the motor control system for different levels of muscular effort could then be tested by observing the variations of the dynamics over a wide range of contraction.

Another possible extension of the present research would be the study of the changes in joint dynamics during imposed and voluntarily produced large motions. An investigation of joint dynamics under these conditions must address the time-varying and nonlinear behaviour which will most certainly be exhibited by the joint. The techniques presented in this thesis will therefore allow quantitative evaluation of motor control of natural activity, and may thus contribute significantly to the study of the neuromuscular system.

APPENDIX A:
IMPLEMENTATION OF THE SVD METHOD

This section presents the ASF code for the NEXUS operator TVFIL, which estimates a series of impulse response functions representing the variation of a system's dynamics over a period of time The theory of the algorithm and details of its implementation are given in chapter 3

```
# TVFIL        V02-01   REK and JBM     Time Varying Filter determination
#
#  Description
#
#     TVFIL determines the filter (impulse response function)
#     between an input and output channel (time series) using ensemble
#     data
#
#-----------------------------------------------------------------------
#
#  Author
#
#       R E  Kearney
#       BioMedical Engineering Unit.
#       McGill University,
#       Montreal, Quebec
#       CANADA
#
#-----------------------------------------------------------------------
#
#  Usage
#
#       Y = TVFIL( X1, X2, [X3] , P1, P2,      )
#
#       where   Y  = filter between X1 and X2
#               X1 = system input data
#               X2 = system output data
#               X3 = starting points for trials [optional]
#               P1,    ,Pn = various parameters
#
#
#       variables created
#
#               VAF = variance accounted for by the filter
#
#-----------------------------------------------------------------------
#
# Notes
#
#       1  Copyright 1981, Hunter & Kearney
#
#       2  The input channel lengths must be  <= 500,000 for VMS
#          <= 2048 for RSX and  <= 1024 for RT-11
#
#       3  The filter (impulse response function) is then calculated
#          by solving a matrix equation using pseudoinversion and
#          singular value decomposition
#
#       5  The resulting filter values are the least-squares estimates
#          for the filter length chosen  Note that with another filter
```

```
#          length different filter values will be obtained  Thus the
#          resulting filter should be inspected to verify that with the
#          filter length used the filter has decayed to zero
#          The filter should be convolved with the original input
#          to get the predicted output  This output should then be
#          compared with the original output
#
#       6  The user is given the option of calculating either a
#          1 or 2 sided filter. The right side (positive time) of the
#          filter is the memory component  The left side (negative
#          time) of the filter, if it has been calculated (i e  2
#          sided filter), is the anticipatory component
#
#       7  Further details on the theory and algorithm used are given
#          in Hunter & Kearney, Med & Biol Eng & Comput, 1983, 21 203-209
#
#---------------------------------------------------------------------
#
# Revisions
#
# V02-01 14 nov 1984 JBM modified TVFIL to get longer filter lengths
#---------------------------------------------------------------------
#
# Linkage
#
#
#---------------------------------------------------------------------
#
# Overlay
#
#
#
#---------------------------------------------------------------------
#
# RT-Build:
#---------------------------------------------------------------------
#
```

```
# INCLUSIONS
    INCLUDE       nx2_:NEXDEF
    INCLUDE       nx2_:SYSDEF
#
# DEFINITIONS
    DEFINE        (_MAXNUMTRIALS, 1000)
    DEFINE        (_FILTERLENMAX, 201)
    DEFINE        (_WORKSIZE, 5000)
    DEFINE        (_NUMINPUTCHANS, 3)
    DEFINE        (_NUMOUTPUTCHANS, 1)
    DEFINE        (_INPUTCHANLEN,2000000)
    DEFINE        (_OUTPUTCHANLEN, 256)
    DEFINE        (_RECORDSIZE, 128)
    DEFINE        (_FILENAMEMAX, 32)
    DEFINE        (_CHANNAMEMAX, 16)
    DEFINE        (_COMMENTMAX, 80)
    DEFINE        (_REAL4, 4)

#
# Declarations for trace
#
    BYTE OPER_NAME(13)
    STRING OPER_NAME 'TVFIL V02-01'
#
# DECLARATIONS
#
    COMMON /RATCOM/JTEMP
    BYTE          INPUT_FILE_NAME(_FILENAMEMAX, _NUMINPUTCHANS)
    BYTE          OUTPUT_FILE_NAME(_FILENAMEMAX, _NUMOUTPUTCHANS)
    INTEGER       IANS
    INTEGER       TERM_LUN
    INTEGER       VAR_LUN, VAF_LUN
    INTEGER       INPUT_LUN(_NUMINPUTCHANS)
    INTEGER       OUTPUT_LUN
    INTEGER       OLUN
    INTEGER       OPEN_FLAG,STOP_FLAG
    INTEGER       CHAN
    INTEGER*4     REC_NUM
    INTEGER       NUM_INPUT_CHANS
    INTEGER       NUM_OUTPUT_CHANS
    INTEGER*4     I, J
    INTEGER*4     INPUT_CHAN_LEN(_NUMINPUTCHANS)
    INTEGER*4     START_INDEX
    INTEGER*4     STOP_INDEX
    INTEGER       TRIAL_LEN,NUM_TRIALS,FILTER_LEN
    INTEGER       OFFSET, OFFSET_START, OFFSET_END, OFFSET_INCREMENT
    REAL          WINDOW(4),PORT(4)
    REAL*4        INPUT_CHAN(_INPUTCHANLEN, _NUMINPUTCHANS)
    REAL*4        OUTPUT_BUFFER (_RECORDSIZE)
    REAL*4        VAF_BUFFER (_RECORDSIZE)
```

```
      INTEGER           OUTPUT_COUNTER, VAF_COUNTER
      INTEGER           OUTPUT_CHAN_LEN, VAF_CHAN_LEN
      INTEGER           OUTPUT_REC_NUM, VAF_REC_NUM

      REAL*4            X1(_INPUTCHANLEN), X2 (_INPUTCHANLEN)
      REAL*8            IMPULSE(_OUTPUTCHANLEN)

      BYTE              TYPE(2)
      INTEGER           INFO
      INTEGER           TWO_SIDES
      INTEGER           DATA_LEN
      INTEGER           LAG_MAX
      INTEGER           LAG_MIN
      REAL*8            I_MEAN
      REAL*8            O_MEAN,O_VAR,R_MEAN,R_VAR
      REAL*4            START (_MAXNUMTRIALS)
      INTEGER*4         START_LEN
      REAL*8            A (_MAXNUMTRIALS,_FILTERLENMAX), B (_MAXNUMTRIALS)
                        C(_MAXNUMTRIALS),D(_MAXNUMTRIALS),
                        X_AVG(_FILTERLENMAX), Y_AVG(_FILTERLENMAX)
      REAL*4            X_MIN, X_MAX, Y_MIN, Y_MAX
      REAL*8            WORK (_WORKSIZE)
      INTEGER           IRANK,LWORK, IFAIL
      LOGICAL           SVD,ERROR_FLAG

      REAL*8            TOL
      REAL*8            SIGMA
      REAL*4            VAF
      REAL*8            SUM
      EQUIVALENCE       (INPUT_CHAN(1,1) X1)
      EQUIVALENCE       (INPUT_CHAN(1,2), X2)
      EQUIVALENCE       (INPUT_CHAN(1,3),START(1))
#
# FILELB Definitions
#
      BYTE              CHAN_NAME(_CHANNAMEMAX)
      BYTE              COMMENT(_COMMENTMAX)

      INTEGER*2         NUM_VERSIONS
      INTEGER*2         NUM_CHANS
      INTEGER*2         CHAN_FORMAT

      INTEGER*4         CHAN_LEN
      REAL*4            CHAN_START
      REAL*4            CHAN_STOP
      REAL*4            CHAN_INCR
      REAL*8            CHAN_TYPE
```

```
# PROGRAM CONTROL
#
       EXECUTE  GET_PIPE_DATA
       IF (STOP_FLAG == _YES) [
          EXECUTE  TERMINATE_PROGRAM
       ]
       EXECUTE  GET_STARTING_INDICES
       EXECUTE  GET_INPUT_DETAILS
       EXECUTE  GET_CONTROL_PARAMETERS
       EXECUTE  CHECK_ARRAY_REFERENCES
       EXECUTE  GET_OUTPUT_DETAILS
       EXECUTE  GET_INPUT_DATA
       DO OFFSET = OFFSET_START, OFFSET_END, OFFSET_INCREMENT [
          EXECUTE  COMPUTE_ENSEMBLE_AVERAGES
          EXECUTE  GENERATE_OUTPUT_DATA
          EXECUTE  GENERATE_PREDICTED_OUTPUT
          EXECUTE  STORE_OUTPUT_DATA
       ]
       EXECUTE FLUSH_OUTPUT_BUFFERS
       EXECUTE STORE_OUTPUT_DETAILS
          CALL NEWL ('EXIT',ANSWER)
       EXECUTE  TERMINATE_PROGRAM
```

```
PROCEDURE  GET_PIPE_DATA [

   OPEN_FLAG = _YES
   I = -_NUMINPUTCHANS
   J = _NUMOUTPUTCHANS
   CALL PIPE (I, NUM_INPUT_CHANS,
            INPUT_FILE_NAME, INPUT_LUN,
            J, NUM_OUTPUT_CHANS,
            OUTPUT_FILE_NAME, OUTPUT_LUN,
            VAR_LUN, TERM_LUN, OPEN_FLAG, STOP_FLAG, OPER_NAME)
   IF (STOP_FLAG == _YES ) [
      TYPE *,'Pipe error'
      STOP ' PIPE error'
   ]

]  #  END OF PROCEDURE  GET_PIPE_DATA
```

```
   PROCEDURE GET_STARTING_INDICES [

      IF (NUM_INPUT_CHANS .NE  3 )
         LEAVE
#
# Get input details
#
      READ (INPUT_LUN(3) ' 1) NUM_VERSIONS, NUM_CHANS,
         CHAN_LEN, CHAN_FORMAT, CHAN_TYPE, CHAN_INCR,
         CHAN_START, CHAN_STOP, (CHAN_NAME(I), I = 1, _CHANNAMEMAX),
         (COMMENT(I), I = 1, _COMMENTMAX)
      START_LEN = CHAN_LEN
      IF (START_LEN > _MAXNUMTRIALS )[
         TYPE *,'** TVFIL - too many trials'
         TYPE *,' Using first ',_MAXNUMTRIALS,' trials'
      ]
#
# Read in starting indices
#
      DO REC_NUM = 2, (START_LEN - 1) / _RECORDSIZE + 2 [
         STOP_INDEX = MIN (_RECORDSIZE,
         START_LEN - (REC_NUM - 2) * _RECORDSIZE)
         J = (REC_NUM-2)*_RECORDSIZE
         READ (INPUT_LUN(3) ' REC_NUM) $
            (INPUT_CHAN(J+I,3), I = 1, STOP_INDEX)
      ]

   ] #End of procedure GET_STARTING_INDICES
```

```
PROCEDURE  GET_INPUT_DETAILS [

   DO CHAN = 1, 2 [
      READ (INPUT_LUN(CHAN) ' 1) NUM_VERSIONS, NUM_CHANS,
         CHAN_LEN, CHAN_FORMAT, CHAN_TYPE, CHAN_INCR,
         CHAN_START, CHAN_STOP, (CHAN_NAME(I), I = 1, _CHANNAMEMAX),
         (COMMENT(I), I = 1, _COMMENTMAX)
         INPUT_CHAN_LEN(CHAN) = CHAN_LEN
   ]
   .IF DF _VMS [
      CHAN_LEN = MIN (INPUT_CHAN_LEN(1),
      INPUT_CHAN_LEN(2))
      IF (CHAN_LEN > _INPUTCHANLEN) [
         TYPE $FORM,_INPUTCHANLEN
(' **** WARNING Input channel too long. Using first ',I6,' points')
      ]
   ]
   INPUT_CHAN_LEN(1) = CHAN_LEN
   INPUT_CHAN_LEN(2) = CHAN_LEN
   DATA_LEN = CHAN_LEN

]  #  END OF PROCEDURE  GET_INPUT_DETAILS
```

```
PROCEDURE GET_CONTROL_PARAMETERS [

    IF (START_LEN == 0 ) [
        CALL NEWJ ('Trial length',TRIAL_LEN, 1, CHAN_LEN)
        NUM_TRIALS = CHAN_LEN/TRIAL_LEN
        CALL NEWJ ('Number of trials to use',NUM_TRIALS,
            1, NUM_TRIALS )
                TYPE $FORM,NUM_TRIALS; (' Number of trials = ,I)
                IF (NUM_TRIALS > _MAXNUMTRIALS)
                    STOP 'Too many trials'
    DO I = 1,NUM_TRIALS [
            START(I) = (I-1)*TRIAL_LEN
        ]
    ]
    ELSE IF (START_LEN > 0 ) [
        NUM_TRIALS = START_LEN
            ]
        TYPE *,NUM_TRIALS
    CALL NEWJ ('Offset start',OFFSET_START,-CHAN_LEN,CHAN_LEN)
    CALL NEWJ ('Offset end',OFFSET_END,OFFSET_START,CHAN_LEN)
    CALL NEWJ ('Offset increment',OFFSET_INCREMENT,
            1,CHAN_LEN/NUM_TRIALS)
    LAG_MAX = MIN (TRIAL_LEN, _FILTERLENMAX)
        CALL NEWJ ('Filter length ', LAG_MAX, 2,
            MIN (_FILTERLENMAX, CHAN_LEN / 2))
            TWO_SIDES = _YES
        CALL NEWL ('Two-sided filter', TWO_SIDES)
    LAG_MIN = 0
    IF (TWO_SIDES == _YES) [
        LAG_MAX = LAG_MAX/2
        LAG_MIN = -LAG_MAX
    ]
    FILTER_LEN = LAG_MAX - LAG_MIN + 1
    IF (FILTER_LEN > _FILTERLENMAX)
        STOP 'Filter too long'
    CHAN_START = LAG_MIN*CHAN_INCR
    CHAN_STOP = LAG_MAX*CHAN_INCR
    XTOL = 5.0E-4
    CALL NEWX ('Tolerance',XTOL,_VSR4,_VLR4)
    TOL = XTOL

] #End of procedure GET_CONTROL_PARAMETERS
```

```
PROCEDURE CHECK_ARRAY_REFERENCES [

   TYPE *,'check array references'
   REPEAT [
   IF ((START(1) + OFFSET_START - LAG_MAX) <= 0 )[
      TYPE *,' ARRAY REFERENCE TOO SMALL - DROPPING TRIAL'
      START_LEN = START_LEN - 1
      NUM_TRIALS = START_LEN
      DO I = 1,START_LEN [
         START(I) = START(I+1)
      ]
   ]
   ELSE
      BREAK
   ]
REPEAT [
      IF ((START(NUM_TRIALS) + OFFSET_END - LAG_MIN) >=  CHAN_LEN)[
      NUM_TRIALS = NUM_TRIALS - 1
      START_LEN = START_LEN -1
      TYPE *,' ARRAY REFERENCE TOO LARGE - DROPPING TRIAL'
      ]
   ELSE
      BREAK
   ]
TYPE *,'Array references o.k '

] #END OF PROCEDURE CHECK_ARRAY_REFERENCES
```

```
   PROCEDURE  GET_OUTPUT_DETAILS [

          CHAN_TYPE = 'LAG  sec'
          CALL ICCS (CHAN_NAME, 1, _CHANNAMEMAX, 'AMPLITUDE',_EOS)
          DO I = 1, _FILENAMEMAX [
             IF (INPUT_FILE_NAME(I, 1) == ' ') [
                INPUT_FILE_NAME(I, 1) = _EOS
                BREAK
             ]
          ]
          DO I = 1, _FILENAMEMAX [
             IF (INPUT_FILE_NAME(I, 2) == ' ') [
                INPUT_FILE_NAME(I, 2) = _EOS
                BREAK
             ]
          ]
          CALL ICCS (COMMENT, 1, _COMMENTMAX, 'FILTER BETWEEN ',  $
                INPUT_FILE_NAME(1,1), ' AND ', _EOS )
          CALL ICCS (COMMENT,LLEN(COMMENT)+1,_COMMENTMAX,  $
                INPUT_FILE_NAME(1,2),_EOS )
#
# Open output file for VAF
#
          VAF_LUN = OUTPUT_LUN + 1
          OPEN (UNIT = VAF_LUN, NAME = 'VAF.NXC', STATUS = 'NEW',
          ACCESS = 'DIRECT', RECORDSIZE = _RECORDSIZE,
             FORM = 'UNFORMATTED',$ERR=ERROR_FLAG )
          IF (ERROR_FLAG)
             STOP 'Error opening output file'
#
# Initialize output counters
#
          OUTPUT_COUNTER = 1
          VAF_COUNTER = 1
          OUTPUT_CHAN_LEN = 0
          VAF_CHAN_LEN = 0
          OUTPUT_REC_NUM = 2
          VAF_REC_NUM = 2

   ] #  END OF PROCEDURE  GET_OUTPUT_DETAILS
```

```
PROCEDURE  GET_INPUT_DATA [

    DO CHAN = 1, 2 [
        CHAN_LEN = INPUT_CHAN_LEN(CHAN)
        DO REC_NUM = 2, (CHAN_LEN - 1) / _RECORDSIZE + 2 [
            STOP_INDEX = MIN (_RECORDSIZE,
            CHAN_LEN - (REC_NUM - 2) * _RECORDSIZE)
            J = (REC_NUM-2)*_RECORDSIZE
            READ (INPUT_LUN(CHAN) ' REC_NUM) $
                (INPUT_CHAN(I + J, CHAN), I = 1, STOP_INDEX)
        ]
    ]

]  #  END OF PROCEDURE  GET_INPUT_DATA
```

```
PROCEDURE COMPUTE_ENSEMBLE_AVERAGES [

    DO I = 1,FILTER_LEN [
        X_AVG(I) = 0
        Y_AVG(I) = 0.
    ]
    X_MIN = INPUT_CHAN ( START (1) + OFFSET, 1)
    X_MAX = X_MIN
    Y_MIN = INPUT_CHAN ( START (1) + OFFSET, 2)
    Y_MAX = Y_MIN
    DO I = 1,NUM_TRIALS [
        J = START(I) + OFFSET
        K = 1
        DO LAG = LAG_MIN,LAG_MAX [
            X_MIN = MIN (X_MIN, INPUT_CHAN (J+LAG,1))
            X_MAX = MAX (X_MAX, INPUT_CHAN (J+LAG,1))
            X_AVG(K) = X_AVG(K) + INPUT_CHAN(J+LAG,1)
            Y_MIN = MIN (Y_MIN, INPUT_CHAN (J+LAG 2))
            Y_MAX = MAX (Y_MAX, INPUT_CHAN (J+LAG,2))
            Y_AVG(K) = Y_AVG(K) + INPUT_CHAN(J+LAG,2)
            K = K + 1
        ]
    ]
    DO I = 1,FILTER_LEN [
        X_AVG(I) = X_AVG(I)/NUM_TRIALS
        Y_AVG(I) = Y_AVG(I)/NUM_TRIALS
    ]

] #End of procedure COMPUTE_ENSEMBLE_AVERAGES
```

```
   PROCEDURE  GENERATE_OUTPUT_DATA [

      K_MAX = LAG_MAX - LAG_MIN + 1
      O_MEAN = 0
      I_MEAN = 0
#
# Remove ensemble mean values
#
      DO I = 1,NUM_TRIALS [
         J = START(I) + OFFSET
         B(I) = INPUT_CHAN(J,2) - Y_AVG(1-LAG_MIN)
         K = 1
         DO LAG = LAG_MIN,LAG_MAX [
            A(I,K) = INPUT_CHAN (J-LAG,1) - X_AVG(K)
            K = K + 1
         ]
      ]
      LWORK = _WORKSIZE
      NRA = _MAXNUMTRIALS
      IFAIL = 1
      FILTER_LEN = LAG_MAX - LAG_MIN + 1
#
# Compute Singular Value Decomposition
#
      CALL F04JGF ( NUM_TRIALS, FILTER_LEN, A, NRA, B, TOL, SVD,
         SIGMA, IRANK, WORK, LWORK, IFAIL )
      IF (IFAIL == 0) [
         TYPE *,'Offset = ',OFFSET, ',Success'
      ]
      ELSE [
         TYPE *,'Offset = ',OFFSET, ' ,Failure  Mode = ',IFAIL
      ]

   ]  #  END OF PROCEDURE  GENERATE_OUTPUT_DATA
```

```
PROCEDURE GENERATE_PREDICTED_OUTPUT [

O_MEAN = 0
O_VAR = 0
R_MEAN = 0
R_VAR = 0
Y_MIN = INPUT_CHAN(OFFSET,2)
Y_MAX = Y_MIN
DO I = 1,NUM_TRIALS [
    J = START(I) + OFFSET
    C(I) = 0.
    K = 1
    DO LAG = LAG_MIN,LAG_MAX [
        C(I) = C(I) + INPUT_CHAN(J-LAG,1) * B(K)
        K = K + 1
    ]
        D(I) = INPUT_CHAN(J,2)
        O_MEAN = O_MEAN + D(I)
            R_MEAN = R_MEAN + C(I)
]
O_MEAN = O_MEAN/NUM_TRIALS
R_MEAN = R_MEAN/NUM_TRIALS
DO I = 1,NUM_TRIALS [
        C(I) = C(I) - R_MEAN
        D(I) = D(I) - O_MEAN
        O_VAR = O_VAR + D(I)**2
        R_VAR = R_VAR + (D(I) - C(I))**2
]
O_VAR =  O_VAR/NUM_TRIALS
R_VAR = R_VAR/NUM_TRIALS
VAF = (1  - R_VAR/O_VAR)*100

] #End of procedure GENERATE_PREDICTED_OUTPUT
```

```
    PROCEDURE  TRANSFORM_DATA_TO_ZERO_MEAN [

#
# Input channel
#
    L = 0
    DO I = 1, NUM_TRIALS [
        SUM = 0 0
        DO J = LAG_MIN,LAG_MAX [
            K = START(I) + OFFSET -  J
            SUM = SUM + INPUT_CHAN(K,1)
            L = L + 1
        ]
    ]
    I_MEAN = SUM/L
    DO I = 1,NUM_TRIALS [
        DO J = LAG_MIN,LAGMAX [
            K = START(I) + OFFSET - J
            INPUT_CHAN(K,1) = INPUT_CHAN(K,1) - I_MEAN
        ]
    ]
#
# Output channel
#
    SUM = 0 0
    DO I = 1, NUM_TRIALS [
        SUM = SUM + INPUT_CHAN(OFFSET + START(I),2)
    ]
    O_MEAN = SUM / NUM_TRIALS
    DO I = 1, NUM_TRIALS [
        J = OFFSET + START(I)
        INPUT_CHAN(J,2) = INPUT_CHAN(J,2) - O_MEAN
    ]

    ] #  END OF PROCEDURE  TRANSFORM_DATA_TO_ZERO_MEAN
```

```
   PROCEDURE   STORE_OUTPUT_DATA [

#
# Store filter
#
   DO I = 1,FILTER_LEN [
      OUTPUT_BUFFER(OUTPUT_COUNTER) = B(I)/CHAN_INCR
      OUTPUT_COUNTER = OUTPUT_COUNTER + 1
      IF (OUTPUT_COUNTER > _RECORDSIZE) [
         WRITE (OUTPUT_LUN ' OUTPUT_REC_NUM) $
            OUTPUT_BUFFER
         OUTPUT_COUNTER = 1
         OUTPUT_REC_NUM = OUTPUT_REC_NUM + 1
      ]
   ]
   OUTPUT_CHAN_LEN = OUTPUT_CHAN_LEN + FILTER_LEN
#
# Store VAF
#
   VAF_BUFFER(VAF_COUNTER) = VAF
   VAF_COUNTER = VAF_COUNTER + 1
   VAF_CHAN_LEN = VAF_CHAN_LEN + 1
   IF (VAF_COUNTER > _RECORDSIZE ) [
      WRITE (VAF_LUN ' VAF_REC_NUM ) VAF_BUFFER
         VAF_COUNTER = 1
         VAF_REC_NUM = VAF_REC_NUM + 1
   ]

   ]#   END OF PROCEDURE   STORE_OUTPUT_DATA
```

```
PROCEDURE FLUSH_OUTPUT_BUFFERS [

    IF (OUTPUT_COUNTER > 1 ) [
       DO I = OUTPUT_COUNTER, _RECORDSIZE [
          OUTPUT_BUFFER(I) = 0
       ]
       WRITE (OUTPUT_LUN ' OUTPUT_REC_NUM) OUTPUT_BUFFER
    ]
    IF (VAF_COUNTER > 1 ) [
       DO I = VAF_COUNTER, _RECORDSIZE [
          VAF_BUFFER(I) = 0
       ]
       WRITE (VAF_LUN ' VAF_REC_NUM) VAF_BUFFER
    ]

] #End of procedure FLUSH_OUTPUT_BUFFERS
```

```
   PROCEDURE STORE_OUTPUT_DETAILS [

   CHAN_FORMAT = _REAL4
#
# Store filter details
#
   CHAN_START = LAG_MIN*CHAN_INCR
   CHAN_STOP = CHAN_START + (OUTPUT_CHAN_LEN -1)*CHAN_INCR
   WRITE (OUTPUT_LUN ´ 1) NUM_VERSIONS, NUM_CHANS,
               OUTPUT_CHAN_LEN, CHAN_FORMAT, CHAN_TYPE, CHAN_INCR,
               CHAN_START, CHAN_STOP, (CHAN_NAME(I), I = 1, _CHANNAMEMAX),
               (COMMENT(I), I = 1, _COMMENTMAX)
   CHAN_LEN = FILTER_LEN
#
# Store VAF details
#
   CALL ICCS (CHAN_NAME, 1, _CHANNAMEMAX, ´VAF´,_EOS)
   CALL ICCS (COMMENT,1,_COMMENTMAX, ´VAF´,_EOS)
   CHAN_START = OFFSET_START*CHAN_INCR
   CHAN_INCR = OFFSET_INCREMENT*CHAN_INCR
   CHAN_STOP = OFFSET_END*CHAN_INCR
   WRITE (VAF_LUN ´ 1) NUM_VERSIONS, NUM_CHANS,
               VAF_CHAN_LEN, CHAN_FORMAT, CHAN_TYPE, CHAN_INCR,
               CHAN_START, CHAN_STOP, (CHAN_NAME(I), I = 1, _CHANNAMEMAX),
               (COMMENT(I), I = 1, _COMMENTMAX)
   CHAN_LEN = FILTER_LEN

   ] #End of procedure STORE_OUTPUT_DETAILS
```

```
    PROCEDURE  TERMINATE_PROGRAM [

       CALL EXIT

    ]  #  END OF PROCEDURE  TERMINATE_PROGRAM




END
```

APPENDIX B: REFERENCES

Agarwal, G.C., and Gottlieb, G.L., "Oscillation of the human ankle joint in response to applied sinusoidal torque on the foot," *J. Physiol. (London)*, 268, 151-176, 1977a.

Agarwal, G.C., and Gottlieb, G.L., "Compliance of the human ankle joint," *Trans. ASME*, 99, 166-170, 1977b.

Akazawa, K., Aldridge, J.W., Steeves, J D., and Stein, R B., "Modulation of stretch reflexes during locomotion in the mesencephalic cat," *J. Physiol. (London)*, 329, 553-567, 1982

Akazawa, K., Milner, T.E., and Stein, R.B., "Modulation of reflex EMG and stiffness in response to stretch of human finger muscle," *J. Neurophysiol.*, 49, 16-27, 1983.

Allum, J.H.J., "Responses to load disturbances in human shoulder muscles: the hypothesis that one component is a pulse test information signal," *Exp. Brain Res.*, 22, 307- 326, 1975

Alnaes, E., "Static and dynamic properties of Golgi tendon organs in the anterior tibial soleus muscles of the cat," *Acta Physiol. Scand.*, 70, 176-187, 1967.

Anderson, J.H., "Dynamic characteristics of Golgi tendon organs," *Brain Res.*, 67, 531-537, 1974.

Aubert, X., Roquet, M.L., and Van der Elst, J., "The tension-length diagram of the frog's sartorius muscle," *Arch. Intern. de Physiol.*, 59, 239-241, 1951.

Bagni, M A., Cecchi, G., Colomo, F., and Tesi, C., "The mechanical characteristics of the contractile machinery at different levels of activation in intact single muscle fibres of the frog," In: Molecular Mechanisms of Muscular Contraction, G.H Pollack and H Sugi, Eds , Plenum Press, New York, 473-487, 1988.

Baldissera, F., Hultborn, H., and Illert, M., "Integration in spinal neuronal systems," In Handbook of Physiology - The Nervous System II, V B Brooks, Ed , American Physiology Society, Bethesda, Md., 509-595, 1981

Baratta, R., and Solomonow, M., "The dynamic response model of nine different skeletal muscles," *IEEE Trans. Biomed. Eng.*, 37, 243-251, 1990.

Basmajian, J.V., Muscles Alive. Their Functions Revealed by Electromyography. Fourth Edition, Williams and Wilkins, Baltimore, 1978.

Basmajian, J.V., and DeLuca, C.J., Muscles Alive. Their Functions Revealed by Electromyography, Fifth Edition, Williams and Wilkins, Baltimore, 1985

Bawa, P., and Stein, R.B., "Frequency response of human soleus muscle," *J. Neurophysiol.*, 39, 788-793, 1976.

Bendat, J.S., and Piersol, A.G., Random Data: Analysis and Measurement Procedures, Second Edition, Wiley, New York, 1986.

Bennet, D.J , Xu, Y., Hollerbach, J.M., and Hunter, I.W., "Mechanical properties of the human arm during voluntary movement," *Proc. 16th CMBEC*, 89-90, 1990.

Bressler, B.H., and Dusik, L.A., "A comparison of muscle stiffness measurements obtained with rapid releases or stretches of frog semitendonosis fibers," In: Contractile Mechanisms in Muscle, G.H. Pollack and H. Sugi, Eds., Plenum Press, New York, 601-604, 1984.

Brooks, V.B , The Neural Basis of Motor Control, Oxford University Press, Oxford, 1986.

Brown, T.I.H., Rack, P.M.H., and Ross, H.F., "Forces generated at the thumb interphalangeal joint during imposed sinusoidal movements," *J. Physiol. (London)*, 332, 69-85, 1982.

Cannon S.C., and Zahalak, G.I., "The mechanical behavior of active human skeletal muscle in small oscillations," *J. Biomech.*,15, 111-121, 1982.

Capaday, C., and Stein, R.B., "Amplitude modulation of the soleus H-reflex in the human during walking and standing," *J., Neurosci.*, 6, 1308-1313, 1986.

Chen, H -F. and Guo, L., "Nonstationary time series identification," *Computers Math. Applic.*, 17, 1247-1258, 1989.

Crowe, A , and Matthews, P.B.C., "The effects of stimulation of static and dynamic fusiform fibres on the response to stretching of the primary endings of muscle spindles," *J. Physiol., (London)*, 174, 109-131, 1964.

Doeblin, E O., Measurement Systems. Application and Design, Third Edition, McGraw-Hill, Montréal, 1983.

Eccles R.M., and Lundberg, A., "Supraspinal control of interneurons mediating spinal reflexes," *J. Physiol. (London)*, 147, 565-584, 1959

Evans, C M , Fellows S.J., Rack, P.M.H., Ross, H.F., and Walters, D.K.W , "Response of the normal human ankle joint to imposed sinusoidal movements," *J. Physiol. (London)*, 344, 483-502, 1983

Eykhoff, P., System Identification, Wiley, New York, 1974.

Gardner, W.A., "Correlation estimation and time-series modeling for nonstationary processes," *Signal Processing*, 15, 31-41, 1988.

Genadry, W.F., Kearney, R.E., and Hunter, I.W , "Dynamic relationship between EMG and torque at the human ankle· variation with contraction level and modulation," *Med & Biol. Eng. & Comput.*, 26, 489-496, 1988.

González-Serratos, H., "Inward spread of activation in vertebrate muscle fibres," *J. Physiol., (London)*, 212, 777-799, 1971.

Gordon, A.M., Huxley, A.F., and Julian, F.J., "The variation in isometric tension with sarcomere length in vertebrate muscle fibers," *J. Physiol., (London)*, 184, 170-192, 1966

Gottlieb, G.L., and Agarwal, G.C., "Dependence of human ankle compliance on joint angle," *J. Biomech.*, 11, 177-181, 1978.

Granit, R., and Kaada, B.R., "Influence of stimulation of central nervous structures on muscle spindles in cat," *Acta Physiol. Scand.*, 27, 130-160, 1952.

Grenier, Y., "Time-dependent ARMA modelling of non-stationary signals," *IEEE Trans. Accoust., Speech and Signal Processing*, 31, 899-911, 1983.

Hall, M., Oppenheim, A.V., and Willsky, A., "Time-varying parametric modelling of speech," *Proc., IEEE Decision and Control Conf.*, 1085-1091, 1977.

Henneman, E., and Olson, C.B., "Relations between structure and design of skeletal muscles," *J. Neurophysiol.*, 28, 581-598, 1965.

Hongo, T., Jankowska, E., and Lundberg, A., "The rubrospinal tract. II, Facilitation of interneuronal transmission in reflex paths to motoneurones," *Exp. Brain Res.*, 7, 365-391, 1969

Houk, J.C., and Henneman, E., "Feedback control of skeletal muscles," *Brain Res.*, 5, 433-451, 1967.

Houk, J.,C., and Henneman, E., "Feedback control of muscle: introductory concepts," In Medical Physiology, Thirteenth Edition, V.B. Mountcastle, Ed., 1, 608-635, 1974

Houk, J.C., and Simon, W., "Responses of Golgi tendon organs to forces applied to the muscle tendon," *J. Neurophysiol.*, 30, 1466-1481, 1967.

Houk, J.C., Singer, J.J., and Goldman, M.R., "An evaluation of length and force feedback to soleus muscle of decerebrate cats," *J. Neurophysiol.*, 33, 784-811, 1970

Hunter, I.W., "Experimental comparison of Wiener and Hammerstein cascade models of frog muscle fiber mechanics," *Biophys J.*, 49, 81a, 1986.

Hunter, I.W., and Kearney, R.E., "Dynamics of human ankle stiffness. Variation with mean ankle torque," *J. Biomech.*, 15, 747-752, 1982.

Hunter, I W., and Kearney, R E., "Two-sided linear filter identification," *Med. & Biol. Eng. & Comput.*, 21, 203-209, 1983.

Hunter, I.W., and Kearney, R.E., "NEXUS: A computer language for physiological systems and signal analysis," *Comput. Biol. & Med.*, 14, 385-401, 1984.

Hunter, I W, and Kearney, R.E., "Quasi-linear, time-varying, and nonlinear approaches to the identification of muscle and joint mechanics," In. Advanced Methods of Physiological System Modeling, Marmarelis, V.Z., Ed., Biomedical Simulation Resource, University of Southern California, Los Angeles, 1, 128-146, 1987

Huxley, A F., and Neidergerke, R., "Structural Changes in muscle during contraction. Interference microscopy of living muscle fibres," *Nature*, 173, 971-973, 1954.

Huxley, A F., "Muscle structure and theories of contraction," *Prog. Biophys. Biophys. Chem.*, 7, 255-318, 1957.

Huxley, H E., and Hanson, J., "Changes in the cross-striations of muscle during contraction and stretch and their structural interpretation," *Nature*, 173, 973-976, 1954

Jansen, J.K.S. and Matthews, P.B.C., "The effects of fusimotor activity on the static responsiveness of primary and secondary endings of muscle spindles in the decerebrate cat," *Acta Physiol. Scand.*, 44, 376-386.

Joyce, G.C., and Rack, P.M.H., "Isotonic lengthening and shortening movements of cat soleus muscle," *J. Physiol. (London)*, 204, 475-491, 1969.

Joyce, G.C., Rack, P.M.H., and Westbury, D.R., "The mechanical properties of cat soleus muscle during controlled lengthening and shortening movements," *J. Physiol. (London)*, 204, 461-474, 1969.

Kalman, R.E., "A new approach to linear filtering and prediction problems," *J. Basic Engineering Trans. ASME*, 82, 35-45, 1960.

Kearney, R E., and Hunter, I.W., "Dynamics of human ankle stiffness: Variation with displacement amplitude," *J. Biomech.*, 15, 753-756, 1982.

Kearney, R E and. Hunter, I.W, "System identification of human stretch reflex dynamics: Tibialis anterior," *Exp. Brain Res.*, 56, 40-49, 1984.

Kearney, R E , and I.W. Hunter, "Evaluation of a technique for the identification of time-varying systems using experimental and simulated data," *Proc. 12th CMBEC*, 12, 75-76, 1986.

Kearney, R E., and Hunter, I.W., "A new method for identification of time-varying biological systems," *Proc. 13th CMBEC*, 127-128, 1987.

Kearney, R.E., Hunter, I W., Weiss, P.L., and Spring, K., "Tilt-table/ankle-actuator system for the study of vestibulospinal reflexes," *Med. & Biol. Eng. & Comput.*, 21, 301-305, 1983.

Lacquaniti, F., Licata, F., and Soechting, J.F., "The mechanical behavior of the human forearm in response to transient perturbations," *Biol. Cybern.*, 44, 25-46, 1982.

Lai, T.L., and Wei, C.Z., "Extended least-squares and their application to adaptive control and prediction in linear systems," *IEEE Trans. Autom. Control*, 31, 898-906, 1986.

Lawrence, P J., and Dawson, R.D., "Identification of periodic nonstationary antenna stabilization control systems by crosscorrelation techniques," *Proc. IEE*, 124, 797-801, 1977

Lindström, L R., "On the frequency spectrum of EMG signals," Technical Report - Research Laboratory of Medical Electronics, Chalmers University of Technology, Göteborg, Sweden, 1970

Ljung, L , and Söderström, T., Theory and Practice of Recursive Identification, MIT Press, Cambridge, Ma., 1983.

Mannard, A., and Stein R.B., "Determination of the frequency response of isometric soleus muscle in the cat using random nerve stimulation," *J. Physiol. (London)*, 229, 275, 1973

Marmarelis, P.Z., and Marmarelis, V.Z., Analysis of Physiological Systems. The White-Noise Approach, Plenum Press, New York, 1978.

Marmarelis, V.Z., "Practicable identification of nonstationary nonlinear systems," *Proc. IEEE*, 128, 211-214, 1981.

Marmarelis, V.Z., "Nonlinear and nonstationary modeling of physiological systems An Overview," In: Advanced Methods of Physiological System Modeling, Marmarelis, V.Z., Ed., Biomedical Simulation Resource, University of Southern California, Los Angeles, 1, 1-24, 1987a.

Marmarelis, V.Z., "Recent advances in nonlinear and nonstationary analysis," In: Advanced Methods of Physiological System Modeling, Marmarelis, V.Z., Ed , Biomedical Simulation Resource, University of Southern California, Los Angeles, 1, 323-336, 1987b.

Marple, S L., Digital Spectral Analysis, Prentice-Hall, Toronto, 1987.

Matthews, P.B.C., and Stein, R.B., "The sensitivity of muscle spindle afferents to small sinusoidal changes in length," *J. Physiol. (London)*, 200, 723-743, 1969.

Mayne, D.Q., "Optimal non-stationary estimation of the parameters of a linear system with Gaussian inputs," *J. Electron. Control*, 14, 101-112, 1963.

McMahon, T.A., Muscles, Reflexes and Locomotion, Princeton University Press, Princeton, 1984

Milner-Brown, H.S., and Stein, R.B., "The relation between the surface electromyogram and muscular force," *J. Physiol. (London)*, 246, 549-565, 1975

Moirier, R.L., Weiss, P.L., and Kearney, R.E , "Low inertia, rigid limb fixation using glass fibre casting bandage," *Med. & Biol. Eng. & Comput.*, 28, 96-99, 1990.

Moser, A T and Graupe, D. "Applicability of Kalman filtering theory to identification of time series with non-stationary covariance structures," *Int. J. Systems Sci.*, 20, 91-96, 1989a

Moser, A.T., and Graupe, D., "Identification of nonstationary models with application to myoelectric signals for controlling electrical stimulation of paraplegics," *IEEE Trans. Accoust. Speech, and Signal Processing*, 37, 713-719, 1989

Neilsen, P.M.F., Hunter, I.W., and Kearney, R.E , "Time-varying identification of isolated muscle mechanics," *Proc. 15th CMBEC*, 121-122, 1989

Numerical Algorithms Group Limited, The NAG Fortran Library Manual -Mark 13 1988

Parker, P.A., Scott, R.N., "Myoelectric control of prostheses," *CRC Critical Reviews in Bioengineering*, 13, 283-309, 1984.

Poppele, R.E., and Bowman, R.J., "Quantitative description of linear behavior of mammalian muscle spindles," *J. Neurophysiol.*, 33, 59-72, 1970.

Press, W.H., Flannery, B.P., Teukolsky, S.A., Vetterling, W.T., Numerical Recipes, Cambridge University Press, Cambridge, 1986.

Proske, U., and Morgan, D.L., "Tendon stiffness: Methods of measurement and significance for the control of movement. A review," *J. Biomech.*, 20, 75-82, 1987

Rack, P.M.H., Ross, H.F., Thilmann, A.F., and Walters, D.K.W., "Reflex responses at the human ankle. the importance of tendon compliance," *J. Physiol. (London)*, 344, 503-524, 1983.

Rack, P.M.H., and Westbury, D.R., "The effects of length and stimulus rate on tension in the isometric cat soleus muscle," *J. Physiol. (London)*, 204, 443-460, 1969.

Rack, PM.H , and Westbury, D.R., "Elastic properties of the cat soleus tendon and their functional importance," *J. Physiol. (London)*, 347, 479-495, 1984.

Rosenthal, N P., McKean, T.A., Roberts, W J., and Terzuolo, C A., "Frequency analysis of stretch reflex and its main subsystems in triceps surae muscles of the cat," *J. Neurophysiol.*, 33, 713-749, 1970.

Rymer, W.Z., and Hasan, Z., "Absence of force-feedback regulation in soleus muscle of the decerebrate cat," *Brain Res.*, 184, 203-209, 1980.

Sammarco, G.J., Burstein, A.H., and Frankel, V H., "Biomechanics of the ankle: A kinematic study," *Orthop. Clin. North Am.*, 4, 75-96, 1973.

Sharman, K.C., and Freidlander, B., "Time-varying modeling of a class of nonstationary signals," *Proc. International Conf. Accoust., Speech and Signal Processing*, San Diego, 22 2 1-22.2.4, 1984.

Smith, A M , "The coactivation of antagonist muscles," *Can. J. Physiol. Pharmacol.*, 59, 733-747, 1981.

Soechting, J F., Dufresne, J.R., and Lacquaniti, F, "Time-varying properties of myotactic response in man during some simple motor tasks," *J. Neurophysiol.*, 46, 1226-1243, 1981.

Stein, R B , "Peripheral control of movement," *Physiol. Rev.*, 54, 215-243, 1974.

Stein, R B , Nerve and Muscle. Plenum Press, New York, 1980.

Stein, R.B , and Gordon, T. "Nonlinear stiffness-force relations in whole mammalian skeletal muscles," *Can. J. Physiol. Pharmacol.*, 64, 1236-1244, 1986

Stein R B , and Parmiggiani, F , "Optimal motor patterns for activating mammalian muscle," *Brain Res.*, 175, 272-276, 1979.

Strang, G., Linear Algebra and its Applications, Second Edition, Academic Press, New York, 1980.

Vander, A.J., Human Physiology: the Mechanisms of Body Function, McGraw-Hill, Montréal, 1985.

Weiss, P.L., Hunter, I.W., and Kearney, RE, "Human ankle joint stiffness over the full range of muscle activation levels," *J. Biomech.*, 21, 539-544, 1988

Weiss, P.L., Kearney, R.E., and Hunter, I.W., "Position dependence of ankle joint dynamics - I: Passive mechanics.," *J. Biomech.*, 19, 727-735, 1986a.

Weiss, P.L., Kearney, R E., and Hunter, I.W., "Position dependence of ankle joint dynamics - II. Active mechanics.," *J. Biomech.*, 19, 737-751, 1986b

Wilkie, D.R., "The relation between force and velocity in human muscle," *J. Physiol. (London)*, 110, 249-280, 1950.

Wilkinson, R.S., and Fukami, Y, "Responses of isolated Golgi tendon organs of cat to sinusoidal stretch," *J. Neurophysiol.*, 49, 976-988, 1983

Zhang, Y.T., Parker, P.A., and Scott, R.N., "Additive noise and the electromyographic channel," *Proc. 15th CMBEC*, 125-126, 1989.